

Renormalization, Complex Mass Scheme, Finite Width Effects and Decay Widths in the Standard Model

Hua-Sheng Shao

PH Department, TH Unit, CERN, CH-1211 Geneva 23, Switzerland

ABSTRACT:

KEYWORDS: [Perturbative Computations](#), [Hadronic Colliders](#).

Contents

1. Introduction	2
2. Renormalization	2
2.1 An example: NLO QCD corrections to Z decays into a quark pair	6
3. Complex Mass Scheme	8
3.1 A useful expansion	10
3.2 Spin decorrelation in Narrow-Width Approximation	10
3.3 A general cancellation in the total cross section	12
3.4 Discussions of the differential distributions	15
3.4.1 Non-resonance region	15
3.4.2 Resonance region	18
3.4.3 ϵ -offshellness method	21
3.5 An example: top quark decay width	25
3.5.1 NLO QCD corrections	26
3.5.2 NLO EW corrections	28
3.5.3 NNLO QCD corrections	34
4. Finite width effects at NNLO QCD level	36
4.1 top quark decay width	36
4.2 W production in hadronic collisions	36
4.3 Z production in hadronic collisions	36
5. SMWIDTH: A package for calculating decay widths of particles in the Standard Model with NNLO QCD and NLO EW accuracy	36
5.1 A quick guide	36
5.2 Illustrative results	36
A. 2-point scalar integrals	38
B. Dangerous in Taylor expansions of renormalization constant in Complex Mass Scheme	40
C. A general strategy for choosing Riemann sheet	42
D. Cancellation of $\alpha \log \Gamma$ between virtual and real	43

E. Cross Checks	46
E.1 $e^+\nu_e \rightarrow W^+ \rightarrow \mu^+\nu_m$	46
E.1.1 Non-resonance region	46
E.1.2 Resonance region: ε -offshellness method	46
E.2 $e^+e^- \rightarrow Z/\gamma^* \rightarrow \mu^+\mu^-$	46
E.2.1 Non-resonance region	46
E.2.2 Resonance region: ε -offshellness method	48
E.3 $e^+\nu_e \rightarrow t\bar{b} \rightarrow W^+b\bar{b}$	49
E.3.1 Non-resonance region	49
E.4 $u\bar{d} \rightarrow W^+ + \gamma \rightarrow e^+\nu_e + \gamma$	51
E.4.1 Non-resonance region	51
E.5 $u\bar{u} \rightarrow Z/\gamma^* + \gamma \rightarrow e^+e^- + \gamma$	51
E.5.1 Non-resonance region	51
E.6 $e^+\nu_e \rightarrow \mu^+\nu_\mu b\bar{b}$	52
E.6.1 Non-resonance region	52
E.7 $gg \rightarrow \mu^+\nu_\mu b\mu^-\bar{\nu}_\mu\bar{b}$	53
E.7.1 Non-resonance region	53
E.8 $b\gamma \rightarrow \mu^+\nu_\mu b\mu^-\bar{\nu}_\mu$	55
E.8.1 Non-resonance region	55

1. Introduction

2. Renormalization

It is well known that perturbative Quantum Field Theory (QFT) should be renormalized since its UltraViolet (UV) divergent in loop Feynman integrals should be absorbed into the redefinition of parameters and fields in the Lagrangian. The so-called bare Lagrangian turns into a renormalized Lagrangian and all of the physical quantities are free of UV divergent contributions in any order of perturbation theory. The most widely used method to perform renormalization order by order in a consistent way is to introduce counterterms following the general Bogoliubov-Parasiuk-Hepp-Zimmermann (BPHZ) renormalization scheme. The UV counterterms are fixed by renormalization conditions as well as the way of renormalization group running for the corresponding renormalized parameters.

In the electroweak theory, a so-called on-shell renormalization scheme [1,2] is frequently used to make sure the renormalized parameters (such as masses of particles M_W, M_Z, M_H and M_f) be equal to the physical parameters. The on-shell renormalization condition guarantees that the renormalized parameter m_R is defined as the real part of the two-point self-energy function $\Sigma(p^2)$ and the bare parameter m_0 via

$$m_{os}^2 = -\text{Re}\Sigma(p^2)|_{p^2=m_{os}^2} + m_0^2, \quad (2.1)$$

and the wavefunction renormalization constant δZ_{os} for field is defined as the real part of its first derivation

$$\delta Z_{os} = -\text{Re}\Sigma'(p^2)|_{p^2=m_{os}^2}. \quad (2.2)$$

It means that

$$\text{Re}\Sigma_{os}(p^2)|_{p^2=m_{os}^2} = 0, \text{Re}\Sigma'_{os}(p^2)|_{p^2=m_{os}^2} = 0, \quad (2.3)$$

which requires both loop diagrams and UV counterterms contribute to $\Sigma_{os}(p^2)$. The advantage of working in on-shell scheme in perturbative computation is to avoid calculating the Feynman diagrams with the loop corrections to external legs since the renormalization condition gurantees that the contribution of these diagrams will cancel with those from the UV counterterm corrections to external legs order by order. We will demonstrate this fact in the following context of this section.

Let us start from the well-known Lehmann-Symanzik-Zimmermann (LSZ) reduction formula [3] to calculate the scattering amplitudes. It reads

$$\begin{aligned} & \langle k_1, \dots, k_n \text{out} | p_1, \dots, p_m \text{in} \rangle \\ &= \prod_{i=1}^n \frac{i(k_i^2 - m_{os}^2)}{\sqrt{(2\pi)^3 Z_{os}}} \prod_{j=1}^m \frac{i(p_j^2 - m_{os}^2)}{\sqrt{(2\pi)^3 Z_{os}}} G(k_1, \dots, k_n; -p_1, \dots, -p_m)|_{k_i^2=m_{os}^2, p_j^2=m_{os}^2}, \end{aligned} \quad (2.4)$$

where the Green function $G(k_1, \dots, k_n; -p_1, \dots, -p_m)$ can be graphically represented as

$$G(k_1, \dots, k_n; -p_1, \dots, -p_m) = \begin{array}{c} \begin{array}{ccc} & p_1 & \\ & \bullet & \\ & \diagdown & \diagup \\ & & k_1 \\ & & \bullet \\ & & \dots \\ & & \bullet \\ & \diagup & \diagdown \\ & p_m & \\ & \bullet & \\ & \diagdown & \diagup \\ & & k_n \\ & & \bullet \end{array} \\ \bullet \\ \bullet \\ \bullet \end{array} \quad (2.5)$$

The LSZ reduction formula (2.4) is valid in both bare Lagrangian and renormalized Lagrangian, and the scattering amplitude should be the same. With the bare Lagrangian, the Green function in the rhs of Eq.(2.4) are expressed in bare parameters, while the renormalized parameters are understood if the rhs is computed with the renormalized Lagrangian. The Green function is understood as the correlation function $\langle 0|T(\phi_0(x_1) \cdots \phi_0(x_{n+m}))|0\rangle$ where ϕ_0 is the bare filed but the correlation function is calculated in the specific Lagrangian. We have the vacuum to single-particle transition amplitude

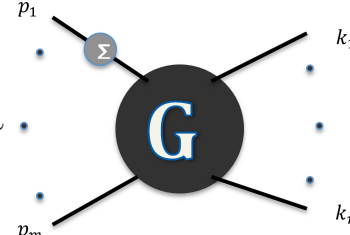
$$\begin{aligned} \langle k|\phi_0|0\rangle_0 &= \langle k|\phi_R|0\rangle_R, \\ \langle k|\phi_0|0\rangle_R &= \sqrt{Z_R}\langle k|\phi_R|0\rangle_R = \sqrt{Z_R}\langle k|\phi_0|0\rangle_0, \end{aligned} \quad (2.6)$$

where the symbol $\langle k|\phi_0|0\rangle_R$ denotes the expectation value of filed ϕ_0 is calculated with the renormalized Lagrangian \mathcal{L}_R and the corresponding wavefunction renormalization constant

is Z_R . With the bare Lagrangian, the rhs of Eq.(2.4) is

$$\begin{aligned} & \prod_{i=1}^n \frac{i(k_i^2 - m_{os}^2)}{\sqrt{(2\pi)^3 Z_{os}}} \prod_{j=1}^m \frac{i(p_j^2 - m_{os}^2)}{\sqrt{(2\pi)^3 Z_{os}}} G_0(k_1, \dots, k_n; -p_1, \dots, -p_m) |_{k_i^2=m_{os}^2, p_j^2=m_{os}^2} \\ &= \prod_{i=1}^n \frac{i(k_i^2 - m_{os}^2)}{\sqrt{(2\pi)^3 Z_{os}}} \prod_{j=1}^m \frac{i(p_j^2 - m_{os}^2)}{\sqrt{(2\pi)^3 Z_{os}}} \langle 0 | T(\phi_0(k_1), \dots, \phi_0(k_n); \phi_0(-p_1), \dots, \phi_0(-p_m)) | 0 \rangle_{0; k_i^2=m_{os}^2, p_j^2=m_{os}^2}. \end{aligned} \quad (2.7)$$

The Green function $G_0(k_1, \dots, k_n; -p_1, \dots, -p_m)$ should have the diagram with two-point self-energy function $\Sigma(p^2)$ inserted at the external legs

$$\begin{aligned} G_0(k_1, \dots, k_n; -p_1, \dots, -p_m) &\sim \text{Diagram} \\ &= \frac{i}{p_1^2 - m_0^2} (i\Sigma(p_1^2)) G_{0,1}(k_1, \dots, k_n; -p_1, \dots, -p_m), \end{aligned}$$


where $G_{0,1}(k_1, \dots, k_n; -p_1, \dots, -p_m)$ is the Green function without loop corrections on external legs and $\Sigma(p_1^2)$ consists of all one-particle irreducible (1PI) two-point Feynman diagrams. In general, we have

$$G_0(k_1, \dots, k_n; -p_1, \dots, -p_m) \sim \frac{(p_1^2 - m_0^2)}{p_1^2 - m_0^2 + \Sigma(p_1^2)} G_{0,1}(k_1, \dots, k_n; -p_1, \dots, -p_m),$$

after taking Dyson-summation. In order to keep unitarity, the imaginary part of $\Sigma(p_1^2)$ is vanishing because the external particle is stable. With the Talyor expansion relation

$$\Sigma(p_1^2) = \Sigma(p_1^2)|_{p_1^2=m_{os}^2} + (p_1^2 - m_{os}^2)\Sigma'(p_1^2)|_{p_1^2=m_{os}^2} + (p_1^2 - m_{os}^2)^2\Sigma_2(p_1^2), \quad (2.8)$$

we have

$$G_0(k_1, \dots, k_n; -p_1, \dots, -p_m) \sim \frac{(p_1^2 - m_0^2)}{(p_1^2 - m_{os}^2)(1 - \delta Z_{os} + (p_1^2 - m_{os}^2)\Sigma_2(p_1^2))} G_{0,1}(k_1, \dots, k_n; -p_1, \dots, -p_m). \quad (2.9)$$

We can transfer the bare Green function $G_{0,1}(k_1, \dots, k_n; -p_1, \dots, -p_m)$ into renormalized Green function

$$G_{0,1}(k_1, \dots, k_n; -p_1, \dots, -p_m) = (Z_{os})^{-1} \frac{p_1^2 - m_{os}^2}{p_1^2 - m_0^2} G_{os}(k_1, \dots, k_n; -p_1, \dots, -p_m), \quad (2.10)$$

because of the pole of the external legs in Green functions and the definition of the Green functions. We can derive the above expression in the following. By definition, we know

$$\begin{aligned} G_{os}(k_1, \dots, k_n; -p_1, \dots, -p_m) &= \langle 0 | T(\phi_0(k_1), \dots, \phi_0(k_n); \phi_0(-p_1), \dots, \phi_0(-p_m)) | 0 \rangle_{os}, \\ G_0(k_1, \dots, k_n; -p_1, \dots, -p_m) &= \langle 0 | T(\phi_0(k_1), \dots, \phi_0(k_n); \phi_0(-p_1), \dots, \phi_0(-p_m)) | 0 \rangle_{\mathcal{R}}. \end{aligned} \quad (2.11)$$

With Eq.(eq:phi0val), we have a factor of $\sqrt{Z_{os}}$ from external wavefunction,i.e.

$$\langle -p_1|\phi_0(-p_1)|0\rangle_{os} = \sqrt{Z_{os}}\langle -p_1|\phi_{os}(-p_1)|0\rangle_{os} = \sqrt{Z_{os}}\langle -p_1|\phi_0(-p_1)|0\rangle_0. \quad (2.12)$$

From vertex renormalization, we have another $\sqrt{Z_{os}}$ from the vertex renormalization. For example, in QED, we have

$$e_0 = Z_e e_R. \quad (2.13)$$

The renormalized vertex would proportional to

$$Z_e e_R \sqrt{Z_R} = e_0 \sqrt{Z_R}. \quad (2.14)$$

The uncanceled $\sqrt{Z_R}$ is one to one correspondent to the external leg. We remind the reader that the renormalized Green function $G_{os}(k_1, \dots, k_n; -p_1, \dots, -p_m)$ is free of loop corrections on external legs. If we defined¹

$$Z_R = \frac{1}{1 - \delta Z_R}, \quad (2.15)$$

and substituted Eqs.(2.9) and (2.10) into Eq.(2.7), we obtained the renormalized form of LSZ formula Eq.(2.4) in on-shell scheme

$$\prod_{i=1}^n -\frac{i(k_i^2 - m_{os}^2)}{\sqrt{(2\pi)^3 Z_{os}}} \prod_{j=1}^m -\frac{i(p_j^2 - m_{os}^2)}{\sqrt{(2\pi)^3 Z_{os}}} G_{os}(k_1, \dots, k_n; -p_1, \dots, -p_m)|_{k_i^2=m_{os}^2, p_j^2=m_{os}^2}, \quad (2.16)$$

where the term $\Sigma_2(p_1^2)$ is dropped after put p_1^2 on-shell $p_1^2 = m_{os}^2$. Then we recover the renormalized form of rhs of LSZ reduction formula Eq.(2.4), where we get rid of loop corrections on external legs in $G_{os}(k_1, \dots, k_n; -p_1, \dots, -p_m)$. In on-shell scheme, the UV counterterms for mass and wavefunction δZ cancel with the loop diagrams on the external legs. The wavefunction renormalization constant δZ_{os} in the prefactor will cancel with those from the Green function via Eq.(2.12). Thus, the remaining wavefunction renormalization counterterm only comes from the uncanceled vertex renormalization.

If one changes the renormalization conditions, for instance, let us take

$$\begin{aligned} \tilde{m}_R^2 &= m_0^2 - \text{Re}\Sigma(p^2)|_{p^2=Q^2}, \\ \delta \tilde{Z} &= -\text{Re}\Sigma(p^2)|_{p^2=Q^2}. \end{aligned} \quad (2.17)$$

Here \tilde{m}_R^2 is not the physical pole m_{os}^2 anymore. Along the same lines, we have

$$\begin{aligned} \Sigma(p_1^2) &= \Sigma(p_1^2)|_{p_1^2=Q^2} + (p_1^2 - Q^2)\Sigma'(p_1^2)|_{p_1^2=Q^2} + (p_1^2 - Q^2)^2\Sigma_2(p_1^2), \\ G_0(k_1, \dots, k_n; -p_1, \dots, -p_m) \\ &\sim \frac{(p_1^2 - m_0^2)}{p_1^2 - \tilde{m}_R^2 - (p_1^2 - Q^2)\delta \tilde{Z} + (p_1^2 - Q^2)^2\Sigma_2(p_1^2)} G_{0,1}(k_1, \dots, k_n; -p_1, \dots, -p_m), \\ G_{0,1}(k_1, \dots, k_n; -p_1, \dots, -p_m) &= (\tilde{Z})^{-1} \frac{p_1^2 - \tilde{m}_R^2}{p_1^2 - m_0^2} \tilde{G}_R(k_1, \dots, k_n; -p_1, \dots, -p_m) \end{aligned} \quad (2.18)$$

¹This definition is consistent with the BPHZ renormalization procedure beyond one-loop.

The derived rhs of Eq.(2.4) becomes

$$\prod_{i=1}^n \left\{ -\frac{i(k_i^2 - m_{os}^2)}{\sqrt{(2\pi)^3 Z_{os}}} F \right\} \prod_{j=1}^m \left\{ -\frac{i(p_j^2 - m_{os}^2)}{\sqrt{(2\pi)^3 Z_{os}}} F \right\} \tilde{G}_R(k_1, \dots, k_n; -p_1, \dots, -p_m) \Big|_{k_i^2=m_{os}^2, p_j^2=m_{os}^2} \quad (2.19)$$

with

$$F = \frac{(1 - \delta\tilde{Z})(m_R^2 - \tilde{m}_R^2)}{m_R^2 - \tilde{m}_R^2 - (m_R^2 - Q^2)\delta\tilde{Z} + (m_R^2 - Q^2)^2 \Sigma_2(m_R^2)}, \quad (2.20)$$

which means one has to calculate the loop diagrams attached on the external particles in the S-matrix. At the one-loop level, it is

$$F = 1 - \delta\tilde{Z} + \frac{m_R^2 - Q^2}{m_R^2 - \tilde{m}_R^2} \delta\tilde{Z} - \frac{(m_R^2 - Q^2)^2}{m_R^2 - \tilde{m}_R^2} \Sigma_2(m_R^2) = 1 - \delta\tilde{Z} - \frac{\Sigma(m_R^2) - \Sigma(Q^2)}{m_R^2 - \tilde{m}_R^2}, \quad (2.21)$$

where $-\frac{\Sigma(m_R^2)}{m_R^2 - \tilde{m}_R^2}$ corresponds to one-loop diagram on external leg, $\frac{\Sigma(Q^2)}{m_R^2 - \tilde{m}_R^2}$ corresponds to mass renormalization insertion diagram on external leg and $-\delta\tilde{Z}$ corresponds to wavefunction renormalization insertion diagram. That means one has to calculate the loop corrections as well as the renormalization insertions to external legs. Moreover, one should keep in mind that the wavefunction renormalization constant from Green function (see Eq.(2.6)) cannot cancel the on-shell wavefunction renormalization constant in the prefactor directly. Then, we will have another term proportional to $\prod \frac{p^2 - m_{os}^2}{p^2 - m_R^2} \frac{\sqrt{Z_R}}{\sqrt{Z_{os}}}$ left at the amplitude level.

2.1 An example: NLO QCD corrections to Z decays into a quark pair

We consider a simple example, i.e. Next-to-Leading Order (NLO) QCD corrections to Z decays into a quark pair in the Standard Model, to illustrate the above arguments. We will work in two renormalization schemes: on-shell renormalization scheme and $\overline{\text{MS}}$ scheme.

For simplicity, let us first examine the case of the massless external quark. Independent of renormalization, it is well known that the (initial helicity averaged) Born amplitude squared is

$$|\overline{\mathcal{M}}_B|^2 = \frac{2N_c e^2 m_Z^2}{3c_w^2 s_w^2} \left[(I_3^q)^2 - 2I_3^q Q_q s_w^2 + 2Q_q^2 s_w^4 \right], \quad (2.22)$$

where c_w, s_w are cosine and sine of Weinberg angle, $N_c = 3$ is the color factor, I_3^q and Q_q are the isospin and charge of the quark. Due to the condition of on-shell renormalization in Eq.(2.3), one can simply ignore to calculate the one-loop diagrams Figs.(1b,1c) and the corresponding UV counter term diagrams Figs.(1e,1f). The contribution of the vertex UV counter term Fig.(1d) is²

$$2\text{Re} \left\{ \overline{\mathcal{M}}_{os}^{\text{UV}} (\overline{\mathcal{M}}_B)^* \right\} = -C_F \frac{\alpha_s}{2\pi} \left(\frac{1}{\epsilon_{\text{UV}}} - \frac{1}{\epsilon_{\text{IR}}} \right) |\overline{\mathcal{M}}_B|^2, \quad (2.23)$$

²We work in Conventional Dimensional Regularization scheme.

where $C_F = \frac{N_c^2 - 1}{2N_c}$ is the color factor of the quark. In the $\overline{\text{MS}}$ renormalization scheme, besides Figs.(1a,1d), we have to include the non-vanishing contributions of Figs.(1b,1c,1e,1f). The expression of Fig.(1a) in $\overline{\text{MS}}$ scheme is the same as that in on-shell scheme, while the expression of the UV one Fig.(1d) becomes

$$2\text{Re} \left\{ \overline{\mathcal{M}_{\overline{\text{MS}},d}^{\text{UV}}} (\overline{\mathcal{M}_B})^* \right\} = -C_F \frac{\alpha_s}{2\pi} \left(\frac{1}{\epsilon_{\text{UV}}} - 1 - \gamma_E + \log(4\pi) \right) |\overline{\mathcal{M}_B}|^2, \quad (2.24)$$

where γ_E is the Euler-Mascheroni constant. Meanwhile, the sum of Figs.(1e,1f) is

$$2\text{Re} \left\{ \overline{\mathcal{M}_{\overline{\text{MS}},e+f}^{\text{UV}}} (\overline{\mathcal{M}_B})^* \right\} = C_F \frac{\alpha_s}{\pi} \left(\frac{1}{\epsilon_{\text{UV}}} - 1 - \gamma_E + \log(4\pi) \right) |\overline{\mathcal{M}_B}|^2, \quad (2.25)$$

and the sum of Figs.(1b,1c) is

$$2\text{Re} \left\{ \overline{\mathcal{M}_{\overline{\text{MS}},b+c}^{\text{one-loop}}} (\overline{\mathcal{M}_B})^* \right\} = -C_F \frac{\alpha_s}{\pi} \left(\frac{1}{\epsilon_{\text{UV}}} - \frac{1}{\epsilon_{\text{IR}}} \right) |\overline{\mathcal{M}_B}|^2. \quad (2.26)$$

Moreover, in $\overline{\text{MS}}$, one has an extra contribution proportional to $|\prod \frac{p^2 - m_{os}^2}{p^2 - m_{\overline{\text{MS}}}^2} \frac{\sqrt{Z_{\overline{\text{MS}}}}}{\sqrt{Z_{os}}}|^2$ at the amplitude squared level. Since the external quark is massless, we have the one-loop level experssion

$$\begin{aligned} m_{\overline{\text{MS}}} &= m_{os} = 0, \\ \delta Z_{os} &= -C_F \frac{\alpha_s}{4\pi} \left(\frac{1}{\epsilon_{\text{UV}}} - \frac{1}{\epsilon_{\text{IR}}} \right), \\ \delta Z_{\overline{\text{MS}}} &= -C_F \frac{\alpha_s}{4\pi} \left(\frac{1}{\epsilon_{\text{UV}}} - \gamma_E + \log(4\pi) \right). \end{aligned} \quad (2.27)$$

At one-loop level, the extra term would be

$$\begin{aligned} &2 \times \left[2 \times \left(\frac{1}{2} \delta Z_{\overline{\text{MS}}} - \frac{1}{2} \delta Z_{os} \right) \right] |\overline{\mathcal{M}_B}|_{\text{CDR}}^2 \\ &= C_F \frac{\alpha_s}{2\pi} \left(-\frac{1}{\epsilon_{\text{IR}}} + 1 + \gamma_E - \log(4\pi) \right) |\overline{\mathcal{M}_B}|^2 \end{aligned} \quad (2.28)$$

where we use

$$|\overline{\mathcal{M}_B}|_{\text{CDR}}^2 = \frac{(d-2)}{2} |\overline{\mathcal{M}_B}|^2. \quad (2.29)$$

The difference between the on-shell renormalization and $\overline{\text{MS}}$ renormalization is Eq.(2.24)+Eq.(2.25)+Eq.(2.26)+Eq.(2.28)−Eq.(2.23)=0. Thus, from this example, we explicitly illustrate the necessacity of the term proportional to $\prod \frac{\sqrt{Z_R}}{\sqrt{Z_{os}}}$ at the one-loop level.

In order to account for the contribution from the ratio of the propagators $\prod \frac{p^2 - m_{os}^2}{p^2 - m_R^2}$, we need to keep the mass of the quark m_q . The Born matrix element squared is

$$|\mathcal{M}_B(m_q)|^2 = \frac{2N_c e^2}{3c_w^2 s_w^2} \left[(I_3^q)^2 (m_Z^2 - m_q^2) - 2I_3^q Q_q s_w^2 (m_Z^2 + 2m_q^2) + 2Q_q^2 s_w^4 (m_Z^2 + 2m_q^2) \right]. \quad (2.30)$$

For simplicity, we just keep trace of the leading pole in $\frac{1}{p^2 - m_{q,\overline{\text{MS}}}^2}$ and the contribution of the ratio in propagators should be taken in to cancel the leading pole. The sum of the diagrams Figs.(1b,1c,1e,1f) is

$$-C_F \frac{2\alpha_s}{\pi} \left(3 \log \frac{m_q^2}{\mu^2} - 4 \right) \frac{1}{p^2 - m_{q,\overline{\text{MS}}}^2} |\overline{\mathcal{M}}_B|^2 + \mathcal{O}(1). \quad (2.31)$$

On the other hand, the ratio of the propagator can be decomposed into

$$\frac{p^2 - m_q^2}{p^2 - m_{q,\overline{\text{MS}}}^2} = 1 - \frac{m_q^2 - m_{q,\overline{\text{MS}}}^2}{p^2 - m_{q,\overline{\text{MS}}}^2} = 1 - (m_q + m_{q,\overline{\text{MS}}}) \frac{\delta m_{\overline{\text{MS}}} - \delta m_{os}}{p^2 - m_{q,\overline{\text{MS}}}^2}, \quad (2.32)$$

where at one-loop level,

$$\begin{aligned} \delta m_{\overline{\text{MS}}} &= -3C_F m_q \frac{\alpha_s}{4\pi} \left(\frac{1}{\epsilon_{\text{UV}}} - \gamma_E + \log 4\pi \right), \\ \delta m_{os} &= -3C_F m_q \frac{\alpha_s}{4\pi} \left(\frac{1}{\epsilon_{\text{UV}}} - \gamma_E + \log 4\pi + \log \frac{\mu^2}{m_q^2} + \frac{4}{3} \right). \end{aligned} \quad (2.33)$$

Then, it contributes an extra term

$$\begin{aligned} &2 \times \left[-2 \times (m_q + m_{q,\overline{\text{MS}}}) \frac{\delta m_{\overline{\text{MS}}} - \delta m_{os}}{p^2 - m_{q,\overline{\text{MS}}}^2} \right] |\overline{\mathcal{M}}_B|^2 \\ &= -C_F \frac{2\alpha_s}{\pi} \left(-3 \log \frac{m_q^2}{\mu^2} + 4 \right) \frac{1}{p^2 - m_{q,\overline{\text{MS}}}^2} |\overline{\mathcal{M}}_B|^2 + \mathcal{O}(1), \end{aligned} \quad (2.34)$$

and it cancels the term in Eq.(2.31).

3. Complex Mass Scheme

However, in the usual perturbative QFT, one encounters the difficulty to handle scattering processes intermediated with unstable particles, such as EW gauge bosons and top quark in the Standard Model theory. It is known for a long time that unitarity on the Hilbert space guarantees only when all of the asymptotic states are stable [4]. A proper treatment of unstable particles in the perturbative scattering amplitude requires a summation of two-point 1PI Feynman diagrams and introduces in a complex pole [5–9] in the denominator of Feynman propagators. However, a naive summation of such self-energy diagrams might violate the gauge invariant in a perturbative theory [10–12].

Despite the fact that there is no fully established treatment of unstable particles in perturbative theories, such issue is usually overlooked since the widths of unstable particles are usually small compared to their masses, in which case the leading approximation (“narrow width approximation”) is frequently applied to calculate physical quantities as long as the dressed propagators [13] are well approximated by the Breit-Wigner (BW) distribution [14]

$$\frac{1}{(p^2 - M^2)^2 + M^2 \Gamma^2}. \quad (3.1)$$

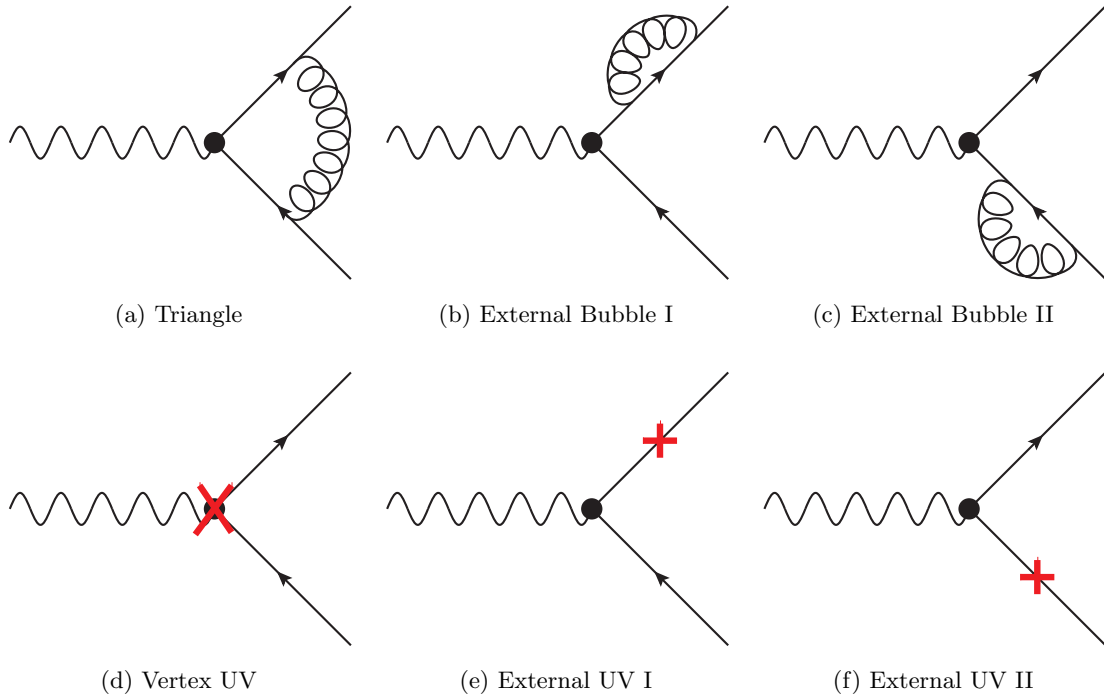


Figure 1: One-loop Feynman diagrams and UV counter terms for $Z \rightarrow q\bar{q}$.

However, finite width effects cannot be ignored anymore when one considers a precision test or one is interested in exclusive observables like the lineshape.

Two general approaches are introduced to handle the unstable particles in a systematic way, which are usually called as *Complex Mass Scheme* (CMS) [15–17] and *unstable-particle effective theory* [18–20]. In this article, we will only focus on the first method, i.e. *complex mass scheme*. It is an extension of the on-shell renormalization scheme. The complex mass and field renormalization constant for the unstable particle field is defined from the residue of the Dyson-summed propagator

$$\frac{i}{p^2 - M_0^2 + \Sigma(p^2)}, \quad (3.2)$$

which is demonstrated in the following way

$$\begin{aligned} m_{cm.s}^2 &= M^2 - i\Gamma M, \\ m_{cm.s}^2 &= M_0^2 - \Sigma(m_{cm.s}^2), \\ \delta Z_{cm.s} &= -\Sigma'(p^2)|_{p^2=m_{cm.s}^2}. \end{aligned} \quad (3.3)$$

The Feynman integrals appearing in self-energy contribution $\Sigma(p^2)$ are defined in the second Riemann sheet [9]. The CMS is a fully gauge-invariant method and it can be applied straightforwardly to the whole phase space. Hence, it is much suitable to realize automation in higher-order calculations. Since the scheme is only a reparameterization of the bare Lagrangian, gauge invariance is assured. However, due to the introduction of complex parameters in CMS, one should concern the unitarity order by order. The perturbative unitarity issue in CMS has already been discussed in Refs. [21, 22].

Since the bare Lagrangian does not change in CMS, in the following we will concern on how to recover the results in CMS to those in on-shell renormalization scheme. From Eq.(3.3), we understand that

$$\begin{aligned} M^2 &= M_0^2 - \text{Re}\Sigma(M^2 - i\Gamma M), \\ \Gamma &= \frac{\text{Im}\Sigma(M^2 - i\Gamma M)}{M}. \end{aligned} \quad (3.4)$$

Since the Feynman prescription $+i\varepsilon$ in $p^2 = p^2 + i\varepsilon$ changes to $-i\varepsilon$ when $\Gamma \rightarrow 0^+$, one should perform the integration in the second Riemann sheet. The second equation in Eq.(3.4) can be thought as the optical theorem for unstable particles. Because no bare parameter enters in Γ , one can think the width Γ is a physical observable that can be obtained in perturbative computation as long as the coupling is weak. In the Standard Model, the relevant unstable particles are electroweak bosons, Higgs bosons and the heavy fermions. At leading order, we have

$$\frac{\Gamma}{M} = \mathcal{O}(\alpha). \quad (3.5)$$

The only way to make a comparison between CMS and on-shell renormalization scheme is by performing coupling constant expansion both in the amplitude and the width Γ .

For simplicity, we only perform the one-loop level comparison though some arguments can be applied to higher orders. Since no sign of the Feynman prescription changes in the loop integrals in CMS and on-shell scheme, the contribution of the one-loop Feynman diagrams in both schemes are the same when taking $\Gamma \rightarrow 0^+$, because no internal loop propagator can be on-shell. Hence, the only difference can be a higher order contribution because of Eq.(3.5). The only relevant

3.1 A useful expansion

$$\begin{aligned} \frac{1}{(s - M^2)^2 + \Gamma^2 M^2} &= \frac{\pi}{\Gamma M} \delta(s - M^2) + \mathcal{P} \left(\frac{1}{(s - M^2)^2} \right)_{M^2} \\ &\quad - \frac{\pi \Gamma M}{2} \delta(s - M^2) \frac{\partial^2}{\partial s^2} + \mathcal{O} \left(\left(\frac{\Gamma}{M} \right)^2 \right), \end{aligned} \quad (3.6)$$

where $\mathcal{P} \left(\frac{1}{(s - M^2)^2} \right)_{M^2}$ is the principle integral

$$\begin{aligned} &\int_{s_{\min}}^{s_{\max}} ds \mathcal{P} \left(\frac{1}{(s - M^2)^2} \right)_{M^2} f(s) \\ &= \int_{s_{\min}}^{M^2-} ds \left(\frac{1}{(s - M^2)^2} \right) f(s) + \int_{M^2+}^{s_{\max}} ds \left(\frac{1}{(s - M^2)^2} \right) f(s). \end{aligned} \quad (3.7)$$

3.2 Spin decorrelation in Narrow-Width Approximation

Let us consider a process with resonant massive vector boson. In the narrow-width approximation, we have the amplitude squared to be

$$|\mathcal{A}|^2 = |\mathcal{A}_p^\mu (-g_{\mu\nu} + \frac{q_\mu q_\nu}{M^2}) \mathcal{A}_d^\nu|^2 \frac{1}{(q^2 - M^2)^2 + \Gamma^2 M^2}. \quad (3.8)$$

The spin-averaged amplitude square is

$$\overline{|\mathcal{A}|^2} = \left[\mathcal{A}_p^\mu (-g_{\mu\nu} + \frac{q_\mu q_\nu}{M^2}) \mathcal{A}_p^{\nu*} \right] \times \frac{1}{3} \left[\mathcal{A}_d^\alpha (-g_{\alpha\beta} + \frac{q_\alpha q_\beta}{M^2}) \mathcal{A}_d^{\beta*} \right]. \quad (3.9)$$

The phase space measure

$$d\Phi_n(\mathbf{P} \rightarrow \mathbf{k}_1, \dots, \mathbf{k}_n) = (2\pi)^4 \delta^{(4)}(\mathbf{P} - \sum_{i=1}^n \mathbf{k}_i) \prod_{i=1}^n \frac{d^3 \tilde{\mathbf{k}}_i}{(2\pi)^3 2E_i} \quad (3.10)$$

can be factorized as (without losing generality, we assume $q = k_1 + k_2$)

$$d\Phi_n(\mathbf{P} \rightarrow \mathbf{k}_1, \dots, \mathbf{k}_n) = d\Phi_{n-1}(\mathbf{P} \rightarrow \mathbf{q}, \mathbf{k}_3, \dots, \mathbf{k}_n) \times \frac{d\mathbf{q}^2}{2\pi} \times d\Phi_2(\mathbf{q} \rightarrow \mathbf{k}_1, \mathbf{k}_2). \quad (3.11)$$

Then, after expanding the Breit-Wigner distribution, we have

$$\begin{aligned} d\Phi_n(\mathbf{P} \rightarrow \mathbf{k}_1, \dots, \mathbf{k}_n) |\mathcal{A}|^2 &= d\Phi_{n-1}(\mathbf{P} \rightarrow \mathbf{q}, \mathbf{k}_3, \dots, \mathbf{k}_n) d\Phi_2(\mathbf{q} \rightarrow \mathbf{k}_1, \mathbf{k}_2) \\ &\times \left. \frac{|\mathcal{A}_p^\mu (-g_{\mu\nu} + \frac{q_\mu q_\nu}{M^2}) \mathcal{A}_d^\nu|^2}{2\Gamma M} \right|_{q^2=M^2}. \end{aligned} \quad (3.12)$$

The difference

$$\Delta = \int d\Phi_2(\mathbf{q} \rightarrow \mathbf{k}_1, \mathbf{k}_2) \left(|\mathcal{A}_p^\mu (-g_{\mu\nu} + \frac{\mathbf{q}_\mu \mathbf{q}_\nu}{M^2}) \mathcal{A}_d^\nu|^2 - \overline{|\mathcal{A}|^2} \right) \quad (3.13)$$

is Lorentz invariant. Hence, we can work it in the rest frame of q , i.e. $q = (M, \vec{0})$. Then,

$$\Delta = \int \frac{|\vec{k}_1|^2 d|\vec{k}_1|}{2E_1} \delta(M - E_1 - E_2) \int d\Omega_1 \left(|\mathcal{A}_p^\mu (-g_{\mu\nu} + \frac{q_\mu q_\nu}{M^2}) \mathcal{A}_d^\nu|^2 - \overline{|\mathcal{A}|^2} \right) \Big|_{\vec{k}_1 + \vec{k}_2 = \vec{0}}. \quad (3.14)$$

The $(-g_{\mu\nu} + \frac{q_\mu q_\nu}{M^2})$ in the rest frame is a diagonal matrix $(0, 1_3)$. Since the decay amplitude $\mathcal{A}_d^\nu = (\mathcal{A}_d^0, \vec{\mathcal{A}}_d)$ is a Lorentz vector, $\vec{\mathcal{A}}_d$ must be proportional to \vec{k}_1 because there is no other independent vector in the decay process when $q = (M, \vec{0})$. Take the direction of the production amplitude $\vec{\mathcal{A}}_p$ to be z axis. We have

$$\begin{aligned} |\mathcal{A}_p^\mu (-g_{\mu\nu} + \frac{q_\mu q_\nu}{M^2}) \mathcal{A}_d^\nu|^2 &= |\vec{\mathcal{A}}_p \cdot \vec{\mathcal{A}}_d|^2 = |\vec{\mathcal{A}}_p|^2 |\vec{\mathcal{A}}_d|^2 \cos^2 \theta_1, \\ \overline{|\mathcal{A}|^2} &= \frac{1}{3} |\vec{\mathcal{A}}_p|^2 |\vec{\mathcal{A}}_d|^2. \end{aligned} \quad (3.15)$$

The integration of the solid angle of Ω_1 to be zero because of

$$|\vec{\mathcal{A}}_p|^2 |\vec{\mathcal{A}}_d|^2 \int d\phi_1 \int_{-1}^1 d\cos \theta_1 \left(\cos^2 \theta_1 - \frac{1}{3} \right) = 0. \quad (3.16)$$

Hence, we prove the spin decorrelation of amplitudes in NWA.

3.3 A general cancellation in the total cross section

The narrow width approximation (NWA) is defined in the usual way, i.e. the total cross section in NWA is the production cross section multiplied with the branching ratio of the decay channel.

Let us consider a process of $e^+\nu_e \rightarrow W^+ \rightarrow \mu^+\nu_\mu$. The comparison of NWA and CMS is the amplitude square by multiplying $(q^2 - M_W^2)^2$. In this section, we will demonstrate that the difference of

$$(q^2 - M_W^2)^2 |\mathcal{A}_{\text{CMS}}|^2 - (q^2 - M_W^2)^2 |\mathcal{A}_{\text{NWA}}|^2 \quad (3.17)$$

is a pure high-order effect after spin decorrelation. At leading order (LO), it is easy to see already from the previous discussion. At next-to-leading order (NLO), we have three classes of topologies in the virtual with CMS. The first one is the factorizable part

$$\begin{aligned} \mathcal{A}_{\text{CMS,Virtual}} &= \text{Diagram 1} + \text{Diagram 2} \\ &= \mathcal{A}_{\text{CMS,Virtual,p}}^\mu \left(-g_{\mu\nu} + \frac{q_\mu q_\nu}{M^2} \right) \mathcal{A}_{\text{CMS,Born,d}}^\nu \\ &+ \mathcal{A}_{\text{CMS,Born,p}}^\mu \left(-g_{\mu\nu} + \frac{q_\mu q_\nu}{M^2} \right) \mathcal{A}_{\text{CMS,Virtual,d}}^\nu, \end{aligned} \quad (3.18)$$

where we have suppressed the W propagator $\frac{1}{(q^2 - M_W^2) - i\Gamma_W M_W}$. Here virtual includes the triangle loop diagrams and the corresponding UV to the vertex. Up to NLO, we only need to keep the first expansion term in Eq.(3.6). Similar to the strategy in the previous section, we can perform the angular integration of μ^+ and ν_μ to get rid of spin correlation between the production and decay amplitudes. After multiplying the Born amplitude, we get a form in the NWA approximation, i.e.

$$2\Re \mathcal{A}_{\text{CMS,Virtual}} \mathcal{A}_{\text{CMS,Born}}^* = \frac{1}{3} [\sigma_{\text{Virtual,p}} \sigma_{\text{Born,d}} + \sigma_{\text{Born,p}} \sigma_{\text{Virtual,d}}], \quad (3.19)$$

where

$$\begin{aligned} \sigma_{\text{Virtual,p/d}} &= 2\Re \left\{ \mathcal{A}_{\text{CMS,Virtual,p/d}}^\mu \left(-g_{\mu\nu} + \frac{q_\mu q_\nu}{M^2} \right) \mathcal{A}_{\text{CMS,Born,p/d}}^{\nu*} \right\}, \\ \sigma_{\text{Born,p/d}} &= \left| \mathcal{A}_{\text{CMS,Born,p/d}}^\mu \left(-g_{\mu\nu} + \frac{q_\mu q_\nu}{M^2} \right) \mathcal{A}_{\text{CMS,Born,p/d}}^{\nu*} \right|. \end{aligned} \quad (3.20)$$

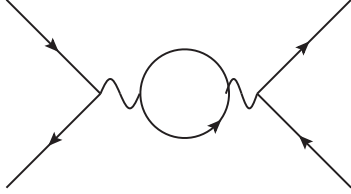
We have suppressed ‘‘CMS’’ in σ because the remaining width effect is a pure higher-order effect³. The argument is valid also for the corresponding real radiation topology following the same argument.

The non-trivial topology is the bubble/tadpole as well as W mass and wavefunction renormalization diagrams⁴. There are two W propagators in the corresponding virtual

³Actually, the W wavefunction renormalization constant in CMS is different to that in NWA. The imaginary part of the difference is not a higher-order effect. Let us keep it in mind.

⁴If we substitute difference of the wavefunction renormalization constant in CMS and NWA from the first class of topology, we can safely replace the wavefunction renormalization constant in CMS to be that in NWA, and then the difference in the first topology would be a pure higher-order effect.

diagrams. The amplitude would be



$$= \mathcal{A}_{\text{CMS,Born,p}}^\mu \left(-g_{\mu\nu} + \frac{q_\mu q_\nu}{M^2} \right) \frac{i}{(q^2 - M_W^2) - i\Gamma_W M_W} i\Sigma \mathcal{A}_{\text{CMS,Born,d}}^\nu, \quad (3.21)$$

where we have suppressed one W propagator $\frac{i}{(q^2 - M_W^2) - i\Gamma_W M_W}$, which will contribute to the Breit-Wigner distribution after multiplying the Born amplitude in CMS. The loop contribution to two-point Green function Σ would be $\Sigma(q^2 + i0)$ and the W mass renormalization is $-\Sigma(M_W^2 - i\Gamma_W M_W)$. After including the difference of wavefunction renormalization from the first class topology, we have the W wavefunction renormalization to be $\delta Z_{\text{os}}^W = -\Re\Sigma'(M_W^2 + i0)$. Remember that the on-shell condition makes sure that⁵

$$\Re\Sigma(q^2 + i0) = \Re\Sigma(M_W^2 + i0) + \Re\Sigma'(M_W^2 + i0)(q^2 - M_W^2) + \mathcal{O}((q^2 - M_W^2)^2). \quad (3.22)$$

Hence, the first and the second term in the real part of the loop contribution cancels the NWA W mass and wavefunction renormalization. The $\mathcal{O}((q^2 - M_W^2)^2)$ only contributes to higher-order term since there is no $\frac{1}{\Gamma_W}$ enhancement but it has an α suppression⁶. Therefore in CMS, the remaining term would be⁷

$$\begin{aligned} & \Sigma(q^2 + i0) - \Sigma(M_W^2 - i\Gamma_W M_W) - \Re\Sigma'(M_W^2 + i0)|_{s_w^2 \rightarrow \Re s_w^2, c_w^2 \rightarrow \Re c_w^2} (q^2 - M_W^2 + i\Gamma_W M_W) \\ &= i\Im\Sigma(q^2 + i0) - (\Sigma(M_W^2 - i\Gamma_W M_W) - \Re\Sigma(M_W^2 + i0)) - i\Gamma_W M_W \Re\Sigma'(M_W^2 + i0)|_{s_w^2 \rightarrow \Re s_w^2, c_w^2 \rightarrow \Re c_w^2} \\ &= i\Im\Sigma(M_W^2 + i0) + i\Im\Sigma'(M_W^2 + i0)(q^2 - M_W^2) + \mathcal{O}((q^2 - M_W^2)^2) \\ &\quad - (i\Im\Sigma(M_W^2 + i0) - i\Gamma_W M_W \Im\Sigma'(M_W^2 + i0)|_{s_w^2 \rightarrow \Re s_w^2, c_w^2 \rightarrow \Re c_w^2} + \mathcal{O}(\alpha^3)) \\ &= i\Im\Sigma'(M_W^2 + i0)(q^2 - M_W^2) + i\Gamma_W M_W \Im\Sigma'(M_W^2 + i0)|_{s_w^2 \rightarrow \Re s_w^2, c_w^2 \rightarrow \Re c_w^2} \\ &\quad + \mathcal{O}(\alpha^3) + \mathcal{O}(\alpha)\mathcal{O}((q^2 - M_W^2)^2) \\ &= [i\Im\Sigma'(M_W^2 + i0)(q^2 - M_W^2 + i\Gamma_W M_W)]|_{s_w^2 \rightarrow \Re s_w^2, c_w^2 \rightarrow \Re c_w^2} + \mathcal{O}(\alpha^3) \\ &= i\frac{\Gamma_W}{M_W}(q^2 - M_W^2 + i\Gamma_W M_W) + \mathcal{O}(\alpha^3). \end{aligned} \quad (3.23)$$

This contribution is a pure imaginary contribution, which should be zero if there is no imaginary part in the Born amplitude, such as in a $2 \rightarrow 2$ process. Here, except the last equation, Γ_W is not necessary to be the exact decay width as long as it is $\mathcal{O}(\alpha)$. In the

⁵There might still remaining some terms that coming from the expansion of the coupling c_w^2 . However, such remaining term will cancel with the coupling effect in the corresponding UV.

⁶Remember that the LO is $\frac{\alpha^2 M_W}{\Gamma_W} \sim \alpha$ and the NLO should be α^2 .

⁷The effect from the complex coupling c_w^2 will cancel exactly between the loop and UV (also in the imaginary part). The effect from the complex coupling c_w^2 for $\Sigma'(M_W^2 + i0)(q^2 - M_W^2)$ is also a higher-order effect.

NWA,

$$\begin{aligned} & \Sigma(q^2 + i0) - \Re\Sigma(M_W^2 + i0) - \Re\Sigma'(M_W^2 + i0)(q^2 - M_W^2) \\ &= i\Im\Sigma(q^2 + i0) = i\Gamma_W M_W + i\frac{\Gamma_W}{M_W}(q^2 - M_W^2) + \mathcal{O}(\alpha^3), \end{aligned} \quad (3.24)$$

where $s_w^2 \rightarrow \Re s_w^2, c_w^2 \rightarrow \Re c_w^2$ is implied. Again, the imaginary part should be zero if there is no imaginary part in the Born amplitude.

An exception happens when there is one loop propagator can be soft and the other loop propagator to be on-shell, e.g.

$$\begin{aligned} & \sim \Sigma(M_W^2 + i0) \\ & \sim i\frac{\alpha}{\pi^3} B_0(M_W^2 + i0, 0, M_W^2 - i\Gamma_W M_W) \\ &= -\frac{\alpha}{\pi} \left[\frac{1}{\epsilon_{UV}} + \left(2 - \gamma_E - \log \pi + \log \frac{\mu^2}{M_W^2 - i\Gamma_W M_W} \right) \right. \\ & \quad \left. - \frac{i\Gamma_W M_W}{M_W^2} \log \frac{-i\Gamma_W M_W}{M_W^2 - i\Gamma_W M_W} \right]. \end{aligned} \quad (3.25)$$

However, in the UV CT, we take $\Sigma(M_W^2 - i\Gamma_W M_W)$. It will result in missing of $\frac{i\Gamma_W M_W}{M_W^2} \log \frac{-i\Gamma_W M_W}{M_W^2 - i\Gamma_W M_W}$ term, which means such term cannot be cancelled by combining loop+UV. Such term will contribute $\log -\frac{i\Gamma_W}{M_W}$ since its prefactor $i\Gamma_W M_W$ will cancel one of the W propagator when the W is on-shell.

The third topology is the interference term between the production part and the decay part. Such term will contribute a higher-order effect except one the boson in the loop can be soft⁸, i.e.

$$= \mathcal{O}(\alpha^3), \quad (3.26)$$

when there is no loop propagator can be soft. If one propagator can be soft, then we will have a box integral

$$D_0(0, 0, 0, 0, p^2, t, 0, 0, M_W^2 - i\Gamma_W M_W, 0) \propto \frac{1}{(p^2 - M_W^2) + i\Gamma_W M_W}. \quad (3.27)$$

In the soft region, we have the loop integral [23]

$$\left(\frac{p^2 - M_W^2 + i\Gamma_W M_W}{M_W^2 - i\Gamma_W M_W} \right)^{d-4} \frac{1}{(p^2 - M_W^2) + i\Gamma_W M_W} C_0(0, t, 0, 0, 0, 0), \quad (3.28)$$

⁸Remember that here the LO is $\mathcal{O}(\alpha)$ and the NLO is $\mathcal{O}(\alpha^2)$.

which cancels all of the divergences as well as $\log(p^2 - M_W^2 + i\Gamma_W M_W)$ in $D_0(0, 0, 0, 0, p^2, t, 0, 0, M_W^2 - i\Gamma_W M_W, 0)$ in the leading term in the expansion of $p^2 \rightarrow M_W^2$. However, there are still remaining leading terms $\frac{1}{p^2 - M_W^2 + i\Gamma_W M_W}$ left that can never be cancelled. This fact can also be understood from the Feynman Tree Theorem (see e.g. Eq.(22) in Ref. [24]). The singularity term from the on-shell photon propagator can be cancelled with the corresponding contribution from the real emission diagrams. However, there are remaining terms from the on-shell fermion propagator(s) only. All these remaining terms can be thought as the finite-width contributions.

The remaining contribution from Born amplitude squared, i.e.

$$|\mathcal{A}_{\text{CMS,Born,p}}^\mu(-g_{\mu\nu} + \frac{q_\mu q_\nu}{M_W^2 - i\Gamma_W M_W})\mathcal{A}_{\text{CMS,Born,d}}^\nu|^2 \mathcal{P} \frac{1}{(q^2 - M_W^2)^2} \quad (3.29)$$

is a pure finite-width effect, which is also a NLO piece. As long as $\mathcal{A}_{\text{CMS,Born,p/d}}^0$ and $\vec{\mathcal{A}}_{\text{CMS,Born,p/d}}$ have the same phase, the second expansion term of $\frac{\Gamma_W}{M_W}$ in $-g_{\mu\nu} + \frac{q_\mu q_\nu}{M_W^2 - i\Gamma_W M_W}$ is a pure imaginary contribution, which will cancel with its complex conjugate one. The second expansion term in the second class of topology would be zero when $q^2 = M_W^2$ since $q^\mu(-g_{\mu\nu} + \frac{q_\mu q_\nu}{M_W^2 - i\Gamma_W M_W}) = 0$. If $q^2 \neq M_W^2$, the term only contribute to a higher-order piece, i.e. NNLO piece.

3.4 Discussions of the differential distributions

The NWA contribution is defined as the amplitude without any width and the renormalization is performed in the on-shell scheme, i.e. applying real part to all of the renormalization constants.

3.4.1 Non-resonance region

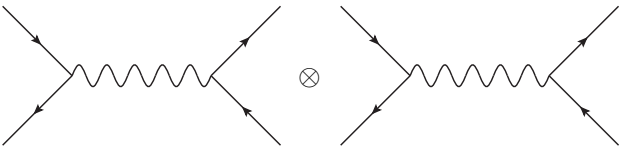
In the region that $|q^2 - M_W^2| \gg \Gamma_W M_W$, the Breit-Wigner distribution can be expanded in $\frac{\Gamma_W M_W}{q^2 - M_W^2}$, i.e.

$$\frac{1}{(q^2 - M_W^2)^2 + \Gamma_W^2 M_W^2} = \frac{1}{(q^2 - M_W^2)^2} \left(1 - \frac{\Gamma_W^2 M_W^2}{(q^2 - M_W^2)^2} + \mathcal{O}(\alpha^4) \right), \quad (3.30)$$

or

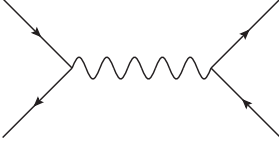
$$\frac{1}{(q^2 - M_W^2) + i\Gamma_W M_W} = \frac{1}{(q^2 - M_W^2)} - i \frac{\Gamma_W M_W}{(q^2 - M_W^2)^2} + \mathcal{O}(\alpha^2). \quad (3.31)$$

In the Born, we need to expand the Breit-Wigner distribution up to second term in R_ξ gauge, i.e.



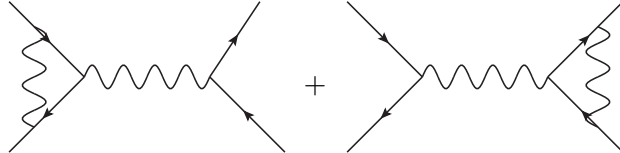
$$\begin{aligned}
&= |\mathcal{A}_{\text{CMS,Born,p}}^\mu \left(-g_{\mu\nu} + (1 - \xi) \frac{q_\mu q_\nu}{q^2 - \xi M_W^2 + \xi i\Gamma_W M_W} \right) \mathcal{A}_{\text{CMS,Born,d}}^{\nu*}|^2 \frac{1}{(q^2 - M_W^2)^2 + \Gamma_W^2 M_W^2} \\
&= \sigma_{\text{Born}}^{\alpha^2} \frac{1}{(q^2 - M_W^2)^2} - \sigma_{\text{Born}}^{\alpha^2} \frac{\Gamma_W^2 M_W^2}{(q^2 - M_W^2)^4} + \mathcal{O}(\alpha^5), \quad (3.32)
\end{aligned}$$

or at the amplitude level



$$\begin{aligned}
&= \mathcal{A}_{\text{CMS,Born,p}}^\mu \left(-g_{\mu\nu} + (1-\xi) \frac{q_\mu q_\nu}{q^2 - \xi M_W^2 + \xi i \Gamma_W M_W} \right) \mathcal{A}_{\text{CMS,Born,d}}^{\nu*} \frac{1}{(q^2 - M_W^2) + i \Gamma_W M_W} \\
&= \mathcal{A}_{\text{CMS,Born,p}}^\mu \left(-g_{\mu\nu} + (1-\xi) \frac{q_\mu q_\nu}{q^2 - \xi M_W^2 + \xi i \Gamma_W M_W} \right) \mathcal{A}_{\text{CMS,Born,d}}^{\nu*} \\
&\times \left[\frac{1}{(q^2 - M_W^2)} - i \frac{\Gamma_W M_W}{(q^2 - M_W^2)^2} + \mathcal{O}(\alpha^2) \right] \\
&= \mathcal{A}_{\text{CMS,Born,p}}^\mu \left(-g_{\mu\nu} + (1-\xi) \frac{q_\mu q_\nu}{q^2 - \xi M_W^2} - (1-\xi) i \frac{\xi \Gamma_W M_W}{q^2 - \xi M_W^2} \frac{q_\mu q_\nu}{q^2 - \xi M_W^2} + \mathcal{O}(\alpha^2) \right) \mathcal{A}_{\text{CMS,Born,d}}^{\nu*} \\
&\times \left[\frac{1}{(q^2 - M_W^2)} - i \frac{\Gamma_W M_W}{(q^2 - M_W^2)^2} + \mathcal{O}(\alpha^2) \right]. \tag{3.33}
\end{aligned}$$

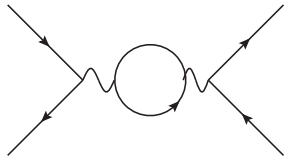
Next, for simplicity, let us work in Feynman gauge, i.e. $\xi = 1$. In the first class of virtual, we only need to keep the first expansion of the W propagator, i.e.



$$\begin{aligned}
&= \left[\mathcal{A}_{\text{CMS,Virtual,p}}^\mu (-g_{\mu\nu}) \mathcal{A}_{\text{CMS,Born,d}}^\nu + \mathcal{A}_{\text{CMS,Born,p}}^\mu (-g_{\mu\nu}) \mathcal{A}_{\text{CMS,Virtual,d}}^\nu \right] \\
&\times \frac{1}{(q^2 - M_W^2)}. \tag{3.34}
\end{aligned}$$

All of the finite-width effect is a pure higher-order effect except the W wavefunction renormalization. Similar argument applies to the third class of the virtual.

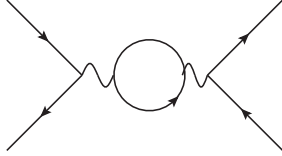
In the second class of virtual, we have



$$\begin{aligned}
&= \mathcal{A}_{\text{CMS,Born,p}}^\mu (-g_{\mu\alpha}) (-g_{\beta\nu}) \mathcal{A}_{\text{CMS,Born,d}}^\nu \frac{1}{(q^2 - M_W^2) + i \Gamma_W M_W} \\
&\times \frac{i}{(q^2 - M_W^2) + i \Gamma_W M_W} i \left[\left(-g_{\alpha\beta} + \frac{q_\alpha q_\beta}{q^2} \right) \Sigma(q^2 + i0) - \frac{q_\alpha q_\beta}{q^2} \Sigma_L(q^2 + i0) \right. \\
&\left. + g_{\alpha\beta} \Sigma(M_W^2 - i \Gamma_W M_W) + g_{\alpha\beta} \Re \Sigma'(M_W^2 + i0) (q^2 - M_W^2 + i \Gamma_W M_W) \right] \tag{3.35}
\end{aligned}$$

where we have replaced the W wavefunction renormalization constant to be the NWA form in the first class of virtual, and take the corresponding contribution into here. Correspond-

ingly, in NWA, we have



$$\begin{aligned}
&= \mathcal{A}_{\text{NWA,Born,p}}^\mu (-g_{\mu\alpha}) (-g_{\beta\nu}) \mathcal{A}_{\text{NWA,Born,d}}^\nu \frac{1}{(q^2 - M_W^2)} \\
&\times \frac{i}{(q^2 - M_W^2)} i \left[\left(-g_{\alpha\beta} + \frac{q_\alpha q_\beta}{q^2} \right) \Sigma(q^2 + i0) - \frac{q_\alpha q_\beta}{q^2} \Sigma_L(q^2 + i0) \right. \\
&\left. + g_{\alpha\beta} \Re \Sigma(M_W^2 + i0) + g_{\alpha\beta} \Re \Sigma'(M_W^2 + i0) (q^2 - M_W^2) \right]. \quad (3.36)
\end{aligned}$$

The difference between Eq.(3.35) and Eq.(3.36) would be proportional to

$$\begin{aligned}
\Sigma(M_W^2 - i\Gamma_W M_W) - \Re \Sigma(M_W^2 + i0) &= i\Im \Sigma(M_W^2 - i0) + \mathcal{O}(\alpha^2) \\
&= i\Gamma_W M_W + \mathcal{O}(\alpha^2). \quad (3.37)
\end{aligned}$$

The expansion of $\frac{\Gamma_W}{M_W}$ in the other pieces is just adding a higher-order effect. Then, Eq.(3.35)–Eq.(3.36) is

$$\mathcal{A}_{\text{CMS,Born,p}}^\mu (-g_{\mu\nu}) \mathcal{A}_{\text{CMS,Born,d}}^\nu \frac{i\Gamma_W M_W}{(q^2 - M_W^2)^2}, \quad (3.38)$$

where we used the fact that the difference between $\mathcal{A}_{\text{CMS,Born,p/d}}^\mu$ and $\mathcal{A}_{\text{NWA,Born,p/d}}^\mu$ in the above equation would only result in a higher-order effect. The above term just cancels the term $-i\frac{\Gamma_W M_W}{(q^2 - M_W^2)^2}$ in Eq.(3.33). In this case, one has to make sure that the LO width is exactly correct to guarantee the cancellation.

The amplitude level cross check can be performed in the non-resonance region after including the Born and virtual contributions.

Method of cross check: In order to avoid the complication of color-structure and helicity dependence of the amplitude, we are trying to multiply the amplitude with the corresponding complex-conjugated Born amplitude and to avoid to adding its complex-conjugated piece. In general, we want to obtain the to be checked piece via

$$\mathcal{A}_{\text{Virtual}}^X \mathcal{A}_{\text{Born}}^{X*}, \quad (3.39)$$

where $X=\text{CMS}$ or NWA . In a $2 \rightarrow 2$ process up to an arbitrary phase, we know one can have

$$\Im \mathcal{A}_{\text{Born}}^{\text{NWA}} = 0, \quad (3.40)$$

and

$$\begin{aligned}
\Re \mathcal{A}_{\text{Born}}^{\text{CMS}} &= \Re \mathcal{A}_{\text{Born}}^{\text{NWA}} (1 + \mathcal{O}(\alpha)), \\
\Im \mathcal{A}_{\text{Born}}^{\text{CMS}} &= \Re \mathcal{A}_{\text{Born}}^{\text{NWA}} \mathcal{O}(\alpha).
\end{aligned} \quad (3.41)$$

The cancellation guarantees that

$$\begin{aligned}
\Re \mathcal{A}_{\text{Virtual/UV}}^{\text{CMS}} &= \Re \mathcal{A}_{\text{Virtual/UV}}^{\text{NWA}} (1 + \mathcal{O}(\alpha)), \\
\Im \mathcal{A}_{\text{Virtual/UV}}^{\text{CMS}} &= \Im \mathcal{A}_{\text{Virtual/UV}}^{\text{NWA}} (1 + \mathcal{O}(\alpha)) - \Im \mathcal{A}_{\text{Born}}^{\text{CMS}}.
\end{aligned} \quad (3.42)$$

Remember that $\mathcal{A}_{\text{Virtual/UV}}^X \sim \Re \mathcal{A}_{\text{Born}}^X \mathcal{O}(\alpha)$. Up to NLO accuracy, we have

$$\begin{aligned} \Re(\mathcal{A}_{\text{Virtual}}^{\text{NWA}} \mathcal{A}_{\text{Born}}^{\text{NWA}*}) &= \Re \mathcal{A}_{\text{Virtual}}^{\text{NWA}} \Re \mathcal{A}_{\text{Born}}^{\text{NWA}} (1 + \mathcal{O}(\alpha)) \\ &= \Re \mathcal{A}_{\text{Virtual}}^{\text{CMS}} \Re \mathcal{A}_{\text{Born}}^{\text{CMS}} (1 + \mathcal{O}(\alpha)) \\ &= \Re(\mathcal{A}_{\text{Virtual}}^{\text{CMS}} \mathcal{A}_{\text{Born}}^{\text{CMS}*}). \end{aligned} \quad (3.43)$$

Hence, the consistent check for the real part of a $2 \rightarrow 2$ process is trivial. On the other hand, the imaginary parts are

$$\begin{aligned} \Im(\mathcal{A}_{\text{Virtual}}^{\text{NWA}} \mathcal{A}_{\text{Born}}^{\text{NWA}*}) &= \Im \mathcal{A}_{\text{Virtual}}^{\text{NWA}} \Re \mathcal{A}_{\text{Born}}^{\text{NWA}} (1 + \mathcal{O}(\alpha)), \\ \Im(\mathcal{A}_{\text{Virtual}}^{\text{CMS}} \mathcal{A}_{\text{Born}}^{\text{CMS}*}) &= \Im \mathcal{A}_{\text{Virtual}}^{\text{CMS}} \Re \mathcal{A}_{\text{Born}}^{\text{CMS}} (1 + \mathcal{O}(\alpha)) \\ &= \Im \mathcal{A}_{\text{Virtual}}^{\text{NWA}} \Re \mathcal{A}_{\text{Born}}^{\text{NWA}} (1 + \mathcal{O}(\alpha)) - \Im \mathcal{A}_{\text{Born}}^{\text{CMS}} \Re \mathcal{A}_{\text{Born}}^{\text{NWA}}. \end{aligned} \quad (3.44)$$

One solution is to add an extra term

$$\Im \mathcal{A}_{\text{Born}}^{\text{CMS}} \mathcal{A}_{\text{Born}}^{\text{NWA}*} = \Im \mathcal{A}_{\text{Born}}^{\text{CMS}} \Re \mathcal{A}_{\text{Born}}^{\text{NWA}} \quad (3.45)$$

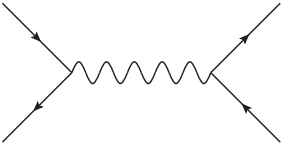
to the CMS one.⁹

However, the situation looks not so simple, because the imaginary part from the coupling constant renormalization (for example $e = \sqrt{4\pi\alpha}$ or in this case Weinberg angles s_w and c_w) can contribute the imaginary part of $\mathcal{A}_{\text{Virtual}}^{\text{CMS}} \mathcal{A}_{\text{Born}}^{\text{CMS}*}$ (which are not necessary to be proportional to $\mathcal{O}(\frac{\Gamma_W}{M_W})$), which should be cancelled out because the coupling constant (at least for e) is factorized out. Hence its imaginary part will not contribute after taking the real of the amplitude squared at NLO level. This situation is not satisfied in $\mathcal{A}_{\text{Virtual}}^{\text{XCMS}} \mathcal{A}_{\text{Born}}^{\text{CMS}*}$, however. We need to take them to be zero at least for the coupling constant renormalization δZ_e .

3.4.2 Resonance region

In the resonance region $|q^2 - M_W^2| \ll \Gamma_W M_W$, the expansion of $\frac{\Gamma_W^{\text{NLO}}}{\Gamma_W^{\text{LO}}}$ in $\Gamma_W = \Gamma_W^{\text{LO}} + \Gamma_W^{\text{NLO}}$ is necessary to guarantee the NLO accuracy. The NWA in this region is ill-defined. However, the NWA amplitude is still well-defined by multiplying $\frac{(q^2 - M_W^2)}{i\Gamma_W M_W}$ and it can be used to compare with the CMS amplitude square in this region.

In CMS, we have the Born amplitude



$$\begin{aligned} &= \mathcal{A}_{\text{CMS,Born,p}}^\mu \left(-g_{\mu\nu} + \frac{q_\mu q_\nu}{M_W^2 - i\Gamma_W M_W} \right) \mathcal{A}_{\text{CMS,Born,d}}^{\nu*} \frac{1}{i\Gamma_W M_W} \\ &= \mathcal{A}_{\text{CMS,Born,p}}^\mu \left(-g_{\mu\nu} + \frac{q_\mu q_\nu}{M_W^2} + i \frac{\Gamma_W M_W}{M_W^2} \frac{q_\mu q_\nu}{M_W^2} + \mathcal{O}(\alpha^2) \right) \mathcal{A}_{\text{CMS,Born,d}}^{\nu*} \frac{1}{i\Gamma_W M_W}. \end{aligned} \quad (3.46)$$

⁹However, the situation would be more complicated because there is also imaginary part from the Weinberg angles s_w and c_w . One should keep these imaginary part in $\mathcal{A}_{\text{Born}}^{\text{NWA}*}$ but only take $M_W^2 - i\Gamma_W M_W$ to be M_W^2 in the W propagator.

while in NWA, it is

$$\begin{aligned}
& \frac{(q^2 - M_W^2)}{i\Gamma_W M_W} \times \text{Diagram} \\
& = \mathcal{A}_{\text{NWA,Born,p}}^\mu \left(-g_{\mu\nu} + \frac{q_\mu q_\nu}{M_W^2} \right) \mathcal{A}_{\text{NWA,Born,d}}^{\nu*} \frac{1}{i\Gamma_W M_W}, \quad (3.47)
\end{aligned}$$

Let us consider the non-trivial second class of virtual topology. In this region, the Eq.(3.35) in unitarity gauge becomes

$$\begin{aligned}
& \text{Diagram} \\
& = \mathcal{A}_{\text{CMS,Born,p}}^\mu \left(-g_{\mu\alpha} + \frac{q_\mu q_\alpha}{M_W^2 - i\Gamma_W M_W} \right) \\
& \quad \times \left(-g_{\beta\nu} + \frac{q_\beta q_\nu}{M_W^2 - i\Gamma_W M_W} \right) \mathcal{A}_{\text{CMS,Born,d}}^\nu \frac{1}{i\Gamma_W M_W} \\
& \quad \times \frac{i}{i\Gamma_W M_W} i \left[\left(-g_{\alpha\beta} + \frac{q_\alpha q_\beta}{M_W^2} \right) \Sigma(M_W^2 + i0) - \frac{q_\alpha q_\beta}{M_W^2} \Sigma_L(M_W^2 + i0) \right. \\
& \quad \left. + g_{\alpha\beta} \Sigma(M_W^2 - i\Gamma_W M_W) + g_{\alpha\beta} \Re \Sigma'(M_W^2 + i0)(i\Gamma_W M_W) \right]. \quad (3.48)
\end{aligned}$$

With $q^\mu(-g_{\mu\nu} + \frac{q_\mu q_\nu}{M_W^2}) = 0^{10}$ when $q^2 = M_W^2$, there is a term

$$\Sigma(M_W^2 + i0) - \Sigma(M_W^2 - i\Gamma_W M_W) - \Re \Sigma'(M_W^2 + i0)(i\Gamma_W M_W), \quad (3.49)$$

which can be simplified following the way of Eq.(3.23)

$$i\Im \Sigma'(M_W^2 + i0, s_w^2)(i\Gamma_W M_W) + \mathcal{O}(\alpha^3) = i\Gamma_W^2 + \mathcal{O}(\alpha^3). \quad (3.50)$$

Similarly, the NWA term is

$$\begin{aligned}
& \frac{(q^2 - M_W^2)}{i\Gamma_W M_W} \times \text{Diagram} \\
& = \mathcal{A}_{\text{NWA,Born,p}}^\mu \left(-g_{\mu\alpha} + \frac{q_\mu q_\alpha}{M_W^2} \right) \\
& \quad \times \left(-g_{\beta\nu} + \frac{q_\beta q_\nu}{M_W^2} \right) \mathcal{A}_{\text{NWA,Born,d}}^\nu \frac{1}{i\Gamma_W M_W} \\
& \quad \times \frac{i}{i\Gamma_W M_W} i \left[\left(-g_{\alpha\beta} + \frac{q_\alpha q_\beta}{M_W^2} \right) \Sigma(M_W^2 + i0) - \frac{q_\alpha q_\beta}{M_W^2} \Sigma_L(M_W^2 + i0) \right. \\
& \quad \left. + g_{\alpha\beta} \Sigma(M_W^2 + i0) \right] \times \frac{i\Gamma_W M_W}{q^2 - M_W^2}. \quad (3.51)
\end{aligned}$$

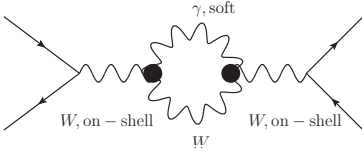
¹⁰It is guaranteed by gauge invariance.

With the help of Eq.(3.24), we simplify the corresponding term to be

$$\begin{aligned}
& \Sigma(q^2 + i0) - \Re\Sigma(M_W^2 + i0) - \Re\Sigma(M_W^2 + i0)(q^2 - M_W^2) \\
&= i\Im\Sigma(q^2 + i0) + \mathcal{O}((q^2 - M_W^2)^2) \\
&= i\Gamma_W M_W + i\Im\Sigma'(M_W^2 + i0)(q^2 - M_W^2) + \mathcal{O}((q^2 - M_W^2)^2). \tag{3.52}
\end{aligned}$$

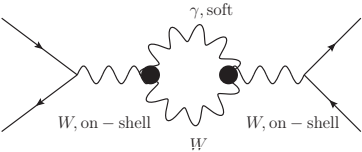
Such realization can be performed with the ε -offshellness method introduced later. One should subtract the $i\Gamma_W M_W$ from the NWA virtual amplitude and then can be compared with the CMS virtual amplitude.

As we already discussed, an exception occurs when there is one loop propagator can be soft and the other loop propagator to be on-shell. For example, in CMS, we have



$$\begin{aligned}
& \sim \Sigma(M_W^2 + i0) \\
& \sim i\frac{\alpha}{\pi^3} B_0(M_W^2 + i0, 0, M_W^2 - i\Gamma_W M_W) \\
&= -\frac{\alpha}{\pi} \left[\frac{1}{\epsilon_{UV}} + \left(2 - \gamma_E - \log \pi + \log \frac{\mu^2}{M_W^2 - i\Gamma_W M_W} \right) \right. \\
& \quad \left. - \frac{i\Gamma_W M_W}{M_W^2} \log \frac{-i\Gamma_W M_W}{M_W^2 - i\Gamma_W M_W} \right]. \tag{3.53}
\end{aligned}$$

However, in the UV CT, we take $\Sigma(M_W^2 - i\Gamma_W M_W)$. It will result in missing of $\frac{i\Gamma_W M_W}{M_W^2} \log \frac{-i\Gamma_W M_W}{M_W^2 - i\Gamma_W M_W}$ term, which means such term cannot be cancelled by combining loop+UV. Such term will contribute $\log -\frac{i\Gamma_W}{M_W}$ since its prefactor $i\Gamma_W M_W$ will cancel one of the W propagator when the W is on-shell. On the other hand, in NWA, we will have

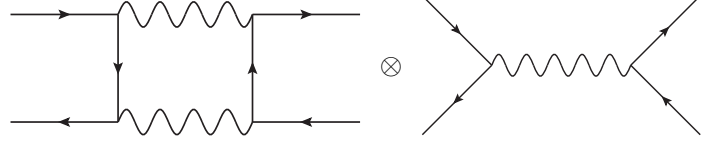


$$\begin{aligned}
& \sim \Sigma(M_W^2 + \varepsilon) \\
& \sim i\frac{\alpha}{\pi^3} B_0(M_W^2 + \varepsilon, 0, M_W^2 - i0) \\
&= -\frac{\alpha}{\pi} \left[\frac{1}{\epsilon_{UV}} + \left(2 - \gamma_E - \log \pi + \log \frac{\mu^2}{M_W^2 - i0} \right) \right. \\
& \quad \left. - \frac{\varepsilon}{M_W^2 + \varepsilon} \log \frac{\varepsilon}{M_W^2 - i0} \right]. \tag{3.54}
\end{aligned}$$

Meanwhile, in the UV CT, we have $\Sigma(M_W^2)$. Hence, the leading term in the expansion of ε in loop+UV would be $\frac{\varepsilon}{M_W^2} \log \frac{\varepsilon}{M_W^2 - i0}$. The prefactor ε cancels with one W propagator. We arrives $\log \frac{\varepsilon}{M_W^2 - i0}$ in NWA. These contributions should be treated properly. For example,

one can take mass in the W mass in the loop to be M_W^2 instead of $M_W^2 - i\Gamma_W M_W$ in CMS and to take ε to be under the on-shell threshold in NWA.

However, in the third class of the topology, we might have the type of

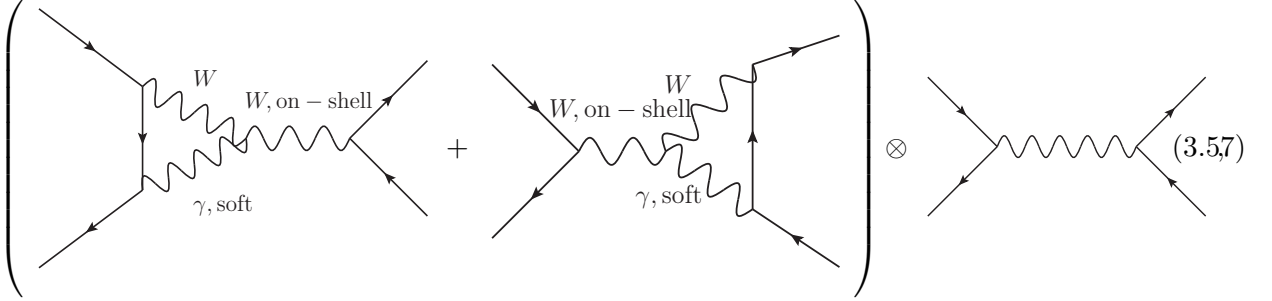


$$(3.55)$$

where one propagator can be soft and it result in a box integral

$$D_0(0, 0, 0, 0, p^2, t, 0, 0, M_W^2 - i\Gamma_W M_W, 0) \propto \frac{1}{(p^2 - M_W^2) + i\Gamma_W M_W}. \quad (3.56)$$

In this case, we will have logarithms like $\log(p^2 - M_W^2 + i\Gamma_W M_W)$ (or in NWA we have $\log \varepsilon$)¹¹. Such logarithms can not be cancelled between CMS and NWA. In the first class of the topology, if the photon loop propagator in the triangle soft

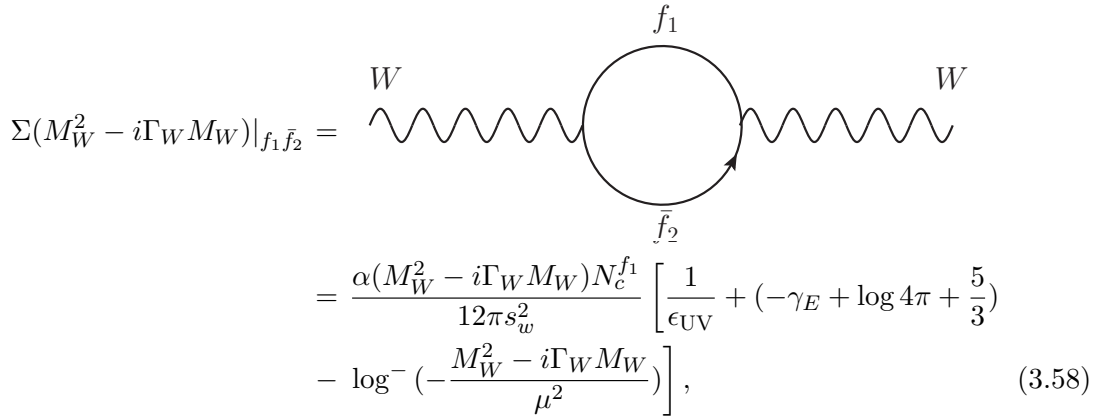


$$(3.57)$$

we will also have logarithms like $\log(p^2 - M_W^2 + i\Gamma_W M_W)$ (or in NWA we have $\log \varepsilon$). All of these type of diagrams should not be included in the following ε -offshellness method.

3.4.3 ε -offshellness method

The ε -offshellness is performed by $\varepsilon = q^2 - M_W^2 \ll \Gamma_W M_W$ and expansion everything in ε .



$$(3.58)$$

¹¹Actually, we will have \log^2 .

where we have defined

$$\log^\pm z = \log z \pm 2i\pi\theta(-\Re z)\theta(\mp\Im z), \quad (3.59)$$

which has the relation

$$\log^\pm z = -\log^\mp \frac{1}{z}. \quad (3.60)$$

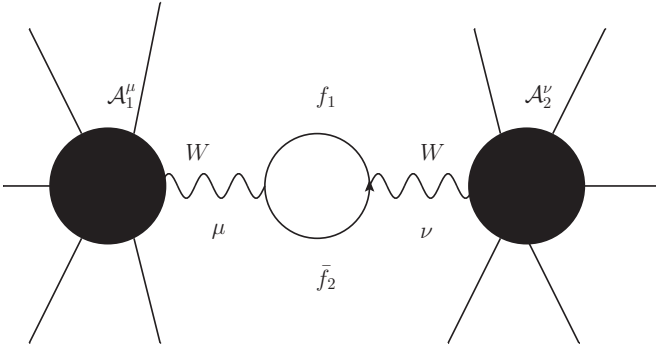
We also have the partial width of $W \rightarrow f_1 \bar{f}_2$

$$\Gamma_W(W \rightarrow f_1 \bar{f}_2) = \frac{\alpha M_W N_c^{f_1}}{12\Re s_w^2}. \quad (3.61)$$

Then, we have

$$\Im\Sigma(M_W^2 - i\Gamma_W M_W)|_{f_1 \bar{f}_2} = \Gamma_W(W \rightarrow f_1 \bar{f}_2) \frac{M_W}{\pi} (-\pi + 2\pi) + \mathcal{O}(\alpha^2). \quad (3.62)$$

Therefore, the extra universal term from this imaginary part when setting W on shell is



$$\begin{aligned}
&= \mathcal{A}_1 \frac{i}{i\Gamma_W(W \rightarrow f_1 \bar{f}_2) M_W} \left[i(-i\Im\Sigma(M_W^2 - i\Gamma_W M_W)|_{f_1 \bar{f}_2}) \right] \\
&\times \frac{i}{i\Gamma_W(W \rightarrow f_1 \bar{f}_2) M_W} \mathcal{A}_2 = \mathcal{A}_1 (+1) \frac{i}{i\Gamma_W(W \rightarrow f_1 \bar{f}_2) M_W} \mathcal{A}_2 \\
&= \mathcal{A}_{\text{Born}}. \quad (3.63)
\end{aligned}$$

After multiplied the conjugated of Born amplitude and take a factor of 2 to the real part of the amplitude square, we have the universal extra term as

$$+2|\mathcal{A}_{\text{Born}}|^2, \quad (3.64)$$

which should be cancelled with the Born term.

In the off-shellness by a small $p^2 = M_W^2 + \varepsilon$, we have the loop contribution

$$\begin{aligned}
\Sigma(M_W^2 + \varepsilon + i0)|_{f_1 \bar{f}_2} &= \text{Diagram: } W \text{ (wavy line) } \rightarrow \text{Circle (loop)} \rightarrow W \text{ (wavy line)} \\
&\quad \text{Top of circle: } f_1, \text{ Bottom: } \bar{f}_2 \\
&= \frac{\alpha(M_W^2 + \varepsilon)N_c^{f_1}}{12\pi\Re s_w^2} \left[\frac{1}{\epsilon_{\text{UV}}} + (-\gamma_E + \log 4\pi + \frac{5}{3}) \right. \\
&\quad \left. - \log\left(-\frac{M_W^2 + \varepsilon + i0}{\mu^2}\right) \right], \tag{3.65}
\end{aligned}$$

while the UV in Narrow-Width Approximation is $-\Re\Sigma(M_W^2 + i0)|_{f_1 \bar{f}_2}$. The sum would be

$$\frac{\varepsilon}{M_W^2} \left[\Re\Sigma(M_W^2 + i0)|_{f_1 \bar{f}_2} - \frac{M_W \Gamma_W(W \rightarrow f_1 \bar{f}_2)}{\pi} \right] + i\Gamma_W(W \rightarrow f_1 \bar{f}_2)M_W \left(1 + \frac{\varepsilon}{M_W^2}\right) \tag{3.66}$$

The UV in Complex-Mass Scheme is $-\Sigma(M_W^2 - i\Gamma_W M_W)|_{f_1 \bar{f}_2}$ with the expansion

$$\begin{aligned}
i\Im\Sigma(M_W^2 - i\Gamma_W M_W)|_{f_1 \bar{f}_2} &= i\Gamma_W(W \rightarrow f_1 \bar{f}_2)M_W - i\frac{\Gamma_W(W \rightarrow f_1 \bar{f}_2)}{M_W} \Re\Sigma(M_W^2 + i0)|_{f_1 \bar{f}_2} \\
&+ i\frac{\Gamma_W(W \rightarrow f_1 \bar{f}_2)}{M_W} \frac{\Gamma_W(W \rightarrow f_1 \bar{f}_2)M_W}{\pi} \\
&- i\frac{\Re c_w^2}{\Re s_w^2} \frac{\Gamma_W(W \rightarrow f_1 \bar{f}_2)}{M_W} \left(1 - \frac{\Gamma_Z}{\Gamma_W(W \rightarrow f_1 \bar{f}_2)} \Re c_w\right) \\
&\times \Re\Sigma(M_W^2 + i0)|_{f_1 \bar{f}_2} + \mathcal{O}(\alpha^3), \tag{3.67}
\end{aligned}$$

and

$$\begin{aligned}
\Re\Sigma(M_W^2 - i\Gamma_W M_W)|_{f_1 \bar{f}_2} &= \Re\Sigma(M_W^2 + i0)|_{f_1 \bar{f}_2} + \Gamma_W(W \rightarrow f_1 \bar{f}_2)^2 \\
&+ \Gamma_W(W \rightarrow f_1 \bar{f}_2)^2 \frac{\Re c_w^2}{\Re s_w^2} \left(1 - \frac{\Gamma_Z}{\Gamma_W(W \rightarrow f_1 \bar{f}_2)} \Re c_w\right) \\
&+ \mathcal{O}(\alpha^3), \tag{3.68}
\end{aligned}$$

where

$$\begin{aligned}
s_w^2 &= 1 - \frac{M_W^2 - i\Gamma_W M_W}{M_Z^2 - i\Gamma_Z M_Z}, \\
\Re s_w^2 &= 1 - \frac{M_W^2}{M_Z^2}, \\
\Re c_w^2 &= 1 - \Re s_w^2. \tag{3.69}
\end{aligned}$$

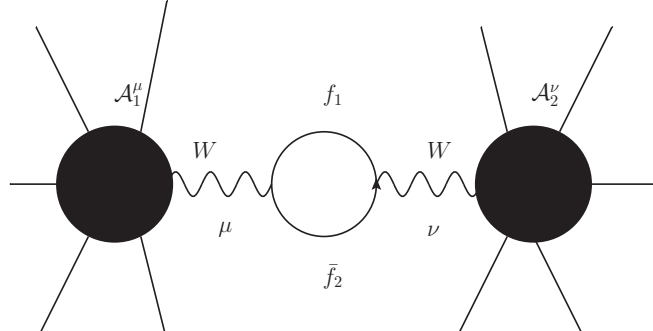
The loop contribution can be expanded as

$$\begin{aligned}
i\Im\Sigma(M_W^2 + i0, s_w^2)|_{f_1\bar{f}_2} &= i\Gamma_W(W \rightarrow f_1\bar{f}_2)M_W \\
&\quad - i\frac{\Re c_w^2}{\Re s_w^2} \frac{\Gamma_W(W \rightarrow f_1\bar{f}_2)}{M_W} \left(1 - \frac{\Gamma_Z}{\Gamma_W(W \rightarrow f_1\bar{f}_2)} \Re c_w\right) \\
&\quad \times \Re\Sigma(M_W^2 + i0)|_{f_1\bar{f}_2} + \mathcal{O}(\alpha^3), \\
\Re\Sigma(M_W^2 + i0, s_w^2)|_{f_1\bar{f}_2} &= \Re\Sigma(M_W^2 + i0)|_{f_1\bar{f}_2} \\
&\quad + \Gamma_W(W \rightarrow f_1\bar{f}_2)^2 \frac{\Re c_w^2}{\Re s_w^2} \left(1 - \frac{\Gamma_Z}{\Gamma_W(W \rightarrow f_1\bar{f}_2)} \Re c_w\right) \\
&\quad + \mathcal{O}(\alpha^3).
\end{aligned} \tag{3.70}$$

After combining UV and loop contributions, we have

$$\begin{aligned}
&- \Gamma_W(W \rightarrow f_1\bar{f}_2)^2 \\
&+ i\frac{\Gamma_W(W \rightarrow f_1\bar{f}_2)}{M_W} \Re\Sigma(M_W^2 + i0)|_{f_1\bar{f}_2} \\
&- i\frac{\Gamma_W(W \rightarrow f_1\bar{f}_2)}{M_W} \frac{\Gamma_W(W \rightarrow f_1\bar{f}_2)M_W}{\pi} + \mathcal{O}(\alpha^3).
\end{aligned} \tag{3.71}$$

In NWA,



$$\begin{aligned}
&= \mathcal{A}_1 \frac{i}{\varepsilon} \left\{ \frac{\varepsilon}{M_W^2} \left[\Re\Sigma(M_W^2 + i0)|_{f_1\bar{f}_2} - \frac{M_W \Gamma_W(W \rightarrow f_1\bar{f}_2)}{\pi} \right] \right. \\
&\quad \left. + i\Gamma_W(W \rightarrow f_1\bar{f}_2)M_W \left(1 + \frac{\varepsilon}{M_W^2}\right) \right\} \\
&\times \frac{i}{\varepsilon} \mathcal{A}_2.
\end{aligned} \tag{3.72}$$

For the $2 \rightarrow 2$, there is no imaginary part and the Born amplitude is¹²

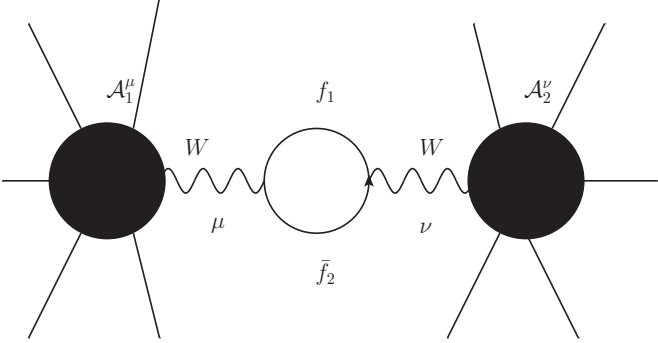
$$\mathcal{A}_{\text{Born}}^{\text{CMS}} \frac{i\Gamma_W M_W}{\varepsilon} = \mathcal{A}_{\text{Born}}^{\text{NWA}} = \mathcal{A}_1 \frac{i}{\varepsilon} \mathcal{A}_2. \tag{3.73}$$

¹²The difference from the coupling $c_w^2 = \frac{M_W^2 - i\Gamma_W M_W}{M_Z^2 - i\Gamma_Z M_Z}$ and $\Re c_w^2 = \frac{M_W^2}{M_Z^2}$ is still possible. However, at the amplitude square level, it would become $|c_w^2|^2 = \frac{M_W^4 + \Gamma_W^2 M_W^2}{M_Z^4 + \Gamma_Z^2 M_Z^2}$ and $\Re c_w^2 = \frac{M_W^4}{M_Z^4}$. The difference is a next-to-next-to-leading order effect.

Hence, we can drop the term $i\Gamma_W(W \rightarrow f_1\bar{f}_2)M_W(1 + \frac{\varepsilon}{M_W^2})$. The final result after multiplying $\varepsilon^2/\Gamma_W^2/M_W^2$ would be

$$\begin{aligned}
& -\frac{1}{M_W^2} \left[\Re\Sigma(M_W^2 + i0)|_{f_1\bar{f}_2} - \frac{M_W\Gamma_W(W \rightarrow f_1\bar{f}_2)}{\pi} \right. \\
& \left. + i\Gamma_W(W \rightarrow f_1\bar{f}_2)M_W \left(\frac{M_W^2}{\varepsilon} + 1 \right) \right] |\mathcal{A}_{\text{Born}}^{\text{CMS}}|^2. \tag{3.74}
\end{aligned}$$

In CMS¹³,



$$\begin{aligned}
& = \mathcal{A}_1 \frac{i}{i\Gamma_W M_W} i \left\{ i \frac{\Gamma_W}{M_W} \Re\Sigma(M_W^2 + i0)|_{f_1\bar{f}_2} \right. \\
& \left. - i \frac{\Gamma_W}{M_W} \frac{\Gamma_W M_W}{\pi} - \Gamma_W^2 + \mathcal{O}(\alpha^3) \right\} \frac{i}{i\Gamma_W M_W} \mathcal{A}_2. \tag{3.75}
\end{aligned}$$

We obtain

$$-\frac{1}{M_W^2} \left[\Re\Sigma(M_W^2 + i0)|_{f_1\bar{f}_2} - \frac{M_W\Gamma_W(W \rightarrow f_1\bar{f}_2)}{\pi} + i\Gamma_W(W \rightarrow f_1\bar{f}_2)M_W \right] |\mathcal{A}_{\text{Born}}^{\text{CMS}}|^2 \tag{3.76}$$

Hence, in general, one should subtract

$$-\frac{i\Gamma_W}{M_W} \frac{M_W^2}{\varepsilon} |\mathcal{A}_{\text{Born}}^{\text{CMS}}|^2 \tag{3.77}$$

from the NWA virtual amplitude squared. Here, we don't need to use the exact width since the comparison does not involve the Born amplitude.

3.5 An example: top quark decay width

In this section, we are trying to determine at which level of the top quark decay width is needed to guarantee the NLO accuracy by demonstrating the top quark decay process, which is already the most complicated decay process in the Standard Model at parton level. From above discussions, we know that in order to guarantee the NLO accuracy in the whole phase space, one should keep the NLO accuracy width at least. For simplify, let us first consider QCD corrections to top quark decay width.

¹³We can drop the term $-\Gamma_W(W \rightarrow f_1\bar{f}_2)^2$ in Eq.(3.71) for a $2 \rightarrow 2$ process but may be not for a $2 \rightarrow n, n > 2$ process, where the amplitude itself has a imaginary part in the same order as the real part.

3.5.1 NLO QCD corrections

There are two loop diagrams in the first class of topology, i.e. the factorized one. We have

$$\begin{aligned}
&= \mathcal{A}_{\text{loop}}^\mu(t \rightarrow bW^+) \left(-g_{\mu\nu} + \frac{p_\mu p_\nu}{M_W^2 - i\Gamma_W M_W} \right) \\
&\times \mathcal{A}_{\text{Born}}^\nu(W^+ \rightarrow f_1 \bar{f}_2) \frac{i}{p^2 - M_W^2 + i\Gamma_W M_W} \quad (3.78)
\end{aligned}$$

and

$$\begin{aligned}
&= \mathcal{A}_{\text{Born}}^\mu(t \rightarrow bW^+) \left(-g_{\mu\nu} + \frac{p_\mu p_\nu}{M_W^2 - i\Gamma_W M_W} \right) \\
&\times \mathcal{A}_{\text{loop}}^\nu(W^+ \rightarrow f_1 \bar{f}_2) \frac{i}{p^2 - M_W^2 + i\Gamma_W M_W}. \quad (3.79)
\end{aligned}$$

Hence, Eq.(3.78) plus its corresponding UV and the real emission diagrams from top quark or bottom quark contribute the NLO QCD corrections to

$$\mathcal{A}_{\text{NLO}}^\mu(t \rightarrow bW^+ + X) \left(-g_{\mu\nu} + \frac{p_\mu p_\nu}{M_W^2 - i\Gamma_W M_W} \right) \mathcal{A}_{\text{Born}}^\nu(W^+ \rightarrow f_1 \bar{f}_2) \frac{i}{p^2 - M_W^2 + i\Gamma_W M_W} \quad (3.80)$$

where $p = p_{f_1} + p_{\bar{f}_2}$. The amplitude squared (after expanding Breit-Wigner distribution and making spin decorrelation) would be

$$|\mathcal{A}_{\text{NLO}}(t \rightarrow bW^+ + X)|^2 |\mathcal{A}_{\text{Born}}(W^+ \rightarrow f_1 \bar{f}_2)|^2 \frac{\pi}{\Gamma_W M_W} \delta(p^2 - M_W^2), \quad (3.81)$$

which after integrating the phase space to f_1 and \bar{f}_2 is

$$|\mathcal{A}_{\text{NLO}}(t \rightarrow bW^+ + X)|^2 \frac{\Gamma_W^{\text{Born}}(W^+ \rightarrow f_1 \bar{f}_2)}{\Gamma_W}. \quad (3.82)$$

Similarly, we have Eq.(3.79) plus its UV and the real emission diagrams from f_1 and \bar{f}_2

$$\mathcal{A}_{\text{Born}}^\mu(t \rightarrow bW^+) \left(-g_{\mu\nu} + \frac{p_\mu p_\nu}{M_W^2 - i\Gamma_W M_W} \right) \mathcal{A}_{\text{NLO}}^\nu(W^+ \rightarrow f_1 \bar{f}_2 + X) \frac{i}{p^2 - M_W^2 + i\Gamma_W M_W} \quad (3.83)$$

where $p = p_t - p_b$. The amplitude squared (after expanding Breit-Wigner distribution and making spin decorrelation) is

$$|\mathcal{A}_{\text{Born}}(t \rightarrow bW^+)|^2 |\mathcal{A}_{\text{NLO}}(W^+ \rightarrow f_1 \bar{f}_2 + X)|^2 \frac{\pi}{\Gamma_W M_W} \delta(p^2 - M_W^2). \quad (3.84)$$

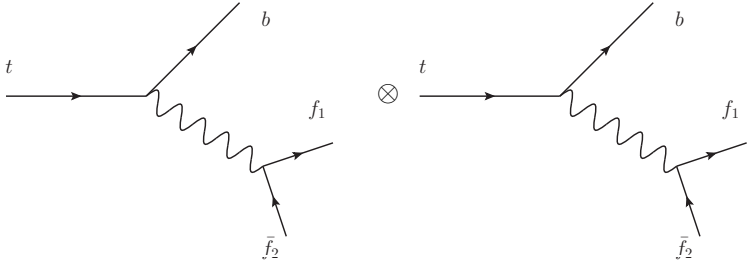
Therefore, one arrives at

$$|\mathcal{A}_{\text{Born}}(t \rightarrow bW^+)|^2 \frac{\Gamma_W^{\text{NLO}}(W^+ \rightarrow f_1 \bar{f}_2 + X)}{\Gamma_W}, \quad (3.85)$$

after phase space integration to f_1, \bar{f}_2 (and the gluon in real). In the above, we take NLO as the pure NLO QCD correction term, which does not include the Born contributions. This form is one can expect from the NLO QCD corrections to top quark decay width in NWA. It means that if one exhausting all possible f_1 and \bar{f}_2 and take Γ_W to be NLO QCD accuracy, we will have

$$\begin{aligned} & \Sigma_{f_1, \bar{f}_2} \left\{ |\mathcal{A}_{\text{Born}}(t \rightarrow bW^+)|^2 \frac{\Gamma_W^{\text{Born}}(W^+ \rightarrow f_1 \bar{f}_2)}{\Gamma_W^{\text{Born}} + \Gamma_W^{\text{NLO}}} + |\mathcal{A}_{\text{NLO}}(t \rightarrow bW^+ + X)|^2 \frac{\Gamma_W^{\text{Born}}(W^+ \rightarrow f_1 \bar{f}_2)}{\Gamma_W^{\text{Born}} + \Gamma_W^{\text{NLO}}} \right. \\ & \left. + |\mathcal{A}_{\text{Born}}(t \rightarrow bW^+)|^2 \frac{\Gamma_W^{\text{NLO}}(W^+ \rightarrow f_1 \bar{f}_2 + X)}{\Gamma_W^{\text{Born}} + \Gamma_W^{\text{NLO}}} \right\} \\ & = |\mathcal{A}_{\text{NLO}}(t \rightarrow bW^+ + X)|^2 \frac{\Gamma_W^{\text{Born}}}{\Gamma_W^{\text{Born}} + \Gamma_W^{\text{NLO}}} + |\mathcal{A}_{\text{Born}}(t \rightarrow bW^+)|^2 \frac{\Gamma_W^{\text{Born}} + \Gamma_W^{\text{NLO}}}{\Gamma_W^{\text{Born}} + \Gamma_W^{\text{NLO}}} \\ & = (|\mathcal{A}_{\text{Born}}(t \rightarrow bW^+)|^2 + |\mathcal{A}_{\text{NLO}}(t \rightarrow bW^+ + X)|^2) + |\mathcal{A}_{\text{NLO}}(t \rightarrow bW^+ + X)|^2 \frac{-\Gamma_W^{\text{NLO}}}{\Gamma_W^{\text{Born}} + \Gamma_W^{\text{NLO}}} \\ & = (|\mathcal{A}_{\text{Born}}(t \rightarrow bW^+)|^2 + |\mathcal{A}_{\text{NLO}}(t \rightarrow bW^+ + X)|^2) + \mathcal{O}(\alpha\alpha_S^2), \end{aligned} \quad (3.86)$$

Hence, we recover the result with NLO QCD corrections in NWA.¹⁴ However, there are still other terms missing in CMS, which can be thought as the pure finite width effects. The first one is the second expansion of the Born amplitude squared, i.e.



$$\begin{aligned} & = |\mathcal{A}_{\text{Born}}(t \rightarrow bW^+)|^2 |\mathcal{A}_{\text{Born}}(W^+ \rightarrow f_1 \bar{f}_2)|^2 \frac{1}{(p^2 - M_W^2)^2 + \Gamma_W^2 M_W^2} \\ & = |\mathcal{A}_{\text{Born}}(t \rightarrow bW^+)|^2 |\mathcal{A}_{\text{Born}}(W^+ \rightarrow f_1 \bar{f}_2)|^2 \left(\frac{\pi}{\Gamma_W M_W} \delta(p^2 - M_W^2) \right. \\ & \left. + \mathcal{P} \left(\frac{1}{(p^2 - M_W^2)^2} \right)_{M_W^2} + \mathcal{O}(\alpha^2) + \mathcal{O}(\alpha\alpha_S) \right). \end{aligned} \quad (3.87)$$

However, because in the Standard Model, the LO W width is $\mathcal{O}(\alpha)$, such finite width effects will not contribute to the result at NLO QCD accuracy but at NLO EW corrections, one should take into account such effect.

¹⁴We have dropped the width dependence from the Weinberg angles s_w, c_w , since they can be factorized out in Born amplitude and the finite width effect in $|s_w|^2$ and $|c_w|^2$ is a NNLO effect.

Due to the color-flow, the interference term of virtual/real gluon exchanging between the $t - b$ fermion line and the $f_1 - \bar{f}_2$ fermion line is zero. Hence, there is no contribution from the third class of topology diagrams in NLO QCD corrections. The second class of topology is zero because W boson is color-singlet.

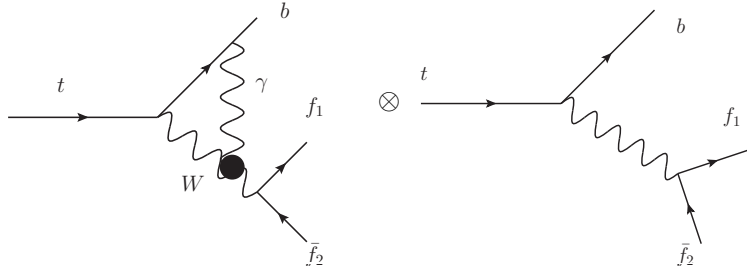
Hence, we have conclusion that: **up to NLO QCD accuracy, we only need to calculate the top quark width in NWA up to NLO QCD level.**

3.5.2 NLO EW corrections

With the same argument in the previous section, for the factorizable topology, we have

$$\begin{aligned}
& \Sigma_{f_1, \bar{f}_2} \left\{ |\mathcal{A}_{\text{Born}}(t \rightarrow bW^+)|^2 \frac{\Gamma_W^{\text{Born}}(W^+ \rightarrow f_1 \bar{f}_2)}{\Gamma_W^{\text{Born}} + \Gamma_W^{\text{NLO}}} + |\mathcal{A}_{\text{NLO}}(t \rightarrow bW^+ + X)|^2 \frac{\Gamma_W^{\text{Born}}(W^+ \rightarrow f_1 \bar{f}_2)}{\Gamma_W^{\text{Born}} + \Gamma_W^{\text{NLO}}} \right. \\
& \left. + |\mathcal{A}_{\text{Born}}(t \rightarrow bW^+)|^2 \frac{\Gamma_W^{\text{NLO}}(W^+ \rightarrow f_1 \bar{f}_2 + X)}{\Gamma_W^{\text{Born}} + \Gamma_W^{\text{NLO}}} \right\} \\
& = |\mathcal{A}_{\text{NLO}}(t \rightarrow bW^+ + X)|^2 \frac{\Gamma_W^{\text{Born}}}{\Gamma_W^{\text{Born}} + \Gamma_W^{\text{NLO}}} + |\mathcal{A}_{\text{Born}}(t \rightarrow bW^+)|^2 \frac{\Gamma_W^{\text{Born}} + \Gamma_W^{\text{NLO}}}{\Gamma_W^{\text{Born}} + \Gamma_W^{\text{NLO}}} \\
& = (|\mathcal{A}_{\text{Born}}(t \rightarrow bW^+)|^2 + |\mathcal{A}_{\text{NLO}}(t \rightarrow bW^+ + X)|^2) + |\mathcal{A}_{\text{NLO}}(t \rightarrow bW^+ + X)|^2 \frac{-\Gamma_W^{\text{NLO}}}{\Gamma_W^{\text{Born}} + \Gamma_W^{\text{NLO}}} \\
& = (|\mathcal{A}_{\text{Born}}(t \rightarrow bW^+)|^2 + |\mathcal{A}_{\text{NLO}}(t \rightarrow bW^+ + X)|^2) + \mathcal{O}(\alpha\alpha_S^2), \tag{3.88}
\end{aligned}$$

up to NLO EW accuracy, where we take NLO as the pure NLO EW correction term here instead. The complication appears in the following diagrams



$$\sim \int d^d q \frac{1}{(q^2 + i0) ((q + p_b)^2 + i0) ((q - p_{f_1} - p_{\bar{f}_2})^2 - M_W^2 + i\Gamma_W M_W)}. \tag{3.89}$$

We consider this Feynman integral via threshold expansion [25]. In the hard region, we know $(q - p_{f_1} - p_{\bar{f}_2})^2 - M_W^2 = q^2 - 2q \cdot (p_{f_1} + p_{\bar{f}_2}) \neq 0$. Hence, the width can be a small parameter to perform the expansion of $\frac{i\Gamma_W M_W}{q^2 + 2q \cdot (p_{f_1} + p_{\bar{f}_2})}$. Hence, the finite width effect is just a higher-order effect. The situation should be taken care of when

$$(q - p_{f_1} - p_{\bar{f}_2})^2 - M_W^2 = q^2 - 2q \cdot (p_{f_1} + p_{\bar{f}_2}) \rightarrow 0. \tag{3.90}$$

The first consideration is the soft region, i.e.

$$q^0 \sim \lambda, |\vec{q}| \sim \lambda, \tag{3.91}$$

where λ is a small parameter. The integral becomes

$$\int d^d q \frac{1}{(q^2 + i0)(2q \cdot p_b + i0)(-2q \cdot (p_{f_1} + p_{\bar{f}_2}) + i\Gamma_W M_W)}. \quad (3.92)$$

One can change the Feynman propagator $G_F(q) = \frac{1}{q^2 + i0}$ to the advanced propagator $G_A(q) = \frac{1}{q^2 + i0q^0}$ via [24]

$$G_A(q) = G_F(q) + 2i\pi\theta(q^0)\delta(q^2), \quad (3.93)$$

which is a direct consequence of the relation

$$\frac{1}{x \pm i0} = \mathcal{P}\left(\frac{1}{x}\right) \mp i\pi\delta(x). \quad (3.94)$$

Hence, Eq.(3.92) becomes

$$\begin{aligned} & \int d^d q \frac{1}{(q^2 + i0q^0)(2q \cdot p_b + i0(q + p_b)^0)(-2q \cdot (p_{f_1} + p_{\bar{f}_2}) + i\Gamma_W M_W)} \\ & - 2i\pi \int d^d q \theta(q^0)\delta(q^2) \frac{1}{(2q \cdot p_b + i0)(-2q \cdot (p_{f_1} + p_{\bar{f}_2}) + i\Gamma_W M_W)} \\ & - 2i\pi \int d^d q \theta((q + p_b)^0)\delta((q + p_b)^2) \frac{1}{(q^2 + i0)(-2q \cdot (p_{f_1} + p_{\bar{f}_2}) + i\Gamma_W M_W)} \end{aligned} \quad (3.95)$$

The first term is zero because all of the residues for q^0 integration are located in the upper-half plane, while the second term will be cancelled by the corresponding real emission diagrams. If the photon is located in the collinear region to p_b , i.e.

$$q \sim \beta p_b + \lambda n, n \cdot p_b = 0, n^2 = -1, \quad (3.96)$$

in such as, however, because of

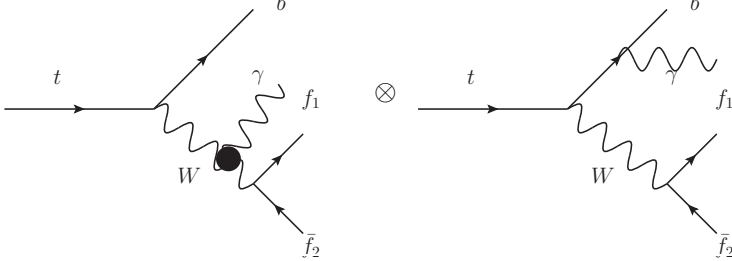
$$\begin{aligned} & (q - p_{f_1} - p_{\bar{f}_2})^2 - M_W^2 = q^2 - 2q \cdot (p_{f_1} + p_{\bar{f}_2}) \\ & = -2\beta p_b \cdot (p_{f_1} + p_{\bar{f}_2}) = -\beta(m_t^2 - M_W^2) \neq 0, \end{aligned} \quad (3.97)$$

the finite width effect is still a higher-order effect.

Let us work in a more direct manner, i.e. to consider the difference

$$\begin{aligned} & \frac{C_0(0, m_t^2, M_W^2, 0, 0, M_W^2 - i\Gamma_W M_W) - C_0(0, m_t^2, M_W^2, 0, 0, M_W^2)}{i\pi^{2-\epsilon}\Gamma(1-\epsilon)^2\Gamma(1+\epsilon)\Gamma(1-2\epsilon)^{-1}} \\ & = -\frac{1}{2(m_t^2 - M_W^2)} \frac{1}{\epsilon_{\text{IR}}} + \frac{1}{2(m_t^2 - M_W^2)} \log\left(-\frac{\Gamma_W^2}{\mu^2}\right) \frac{1}{\epsilon_{\text{IR}}} \\ & + \frac{1}{2(m_t^2 - M_W^2)} \left(-\frac{\pi^2}{2} - \frac{1}{2} \log^2\left(-\frac{\Gamma_W^2}{\mu^2}\right)\right). \end{aligned} \quad (3.98)$$

Correspondingly, the real emission in the soft region would be



$$\begin{aligned}
\text{Real}^\pm(\Gamma_W) &= (2i\pi) \frac{2M_W}{m_t^2 - M_W^2} \int \frac{d^{d-1}\vec{q}}{2|\vec{q}|} \frac{1}{2|\vec{q}|(1 - \cos\theta) (-2|\vec{q}|M_W \pm i\Gamma_W M_W)} \\
&= (2i\pi) \frac{\pi^{1-\epsilon} \sqrt{\pi}}{-2\epsilon_{\text{IR}}} \frac{1}{\Gamma(\frac{1}{2} - \epsilon)} \frac{2M_W}{m_t^2 - M_W^2} \int d|\vec{q}| \frac{|\vec{q}|^{-2\epsilon}}{-2|\vec{q}|M_W \pm i\Gamma_W M_W} \\
&= (2i\pi) \frac{\pi^{1-\epsilon} \sqrt{\pi}}{-2\epsilon_{\text{IR}}} \frac{1}{\Gamma(\frac{1}{2} - \epsilon)} 2^{2\epsilon} \times \begin{cases} \left(\frac{m_t^2 - M_W^2}{M_W \mu} \right)^{-2\epsilon} \frac{1}{2(m_t^2 - M_W^2) \epsilon_{\text{IR}}} & \text{when } \Gamma_W = 0 \\ \log \frac{\pm i\Gamma_W M_W}{m_t^2 - M_W^2} - \epsilon & \text{when } \Gamma_W \neq 0 \\ \times \frac{\frac{\pi^2}{3} + \log \left(-\frac{m_t^2 - M_W^2}{\pm i\Gamma_W M_W} \right) \log \left(-\frac{M_W^2 \mu^2}{\pm i\Gamma_W M_W (m_t^2 - M_W^2)} \right)}{m_t^2 - M_W^2} \end{cases} \quad (3.99)
\end{aligned}$$

Therefore,

$$\begin{aligned}
&\frac{\text{Real}^\pm(\Gamma_W) - \text{Real}^\pm(0)}{i\pi^{2-\epsilon} \Gamma(1 - \epsilon)^2 \Gamma(1 + \epsilon) \Gamma(1 - 2\epsilon)^{-1}} \quad (3.100) \\
&= \left(-\frac{1}{\epsilon_{\text{IR}}} + \frac{\pi^2 \epsilon}{6} \right) \times \left(-\frac{1}{2(m_t^2 - M_W^2)} \frac{1}{\epsilon_{\text{IR}}} + \frac{1}{2(m_t^2 - M_W^2)} \log \left(-\frac{\Gamma_W^2}{\mu^2} \right) - \epsilon \frac{\frac{\pi^2}{3} + \frac{\log^2 \left(-\frac{\Gamma_W^2}{\mu^2} \right)}{4}}{m_t^2 - M_W^2} \right).
\end{aligned}$$

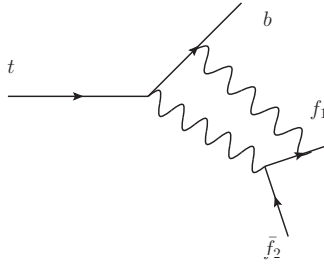
Hence, the real emission and the virtual cancels exactly. This conclusion should be true to other triangle diagrams with one photon loop propagator.

The finite width effect from the second expansion term of Eq.(3.87) should be added to the top quark decay width at NLO EW accuracy. It can be guaranteed by subtracting the LO top quark width in NWA from the LO top quark width in CMS with the LO W

width, because of

$$\begin{aligned}
& \Sigma_{f_1, \bar{f}_2} |\mathcal{A}_{\text{Born}}(t \rightarrow bW^+)|^2 \left(\frac{\Gamma_W^{\text{Born}}(W^+ \rightarrow f_1 \bar{f}_2)}{\Gamma_W^{\text{Born}} + \Gamma_W^{\text{NLO}}} \right) \\
& + \int d\Phi(W^+ \rightarrow f_1 \bar{f}_2) \mathcal{P} \left(\frac{1}{(p^2 - M_W^2)^2} \right) |\mathcal{A}_{\text{Born}}(W^+ \rightarrow f_1 \bar{f}_2)|^2 + \mathcal{O}(\alpha^n \alpha_S^m, n+m \geq 3) \\
& - \Sigma_{f_1, \bar{f}_2} |\mathcal{A}_{\text{Born}}(t \rightarrow bW^+)|^2 \frac{\Gamma_W^{\text{Born}}(W^+ \rightarrow f_1 \bar{f}_2)}{\Gamma_W^{\text{Born}} + \Gamma_W^{\text{NLO}}} \\
& = \Sigma_{f_1, \bar{f}_2} |\mathcal{A}_{\text{Born}}(t \rightarrow bW^+)|^2 \left(\frac{\Gamma_W^{\text{Born}}(W^+ \rightarrow f_1 \bar{f}_2)}{\Gamma_W^{\text{Born}}} \right) \\
& + \int d\Phi(W^+ \rightarrow f_1 \bar{f}_2) \mathcal{P} \left(\frac{1}{(p^2 - M_W^2)^2} \right) |\mathcal{A}_{\text{Born}}(W^+ \rightarrow f_1 \bar{f}_2)|^2 \Big|_{\Gamma_W = \Gamma_W^{\text{Born}}} + \mathcal{O}(\alpha^n \alpha_S^m, n+m \geq 3) \\
& - \Sigma_{f_1, \bar{f}_2} |\mathcal{A}_{\text{Born}}(t \rightarrow bW^+)|^2 \frac{\Gamma_W^{\text{Born}}(W^+ \rightarrow f_1 \bar{f}_2)}{\Gamma_W^{\text{Born}}} \\
& = \Sigma_{f_1, \bar{f}_2} \Gamma_{\text{Born}}^{\text{CMS}}(t \rightarrow bW^+ \rightarrow b f_1 \bar{f}_2) \Big|_{\Gamma_W = \Gamma_W^{\text{Born}}} - \Gamma_{\text{Born}}^{\text{NWA}}(t \rightarrow bW^+) \\
& = \left[\Sigma_{f_1, \bar{f}_2} \Gamma_{\text{Born}}^{\text{CMS}}(t \rightarrow bW^+ \rightarrow b f_1 \bar{f}_2) - \Gamma_{\text{Born}}^{\text{NWA}}(t \rightarrow bW^+) \frac{\Gamma_W^{\text{Born}}}{\Gamma_W} \right] \Big|_{\Gamma_W = \Gamma_W^{\text{Born}} + \Gamma_W^{\text{NLO}}}. \tag{3.101}
\end{aligned}$$

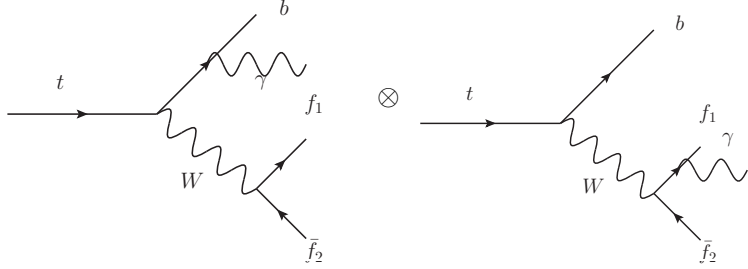
Now, let us consider the interference pieces from the third class of topology. The box diagram cannot have any $\frac{M}{\Gamma}$ enhancement except one loop propagator can be soft, e.g. one can be a photon in this case.



$$\begin{aligned}
& \sim D_0(0, 0, m_t^2, 0, M_W^2, t, 0, 0, M_W^2 - i\Gamma_W M_W, 0) \\
& \stackrel{t \rightarrow m_t^2 - M_W^2}{\sim} \frac{i\pi^2}{m_t^2 - M_W^2} \frac{1}{i\Gamma_W M_W} \pi^{-\epsilon} \frac{\Gamma(1-\epsilon)^2 \Gamma(1+\epsilon)}{\Gamma(1-2\epsilon)} \\
& \times \left[\frac{1}{\epsilon_{\text{IR}}^2} - \frac{1}{\epsilon_{\text{IR}}} \log \left(-\frac{\Gamma_W^2}{\mu^2} \right) + \frac{\pi^2}{2} + \frac{\log^2 \left(-\frac{\Gamma_W^2}{\mu^2} \right)}{2} \right], \tag{3.102}
\end{aligned}$$

where $t \rightarrow m_t^2 - M_W^2$ means f_1 and b is back-to-back. Hence, the pure $\log \left(-\frac{\Gamma_W^2}{\mu^2} \right)$ term is universal and should be cancelled by the real emission (in the soft region) with $(p_{f_1} + p_{\bar{f}_2})^2 =$

M_W^2 ¹⁵



$$\begin{aligned}
&= \text{Real}(\Gamma_W) \\
&= (-2i\pi) \int d^d q \theta(q^0) \delta(q^2) \frac{1}{(q+p_b)^2 (q+p_{f_1})^2 ((q+p_{f_1}+p_{\bar{f}_2})^2 - M_W^2 - i\Gamma_W M_W)} \\
&\times \frac{1}{(p_{f_1}+p_{\bar{f}_1})^2 - M_W^2 + i\Gamma_W M_W} \\
&\stackrel{t \rightarrow m_t^2 - M_W^2}{\sim} \frac{1}{i\Gamma_W M_W} \frac{(-2i\pi)}{m_t^2 - M_W^2} \int \frac{d^{d-1} \vec{q}}{2|\vec{q}|} \frac{1}{|\vec{q}|^2 (2|\vec{q}|M_W - i\Gamma_W M_W) (1 - \cos^2 \theta)} \\
&= \frac{1}{i\Gamma_W M_W} \frac{-i\pi}{m_t^2 - M_W^2} \frac{2\pi^{1-\epsilon}}{\Gamma(1-\epsilon)} \frac{\sqrt{\pi}\Gamma(-\epsilon)}{\Gamma(\frac{1}{2}-\epsilon)} \int d|\vec{q}| \frac{|\vec{q}|^{d-5}}{2|\vec{q}|M_W - i\Gamma_W M_W} \\
&= \frac{1}{i\Gamma_W M_W} \frac{-i\pi}{m_t^2 - M_W^2} \frac{2\pi^{1-\epsilon}}{\Gamma(1-\epsilon)} \frac{\sqrt{\pi}\Gamma(-\epsilon)}{\Gamma(\frac{1}{2}-\epsilon)} i \left(-\frac{1}{2\Gamma_W M_W} \frac{1}{\epsilon_{\text{IR}}} \right. \\
&+ \left. \frac{\log\left(-\frac{\Gamma_W^2}{4\mu^2}\right)}{2\Gamma_W M_W} - \epsilon \frac{\left(\frac{\pi^2}{3} + \frac{\log^2\left(-\frac{\Gamma_W^2}{4\mu^2}\right)}{4}\right)}{\Gamma_W M_W} + \mathcal{O}(1) \right) \\
&= -\frac{1}{\Gamma_W^2 M_W^2} \frac{i\pi^2}{m_t^2 - M_W^2} \pi^{-\epsilon} \frac{\Gamma(1-\epsilon)^2 \Gamma(1+\epsilon)}{\Gamma(1-2\epsilon)} \\
&\times \left(\frac{1}{\epsilon_{\text{IR}}^2} - \frac{1}{\epsilon_{\text{IR}}} \log\left(-\frac{\Gamma_W^2}{\mu^2}\right) + \frac{\pi^2}{2} + \frac{\log^2\left(-\frac{\Gamma_W^2}{\mu^2}\right)}{2} \right). \tag{3.103}
\end{aligned}$$

Therefore, $\text{Real}(\Gamma_W) + \text{loop} \times \frac{1}{-i\Gamma_W M_W}$ cancels exactly. **The universal term of $\log\left(-\frac{\Gamma_W^2}{\mu^2}\right)$ is a global prefactor $\left(\frac{\Gamma_W^2}{\mu^2}\right)^\epsilon$ to the leading singularity (i.e. $\frac{1}{\epsilon_{\text{IR}}}$ in the above triangle/box examples) of the difference between CMS and NWA virtual/loop/real amplitudes.**

The second class of topology is also the new topology in CMS. There is no such contribution in NWA because of the on-shell renormalization condition. In order to make the equivalence between CMS and NWA, we still include loop+UV on the W propagator. First, let us consider the virtual one. With the exactly same argument in the W production

¹⁵Note, to guarantee the same phase space point, one should write one W propagator to be $\frac{1}{(q+p_{f_1}+p_{\bar{f}_2})^2 - M_W^2 - i\Gamma_W M_W}$ instead of $\frac{1}{(p_t - p_b)^2 - M_W^2 - i\Gamma_W M_W}$.

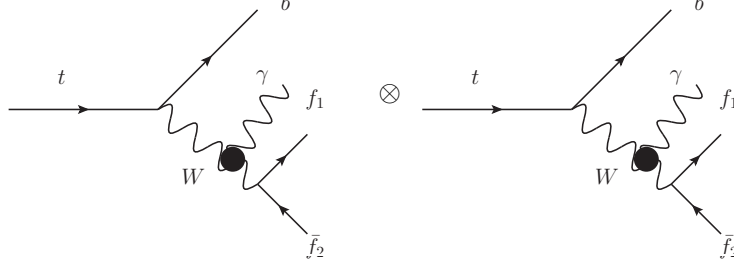
case, the result between CMS and NWA are same. The only “exception” can be the photon in the loop propagator. We will demonstrate that this “exception” is also not an exception after including the corresponding soft real emission. For this diagram, the difference of the corresponding UV is beyond NLO level. Let us apply the similar argument in Sec.D. For example, the loop diagram have

$$\begin{aligned}
& \sim \frac{1}{i\Gamma_W M_W} B_0(M_W^2, 0, M_W^2 - i\Gamma_W M_W) \\
& = \frac{1}{i\Gamma_W M_W} i\pi^2 \left(\frac{1}{\epsilon_{UV}} - \gamma_E + 2 - \log \pi + \log \frac{\mu^2}{M_W^2 - i\Gamma_W M_W} \right. \\
& \quad \left. - \frac{i\Gamma_W}{M_W} \log \frac{-i\Gamma_W M_W}{M_W^2 - i\Gamma_W M_W} \right). \tag{3.104}
\end{aligned}$$

The real part would be cancelled by W mass UV (though not the same as that in NWA), while the term $-\frac{i\Gamma_W}{M_W} \log \frac{-i\Gamma_W M_W}{M_W^2 - i\Gamma_W M_W}$ is an extra term in CMS. Moreover, one should also include the W wavefunction renormalization, which is

$$\begin{aligned}
& -\frac{1}{i\Gamma_W M_W} i\Gamma_W M_W i\pi^2 \left[\frac{d}{dp^2} \int d^d q \frac{1}{q^2((q+p)^2 - M_W^2 + i\Gamma_W M_W)} \right] \Big|_{p^2 \rightarrow M_W^2 - i\Gamma_W M_W} \\
& = -\frac{1}{i\Gamma_W M_W} i\Gamma_W M_W i\pi^2 \left[\int d^{d+2} q \frac{1}{q^4((q+p)^2 - M_W^2 + i\Gamma_W M_W)^2} \right] \Big|_{p^2 \rightarrow M_W^2 - i\Gamma_W M_W} \tag{3.105} \\
& = -\frac{1}{i\Gamma_W M_W} i\Gamma_W M_W i\pi^2 \frac{1}{2(M_W^2 - i\Gamma_W M_W)} \left(-\frac{1}{\epsilon_{IR}} + \gamma_E - 2 + \log \pi - \log \frac{\mu^2}{M_W^2 - i\Gamma_W M_W} \right)
\end{aligned}$$

Let us consider the corresponding real emission diagrams



$$\begin{aligned}
\text{Real}(\Gamma_W) &\sim (-2i\pi) \int d^d q \theta(q^0) \delta(q^2) \frac{1}{(p-q)^2 - M_W^2 + i\Gamma_W M_W} \frac{1}{(p-q)^2 - M_W^2 - i\Gamma_W M_W} \\
&= (-2i\pi) \int \frac{d^{d-1} \vec{q}}{2|\vec{q}|} \frac{1}{((p-q)^2 - M_W^2)^2 + \Gamma_W^2 M_W^2} \\
&= (-2i\pi) \int \frac{d|\vec{q}| d^{d-1} \Omega}{2} \frac{|\vec{q}|^{d-3}}{4|\vec{q}|^2 M_W^2 + \Gamma_W^2 M_W^2} \\
&= (-2i\pi) \frac{\pi^{1-\epsilon} \sqrt{\pi}}{4M_W^2} \frac{1}{\Gamma(\frac{3}{2} - \epsilon)} 2^{2\epsilon} \times \begin{cases} -\left(\frac{m_t^2 - M_W^2}{M_W \mu}\right)^{-2\epsilon} \frac{1}{2\epsilon_{\text{IR}}} & \text{when } \Gamma_W = 0 \\ \log \frac{m_t^2 - M_W^2}{\Gamma_W M_W} & \text{when } \Gamma_W \neq 0 \end{cases}, \quad (3.106)
\end{aligned}$$

Therefore, Eq.(3.104)+Eq.(3.106)+Real(Γ_W)-Real(0) plus mass UV in CMS would cancel out completely. We should note that when $p^2 = (p_t - p_b)^2 = M_W^2$ the real emission is corresponding to EW corrections in the decay process in NWA, while when $p^2 = (p_{f_1} + p_{\bar{f}_2})^2 = M_W^2$ the real emission corresponds to EW corrections in the production process in NWA. The different two phase space point would also contribute a factor of 2 in the real emission and it will compensant the factor 2 in the virtual pieces.

In conclusion, we illustrated that : **up to NLO QED accuracy, we only need to calculate the top quark width in NWA up to NLO QED level plus the finite W width effect via $\Sigma_{f_1, \bar{f}_2} \Gamma_{\text{Born}}^{\text{CMS}}(t \rightarrow bW^+ \rightarrow bf_1 \bar{f}_2)|_{\Gamma_W = \Gamma_W^{\text{Born}}} - \Gamma_{\text{Born}}^{\text{NWA}}(t \rightarrow bW^+)$.**

3.5.3 NNLO QCD corrections

Similar exercise can be generalized to higher-order, where we consider NNLO QCD corrections, in which we have With the same argument in the previous section, for the factorizable

topology, we have

$$\begin{aligned}
& \Sigma_{f_1, \bar{f}_2} \left\{ |\mathcal{A}_{\text{Born}}(t \rightarrow bW^+)|^2 \frac{\Gamma_W^{\text{Born}}(W^+ \rightarrow f_1 \bar{f}_2)}{\Gamma_W^{\text{Born}} + \Gamma_W^{\text{NLO}} + \Gamma_W^{\text{NNLO}}} \right. \\
& + |\mathcal{A}_{\text{NLO}}(t \rightarrow bW^+ + X)|^2 \frac{\Gamma_W^{\text{Born}}(W^+ \rightarrow f_1 \bar{f}_2)}{\Gamma_W^{\text{Born}} + \Gamma_W^{\text{NLO}} + \Gamma_W^{\text{NNLO}}} + |\mathcal{A}_{\text{Born}}(t \rightarrow bW^+)|^2 \frac{\Gamma_W^{\text{NLO}}(W^+ \rightarrow f_1 \bar{f}_2 + X)}{\Gamma_W^{\text{Born}} + \Gamma_W^{\text{NLO}} + \Gamma_W^{\text{NNLO}}} \\
& + |\mathcal{A}_{\text{NNLO}}(t \rightarrow bW^+ + X)|^2 \frac{\Gamma_W^{\text{Born}}(W^+ \rightarrow f_1 \bar{f}_2)}{\Gamma_W^{\text{Born}} + \Gamma_W^{\text{NLO}} + \Gamma_W^{\text{NNLO}}} + |\mathcal{A}_{\text{NLO}}(t \rightarrow bW^+ + X)|^2 \frac{\Gamma_W^{\text{NLO}}(W^+ \rightarrow f_1 \bar{f}_2)}{\Gamma_W^{\text{Born}} + \Gamma_W^{\text{NLO}} + \Gamma_W^{\text{NNLO}}} \\
& \left. + |\mathcal{A}_{\text{Born}}(t \rightarrow bW^+ + X)|^2 \frac{\Gamma_W^{\text{NNLO}}(W^+ \rightarrow f_1 \bar{f}_2)}{\Gamma_W^{\text{Born}} + \Gamma_W^{\text{NLO}} + \Gamma_W^{\text{NNLO}}} \right\} \\
& = |\mathcal{A}_{\text{NLO}}(t \rightarrow bW^+ + X)|^2 \frac{\Gamma_W^{\text{Born}} + \Gamma_W^{\text{NLO}}}{\Gamma_W^{\text{Born}} + \Gamma_W^{\text{NLO}} + \Gamma_W^{\text{NNLO}}} + |\mathcal{A}_{\text{Born}}(t \rightarrow bW^+)|^2 \frac{\Gamma_W^{\text{Born}} + \Gamma_W^{\text{NLO}} + \Gamma_W^{\text{NNLO}}}{\Gamma_W^{\text{Born}} + \Gamma_W^{\text{NLO}} + \Gamma_W^{\text{NNLO}}} \\
& + |\mathcal{A}_{\text{NNLO}}(t \rightarrow bW^+ + X)|^2 \frac{\Gamma_W^{\text{Born}}}{\Gamma_W^{\text{Born}} + \Gamma_W^{\text{NLO}} + \Gamma_W^{\text{NNLO}}} \\
& = (|\mathcal{A}_{\text{Born}}(t \rightarrow bW^+)|^2 + |\mathcal{A}_{\text{NLO}}(t \rightarrow bW^+ + X)|^2 + |\mathcal{A}_{\text{NNLO}}(t \rightarrow bW^+ + X)|^2) \\
& + |\mathcal{A}_{\text{NLO}}(t \rightarrow bW^+ + X)|^2 \frac{-\Gamma_W^{\text{NNLO}}}{\Gamma_W^{\text{Born}} + \Gamma_W^{\text{NLO}} + \Gamma_W^{\text{NNLO}}} \\
& + |\mathcal{A}_{\text{NNLO}}(t \rightarrow bW^+ + X)|^2 \frac{-\Gamma_W^{\text{NLO}} - \Gamma_W^{\text{NNLO}}}{\Gamma_W^{\text{Born}} + \Gamma_W^{\text{NLO}} + \Gamma_W^{\text{NNLO}}} \\
& = (|\mathcal{A}_{\text{Born}}(t \rightarrow bW^+)|^2 + |\mathcal{A}_{\text{NLO}}(t \rightarrow bW^+ + X)|^2 + |\mathcal{A}_{\text{NNLO}}(t \rightarrow bW^+ + X)|^2) \\
& + \mathcal{O}(\alpha^n \alpha_S^m, n + m \geq 4). \tag{3.107}
\end{aligned}$$

Hence, the finite width effect at NNLO level in general would be

$$\begin{aligned}
& \left\{ \Sigma_{f_1, \bar{f}_2} |\mathcal{A}_{\text{Born}}(t \rightarrow bW^+)|^2 \left(\frac{\Gamma_W^{\text{Born}}(W^+ \rightarrow f_1 \bar{f}_2) + \Gamma_W^{\text{NLO}}(W^+ \rightarrow f_1 \bar{f}_2)}{\Gamma_W^{\text{Born}} + \Gamma_W^{\text{NLO}} + \Gamma_W^{\text{NNLO}}} \right) \right. \\
& + \int d\Phi(W^+ \rightarrow f_1 \bar{f}_2 + X) \mathcal{P} \left(\frac{1}{(p^2 - M_W^2)^2} \right) (|\mathcal{A}_{\text{Born}}(W^+ \rightarrow f_1 \bar{f}_2)|^2 + |\mathcal{A}_{\text{NLO}}(W^+ \rightarrow f_1 \bar{f}_2)|^2) \\
& - \int d\Phi(W^+ \rightarrow f_1 \bar{f}_2) \frac{\pi \Gamma_W M_W}{2} \delta(p^2 - M_W^2) \left(\frac{\partial}{\partial p^2} \right)^2 |\mathcal{A}_{\text{Born}}(W^+ \rightarrow f_1 \bar{f}_2)|^2 \left. + \mathcal{O}(\alpha^n \alpha_S^m, n + m \geq 4) \right. \\
& - \Sigma_{f_1, \bar{f}_2} |\mathcal{A}_{\text{Born}}(t \rightarrow bW^+)|^2 \frac{\Gamma_W^{\text{Born}}(W^+ \rightarrow f_1 \bar{f}_2) + \Gamma_W^{\text{NLO}}(W^+ \rightarrow f_1 \bar{f}_2)}{\Gamma_W^{\text{Born}} + \Gamma_W^{\text{NLO}} + \Gamma_W^{\text{NNLO}}} \left. \right\} \\
& + \left\{ \Sigma_{f_1, \bar{f}_2} |\mathcal{A}_{\text{NLO}}(t \rightarrow bW^+)|^2 \left(\frac{\Gamma_W^{\text{Born}}(W^+ \rightarrow f_1 \bar{f}_2)}{\Gamma_W^{\text{Born}} + \Gamma_W^{\text{NLO}} + \Gamma_W^{\text{NNLO}}} \right) \right. \\
& + \int d\Phi(W^+ \rightarrow f_1 \bar{f}_2) \mathcal{P} \left(\frac{1}{(p^2 - M_W^2)^2} \right) |\mathcal{A}_{\text{Born}}(W^+ \rightarrow f_1 \bar{f}_2)|^2 \left. \right. \\
& - \Sigma_{f_1, \bar{f}_2} |\mathcal{A}_{\text{NLO}}(t \rightarrow bW^+)|^2 \frac{\Gamma_W^{\text{Born}}(W^+ \rightarrow f_1 \bar{f}_2)}{\Gamma_W^{\text{Born}} + \Gamma_W^{\text{NLO}} + \Gamma_W^{\text{NNLO}}} \left. \right\} \\
& = \Sigma_{f_1, \bar{f}_2} \Gamma_{\text{Born+NLO}}^{\text{CMS}}(t \rightarrow bW^+ \rightarrow b f_1 \bar{f}_2 + X) |_{\Gamma_W = \Gamma_W^{\text{Born}} + \Gamma_W^{\text{NLO}}} - \Gamma_{\text{Born+NLO}}^{\text{NWA}}(t \rightarrow bW^+). \tag{3.108}
\end{aligned}$$

However, because of $\Gamma_W^{\text{Born}} \sim \mathcal{O}(\alpha)$ only, such finite width effect need at least one EW/QED corrections, i.e. at NNLO level, it only appears when performing NNLO EW/QED cor-

rections or NLO QCD \otimes NLO EW/QED corrections. In the later case, one just replace NLO=NLO QCD+NLO EW/QED and NNLO=NLO QCD \otimes NLO EW/QED.

4. Finite width effects at NNLO QCD level

4.1 top quark decay width

4.2 W production in hadronic collisions

4.3 Z production in hadronic collisions

5. SMWIDTH: A package for calculating decay widths of particles in the Standard Model with NNLO QCD and NLO EW accuracy

5.1 A quick guide

5.2 Illustrative results

The parameter setup in $\alpha(M_Z)$ renormalization scheme is:

Parameter	value	Parameter	value
G_μ	$1.1987498350461625 \cdot 10^{-5}$	$\alpha(M_Z)^{-1}$	128.930
m_t	173.3	y_t	173.3
M_W	80.419	M_Z	91.188
M_H	125.0	V_{ij}	δ_{ij}

We have presented the widths for W, Z and top quark from SMWIDTH in $\alpha(M_Z)$ renormalization scheme in Tab.1, where we have defined

$$\begin{aligned}
 \Gamma_W &= \Gamma_W^{\text{LO}} (1 + \delta_{\alpha_S} + \delta_\alpha + \delta_{m_f}), \\
 \Gamma_Z &= \Gamma_Z^{\text{LO}} (1 + \delta_{\alpha_S} + \delta_\alpha + \delta_{m_f}), \\
 \Gamma_t &= \Gamma_t^{\text{LO}} (1 + \delta_{\alpha_S} + \delta_\alpha + \delta_{m_f} + \delta_{\Gamma_W}).
 \end{aligned} \tag{5.1}$$

Here, $\delta_{\alpha_S, \alpha, m_f, \Gamma_W}$ represent the QCD corrections, EW corrections, finite fermion mass effect and finite width effect respectively. For the renormalization of $\alpha_S(\mu_R)$, we have setting μ_R to be the mother particle's mass. In the finite fermion mass effect, we have taken them to be:

Parameter	value	Parameter	value
m_b	4.49	m_c	1.42
m_τ	1.77684	m_μ	0.105658367

Similarly, in the G_μ renormalization scheme, we use the same parameter setup except using

$$G_\mu = 1.16639 \cdot 10^{-5} \rightarrow \alpha_{G_\mu}^{-1} = 132.23. \tag{5.2}$$

The corresponding results are presented in Fig.2. To the Z boson width, the contribution from $Z \rightarrow W^\pm f_1 \bar{f}_2$ is negligible because of the phase space suppression.

	Γ^{LO} [GeV]	δ_{α_S} (%)	δ_α (%)	δ_{m_f} (%)	δ_{Γ_W} (%)
W^\pm	2.10490	2.55	-3.51	-0.0238	-
Z	2.51376	2.61	-3.34	-0.0374	-
t	1.54624	-8.58	-1.41	-0.239	-1.58

Table 1: The widths calculated by SMWIDTH in $\alpha(M_Z)$ renormalization scheme.

	Γ^{LO} [GeV]	δ_{α_S} (%)	δ_α (%)	δ_{m_f} (%)	δ_{Γ_W} (%)
W^\pm	2.04808	2.55	-0.364	-0.0238	-
Z	2.44591	2.61	-0.197	-0.0374	-
t	1.50450	-8.58	1.68	-0.239	-1.54

Table 2: The widths calculated by SMWIDTH in G_μ renormalization scheme.

A. 2-point scalar integrals

In the physical region, i.e.

$$p^2 \rightarrow p^2 + i0, m_i^2 \rightarrow m_i^2 - i0, \quad (\text{A.1})$$

we have

$$\begin{aligned} & \text{---} \overset{p^2}{\text{---}} \text{---} \text{---} \overset{m_1}{\text{---}} \text{---} \text{---} \overset{p^2}{\text{---}} \text{---} \text{---} \underset{m_2}{\text{---}} \text{---} \text{---} = B_0(p^2, m_1^2, m_2^2) \\ & = \mu^{2\epsilon} \left\{ \frac{1}{\epsilon_{\text{UV}}} + 2 - \log(p^2 + i0) + \sum_{i=0}^1 \left[\gamma_i \log \frac{\gamma_i - 1}{\gamma_i} - \log(\gamma_i - 1) \right] \right\}, \end{aligned} \quad (\text{A.2})$$

where γ_0 and γ_1 are the two roots of the quadratic equation

$$-\gamma(1-\gamma)p^2 + \gamma m_2^2 + (1-\gamma)m_1^2 = 0, \quad (\text{A.3})$$

which are

$$\begin{aligned} \gamma_i &= \frac{p^2 - m_2^2 + m_1^2 + (-)^i \sqrt{\lambda(p^2, m_1^2, m_2^2)}}{2p^2}, \\ \lambda(a, b, c) &= a^2 + b^2 + c^2 - 2ab - 2ac - 2bc. \end{aligned} \quad (\text{A.4})$$

Without losing generality, we can assume $m_1 \geq m_2$. For the relevant to the complex mass scheme, we have

$$\Re p^2 \geq 0, \Re m_i^2 \geq 0, \Im m_i^2 \leq 0, \quad (\text{A.5})$$

and $\Im p^2 \ll \Re p^2, \Im m_i^2 \ll \Re m_i^2$.

The criterion is that $p^2 + i0 \rightarrow p^2 - i0$ will not flip the sign of the imaginary part of the loop integral.

Case 1:

$$\Re \lambda(p^2, m_1^2, m_2^2) \geq 0, \text{ i.e. } \Re p^2 \geq (\Re m_1 + \Re m_2)^2 \text{ or } \Re p^2 \leq (\Re m_1 - \Re m_2)^2. \quad (\text{A.6})$$

Case 1.1, when

$$\Re p^2 \leq (\Re m_1 - \Re m_2)^2, \quad (\text{A.7})$$

we have

$$\begin{aligned} \Re \frac{\gamma_0 - 1}{\gamma_0} &= \Re \frac{(m_1 - m_2)(m_1 + m_2) - p^2 + \sqrt{\lambda(p^2, m_1^2, m_2^2)}}{(m_1 - m_2)(m_1 + m_2) + p^2 + \sqrt{\lambda(p^2, m_1^2, m_2^2)}} \geq 0, \\ \Re(\gamma_0 - 1) &= \Re \frac{(m_1 - m_2)(m_1 + m_2) - p^2 + \sqrt{\lambda(p^2, m_1^2, m_2^2)}}{2p^2} \geq 0, \end{aligned} \quad (\text{A.8})$$

and

$$\begin{aligned}\Re \frac{\gamma_1 - 1}{\gamma_1} &= \Re \frac{(m_1 - m_2)(m_1 + m_2) - p^2 - \sqrt{\lambda(p^2, m_1^2, m_2^2)}}{(m_1 - m_2)(m_1 + m_2) + p^2 - \sqrt{\lambda(p^2, m_1^2, m_2^2)}} \geq 0, \\ \Re(\gamma_1 - 1) &= \Re \frac{(m_1 - m_2)(m_1 + m_2) - p^2 - \sqrt{\lambda(p^2, m_1^2, m_2^2)}}{2p^2} \geq 0.\end{aligned}\quad (\text{A.9})$$

Hence, in this case, logarithm is the normal one.

Case 1.2, when

$$\Re p^2 \geq (\Re m_1 + \Re m_2)^2, \quad (\text{A.10})$$

we have

$$\begin{aligned}m_1^2 - m_2^2 - p^2 &\leq -\sqrt{\lambda(p^2, m_1^2, m_2^2)} \\ \rightarrow \Re \gamma_0 &\geq \frac{1}{2}, \Re \gamma_0 - 1 \leq 0,\end{aligned}\quad (\text{A.11})$$

and

$$\begin{aligned}m_1^2 - m_2^2 + p^2 &\geq \sqrt{\lambda(p^2, m_1^2, m_2^2)} \\ \rightarrow \Re \gamma_1 &\geq 0, \Re \gamma_1 - 1 \leq 0.\end{aligned}\quad (\text{A.12})$$

If $\Re p^2 \geq 2(\Re m_1^2 + \Re m_2^2)$, we have

$$\frac{1}{2} \geq \Re \gamma_1 \geq 0, \quad (\text{A.13})$$

while $\Re p^2 \leq 2(\Re m_1^2 + \Re m_2^2)$, we have

$$1 \geq \Re \gamma_1 \geq \frac{1}{2}. \quad (\text{A.14})$$

We can also expand the imaginary part to the first order, i.e.

$$\Im \gamma_0 = -\Re \gamma_0 \frac{\Im p^2}{\Re p^2} + \frac{\Im m_1^2 - \Im m_2^2 + \Im p^2}{2\Re p^2} - \frac{g(p^2, m_1^2, m_2^2)}{2\Re p^2 \sqrt{\lambda(\Re p^2, \Re m_1^2, \Re m_2^2)}}, \quad (\text{A.15})$$

where

$$g(a, b, c) = \Im a \Re(b + c - a) + \Im b \Re(a + c - b) + \Im c \Re(a + b - c) \quad (\text{A.16})$$

In this case, the logarithms should be generalized to \log^- defined in Eq.3.59 only when the sign of the imaginary part is determined by the imaginary part of $\Im p^2$. This condition makes it is easier to use the $\Im p^2$ expansion only. However, in Standard Model, we have such condition only happens when $t \rightarrow W + b$, where we have $\Im m_2^2 = 0$ and $\Re m_2^2 \ll \Re m_1^2, \Re p^2$. Then

$$\Im \gamma_0 = (1 - \Re \gamma_0) \frac{\Im p^2}{\Re p^2} \geq 0, \quad (\text{A.17})$$

However, in the Taylor expansion, we have

$$\begin{aligned}
& B_0(M_W^2 + i0, 0, M_W^2 - i\Gamma_W M_W) \\
& + (M_W^2 - i\Gamma_W M_W - M_W^2) B'_0(p^2, 0, M_W^2 - i\Gamma_W M_W) \Big|_{p^2 \rightarrow M_W^2 + i0} \\
& + \mathcal{O}((M_W^2 - i\Gamma_W M_W - M_W^2)^2).
\end{aligned} \tag{B.2}$$

The difference between Eq.(B.2) and $B_0(M_W^2 - i\Gamma_W M_W, 0, M_W^2 - i\Gamma_W M_W)$ would be

$$\begin{aligned}
& -\frac{\pi^2 \Gamma_W \left[M_W - i\Gamma_W \log\left(-\frac{i\Gamma_W}{M_W - i\Gamma_W}\right) \right]}{M_W^2} + \mathcal{O}\left(\left(\frac{\Gamma_W}{M_W}\right)^2\right) \\
& = \frac{\pi^2 \Gamma_W}{M_W} + \mathcal{O}\left(\left(\frac{\Gamma_W}{M_W}\right)^2\right),
\end{aligned} \tag{B.3}$$

which means they are not the same up to $\mathcal{O}\left(\left(\frac{\Gamma_W}{M_W}\right)\right)$. The problem comes from the term $\frac{p^2 - M_W^2 + i\Gamma_W M_W}{p^2} \log \frac{M_W^2 - i\Gamma_W M_W - p^2}{M_W^2 - i\Gamma_W M_W}$. Because the derivation of the logarithm will result in $\frac{1}{p^2 - M_W^2 + i\Gamma_W M_W}$, i.e. $\frac{1}{i\Gamma_W M_W}$ when $p^2 = M_W^2$. Hence, one should also include the higher-order expansions from the above Taylor expansion Eq.(B.2). If we expand it up to the next term, i.e.

$$\begin{aligned}
& B_0(M_W^2 + i0, 0, M_W^2 - i\Gamma_W M_W) \\
& + (M_W^2 - i\Gamma_W M_W - M_W^2) B'_0(p^2, 0, M_W^2 - i\Gamma_W M_W) \Big|_{p^2 \rightarrow M_W^2 + i0} \\
& + \frac{(M_W^2 - i\Gamma_W M_W - M_W^2)^2}{2} B''_0(p^2, 0, M_W^2 - i\Gamma_W M_W) \Big|_{p^2 \rightarrow M_W^2 + i0} \\
& + \mathcal{O}((M_W^2 - i\Gamma_W M_W - M_W^2)^3).
\end{aligned} \tag{B.4}$$

In this case, the difference between Eq.(B.4) and $B_0(M_W^2 - i\Gamma_W M_W, 0, M_W^2 - i\Gamma_W M_W)$ would become

$$-\frac{\pi^2 \Gamma_W}{2M_W} + \mathcal{O}\left(\left(\frac{\Gamma_W}{M_W}\right)^2\right). \tag{B.5}$$

In general, if one expands to $\mathcal{O}((M_W^2 - i\Gamma_W M_W - M_W^2)^n)$, the difference would reduce to

$$-\frac{\pi^2 \Gamma_W}{nM_W} + \mathcal{O}\left(\left(\frac{\Gamma_W}{M_W}\right)^2\right). \tag{B.6}$$

Hence, only when one includes all order Taylor expansion, one can get the correct result for the UV renormalization constant in complex mass scheme.

This fact is indeed has been noticed in the Erratum of Ref. [15], where it was proposed to use two methods to cure it:

1. Do not expand the counterterm $\Sigma(p^2, M_W^2 - i\Gamma_W M_W)$ at least for diagrams with photon or gluon exchange.

2. Add the missing term back to the expanded counterterm.

Hence, the Taylor expansion method can be used directly only satisfy the following two conditions

1. The width is $\mathcal{O}(\alpha)$ and its coefficients to the coupling constant α is $\mathcal{O}(1)$, where α is the perturbative expansion coupling constant we are considering. In other words, it will not be applied if the width is not small, e.g. the Higgs boson with mass larger than 400 GeV.
2. There is Feynman diagrams with branching cuts at $p^2 = M^2 - i\Gamma M$, which is the case when one loop propagator can be soft and the other loop propagator can be on-shell (at the level no width effect or $q^2 \rightarrow M^2$).

C. A general strategy for choosing Riemann sheet

We propose a general strategy for choosing a correct Riemann sheet in UV/logarithms without the Taylor expansion as proposed in Ref. [15]. The necessity to do so relies on the motivation for a general implementation of complex-mass scheme in SM and BSM. It based on the fact that the logarithms are in the first Riemann sheet if one is in the physical region, i.e. in

$$p^2 \rightarrow p^2 + i0, m^2 \rightarrow m^2 - i0. \quad (\text{C.1})$$

Let us consider a general case $\log f(\{p_i^2\}, \{m_i^2 - i\gamma_i m_i\}, \mu^2 - i0)$. The choosing of the Riemann sheet in principle depends on all scales enters into function f . Hence, in general, based on the mass spectrum, the log should be changed to \log^+, \log^- or the normal logarithm (in the first Riemann sheet). For simplicity, first let us assume the real part of $f(\{p_i^2\}, \{m_i^2 - i\Gamma_i m_i\}, \mu^2 - i0)$ will not change from $p_i^2 = M_i^2 + i0$ to $p_i^2 = M_i^2 - i\Gamma_i M_i$, which is the usual case when $\Gamma_i \ll M_i$.¹⁶ In this case, one can always use $f(\{M_i^2 + i0\}, \{m_i^2 - i\gamma_i m_i\}, \mu^2 - i0)$ as a reference. One should use \log^\pm only when one encounters the following two cases with the real part $\Re f(\{M_i^2 + i0\}, \{m_i^2 - i\gamma_i m_i\}, \mu^2 - i0) < 0$:

1. when $\Im f(\{M_i^2 + i0\}, \{m_i^2 - i\gamma_i m_i\}, \mu^2 - i0)$ is negative and $\Im f(\{M_i^2 - i\Gamma_i M_i\}, \{m_i^2 - i\gamma_i m_i\}, \mu^2 - i0)$ is positive, one should continue log to \log^- ;
2. when $\Im f(\{M_i^2 + i0\}, \{m_i^2 - i\gamma_i m_i\}, \mu^2 - i0)$ is positive and $\Im f(\{M_i^2 - i\Gamma_i M_i\}, \{m_i^2 - i\gamma_i m_i\}, \mu^2 - i0)$ is negative, one should continue log to \log^+ .

¹⁶For a complicated cases when $\Re f(\{M_i^2 + i0\}, \{m_i^2 - i\gamma_i m_i\}, \mu^2 - i0)$ and $\Re f(\{M_i^2 - i\Gamma_i M_i\}, \{m_i^2 - i\gamma_i m_i\}, \mu^2 - i0)$ are not in same sign. One should in principle use another reference p_i^2 in the physical region.

D. Cancellation of $\alpha \log \Gamma$ between virtual and real

As we already discussed in section 3.4.2, after combing loop+UV=virtual, there are still remaining $\alpha \log \Gamma_W$ terms, which might spoil the perturbation convergence since Γ_W is small. In this section, we will illustrate that such logarithms will be cancelled by including the real emission contributions. For example, we have

$$\begin{aligned}
 & 2\Re \left(\text{Diagram 1} \otimes \text{Diagram 2} \right) \\
 & \sim 2 \frac{1}{i\Gamma_W M_W} B_0(M_W^2 + i0, 0, M_W^2 - i\Gamma_W M_W) \sim -\frac{2i\pi^2}{M_W^2} \log \Gamma_W. \quad (\text{D.1})
 \end{aligned}$$

Correspondingly, in the real emission, we have

$$\begin{aligned}
 & \left(\text{Diagram 3} \otimes \text{Diagram 4} \right) \\
 & \sim (-2i\pi) \int d^4 q \theta(q^0) \delta(q^2) \frac{1}{(p-q)^2 - M_W^2 + i\Gamma_W M_W} \frac{1}{(p-q)^2 - M_W^2 - i\Gamma_W M_W} \\
 & = (-2i\pi) \int \frac{d^3 \vec{q}}{2|\vec{q}|} \frac{1}{((p-q)^2 - M_W^2)^2 + \Gamma_W^2 M_W^2} \\
 & \stackrel{q \text{ soft}}{\sim} (-2i\pi) \int \frac{d|\vec{q}| d\Omega}{2} \frac{|\vec{q}|}{4|\vec{q}|^2 M_W^2 + \Gamma_W^2 M_W^2} \sim \frac{i\pi^2}{M_W^2} \log \Gamma_W, \quad (\text{D.2})
 \end{aligned}$$

and

$$\begin{aligned}
& \left(\begin{array}{c} \text{Diagram 1} \otimes \text{Diagram 2} \end{array} \right) \\
& \sim (-2i\pi) \int d^4 q \theta(q^0) \delta(q^2) \frac{1}{(q+p)^2 - M_W^2 + i\Gamma_W M_W} \frac{1}{(q+p)^2 - M_W^2 - i\Gamma_W M_W} \\
& = (-2i\pi) \int \frac{d^3 \vec{q}}{2|\vec{q}|} \frac{1}{((q+p)^2 - M_W^2)^2 + \Gamma_W^2 M_W^2} \\
& \stackrel{q \text{ soft}}{\sim} (-2i\pi) \int \frac{d|\vec{q}| d\Omega}{2} \frac{|\vec{q}|}{4|\vec{q}|^2 M_W^2 + \Gamma_W^2 M_W^2} \sim \frac{i\pi^2}{M_W^2} \log \Gamma_W. \tag{D.3}
\end{aligned}$$

Therefore, the $\log \Gamma_W$ cancels in Eq.(D.1)+Eq.(D.2)+Eq.(D.3). We would like to emphasize that Eq.(D.2) and Eq.(D.3) represent two different phase space regions.

Similarly, I would expect that the $\log \Gamma_W$ term would cancel in

$$\begin{aligned}
& 2\Re \left(\begin{array}{c} \text{Diagram 1} \otimes \text{Diagram 2} \end{array} \right) \\
& + \left(\begin{array}{c} \text{Diagram 3} \otimes \text{Diagram 4} \end{array} \right) \\
& + \left(\begin{array}{c} \text{Diagram 5} \otimes \text{Diagram 6} \end{array} \right) \tag{D.4}
\end{aligned}$$

and in

$$\begin{aligned}
 & \left. \left. \left. \left. \left. \begin{array}{c} \text{Diagram 1} \\ \text{Diagram 2} \end{array} \right. \right. \right. \right. \otimes \left. \left. \left. \left. \begin{array}{c} \text{Diagram 3} \end{array} \right. \right. \right. \right) \\
 & + \left. \left. \left. \left. \begin{array}{c} \text{Diagram 4} \\ \text{Diagram 5} \end{array} \right. \right. \right. \otimes \left. \left. \left. \left. \begin{array}{c} \text{Diagram 6} \\ \text{Diagram 7} \end{array} \right. \right. \right. \right) \\
 & + \left. \left. \left. \left. \begin{array}{c} \text{Diagram 8} \\ \text{Diagram 9} \end{array} \right. \right. \right. \otimes \left. \left. \left. \left. \begin{array}{c} \text{Diagram 10} \\ \text{Diagram 11} \end{array} \right. \right. \right. \right) \\
 & + \left. \left. \left. \left. \begin{array}{c} \text{Diagram 12} \\ \text{Diagram 13} \end{array} \right. \right. \right. \otimes \left. \left. \left. \left. \begin{array}{c} \text{Diagram 14} \\ \text{Diagram 15} \end{array} \right. \right. \right. \right) .
 \end{aligned}
 \tag{D.5}$$

The diagrams are Feynman diagrams for a process involving two incoming fermions and two outgoing fermions. The diagrams are organized into four rows, each starting with a plus sign. The first row is enclosed in a large curly bracket on the left, labeled $2\mathcal{R}$. The diagrams are connected by plus signs and tensor products (\otimes).

- Diagram 1:** Two incoming fermions meet at a vertex, producing a W boson (wavy line) and a γ photon (wavy line). The W boson is labeled "W, on-shell" and the γ photon is labeled " γ , soft". They then meet at a second vertex to produce two outgoing fermions.
- Diagram 2:** Similar to Diagram 1, but the W boson and γ photon are swapped in the intermediate state.
- Diagram 3:** A W boson (wavy line) is exchanged between the two vertices. The W boson is labeled "W, on-shell". A γ photon (wavy line) is attached to the W boson line, labeled " γ , soft".
- Diagram 4:** A γ photon (wavy line) is attached to the incoming fermion line. The photon is labeled " γ , soft". The W boson (wavy line) is labeled "W, on-shell". The photon's momentum is q . The W boson's momentum is $p^2 = M_W^2$. The W boson is attached to the outgoing fermion line.
- Diagram 5:** Similar to Diagram 4, but the W boson is attached to the incoming fermion line and the photon is attached to the outgoing fermion line.
- Diagram 6:** Similar to Diagram 4, but the photon's momentum is $q+p$ and the W boson's momentum is $p^2 = M_W^2$.
- Diagram 7:** Similar to Diagram 6, but the W boson is attached to the outgoing fermion line.
- Diagram 8:** Similar to Diagram 6, but the W boson is attached to the incoming fermion line.
- Diagram 9:** Similar to Diagram 8, but the photon is attached to the outgoing fermion line.
- Diagram 10:** Similar to Diagram 4, but the photon's momentum is q and the W boson's momentum is $p^2 = M_W^2$.
- Diagram 11:** Similar to Diagram 10, but the W boson is attached to the outgoing fermion line.
- Diagram 12:** Similar to Diagram 10, but the W boson is attached to the incoming fermion line.
- Diagram 13:** Similar to Diagram 12, but the photon is attached to the outgoing fermion line.
- Diagram 14:** Similar to Diagram 10, but the photon's momentum is $p-q$ and the W boson's momentum is $p^2 = M_W^2$.
- Diagram 15:** Similar to Diagram 14, but the W boson is attached to the outgoing fermion line.

E. Cross Checks

E.1 $e^+\nu_e \rightarrow W^+ \rightarrow \mu^+\nu_m$

E.1.1 Non-resonance region

As we already discussed, in a $2 \rightarrow 2$ process, there is no imaginary part in the Born amplitude. Hence, the cross check for the real part of virtual is a trivial cross check. We have shown it in Fig.2. The symbols in Fig.2 are defined as

$$\begin{aligned} \text{CMS} &= \frac{2\Re\mathcal{A}_{\text{Virtual}}^{\text{CMS}}\mathcal{A}_{\text{Born}}^{\text{CMS}*}}{\alpha_{ew}|\mathcal{A}_{\text{Born}}^{\text{NWA}}|^2}, \\ \text{NWA} &= \frac{2\Re\mathcal{A}_{\text{Virtual}}^{\text{NWA}}\mathcal{A}_{\text{Born}}^{\text{NWA}*}}{\alpha_{ew}|\mathcal{A}_{\text{Born}}^{\text{NWA}}|^2}, \\ \text{diff} &= (\text{CMS} - \text{NWA})/\alpha_{ew}. \end{aligned} \quad (\text{E.1})$$

We define the following notations for comparison between the results in CMS and NWA:

$$\begin{aligned} \text{CMS} \times \alpha_{ew}|\mathcal{A}_{\text{Born}}^{\text{NWA}}|^2 &= 2\Im\mathcal{A}_{\text{Virtual}}^{\text{CMS}}\mathcal{A}_{\text{Born}}^{\text{CMS}*}|_{\delta Z_e=0, \delta s_w=0} \\ &\quad + 2\Im\mathcal{A}_{\text{Born}}^{\text{CMS}}(\mathcal{A}_{\text{Born}}^{\text{CMS}*}|_{(\Gamma_W=0 \text{ in } W \text{ propagator only})}), \\ \text{NWA} \times \alpha_{ew}|\mathcal{A}_{\text{Born}}^{\text{NWA}}|^2 &= 2\Im\mathcal{A}_{\text{Virtual}}^{\text{NWA}}\mathcal{A}_{\text{Born}}^{\text{NWA}*}, \\ \text{diff} &= (\text{CMS} - \text{NWA})/\alpha_{ew}. \end{aligned} \quad (\text{E.2})$$

E.1.2 Resonance region: ε -offshellness method

We define the following notations for comparison between the results in CMS and NWA:

$$\begin{aligned} \text{CMS} &= 2\Re(\mathcal{A}_{\text{Virtual}}^{\text{CMS}})\mathcal{A}_{\text{Born}}^{\text{CMS}*}/\alpha_{ew} \\ \text{NWA} &= 2\Re\mathcal{A}_{\text{Virtual}}^{\text{NWA}}\mathcal{A}_{\text{Born}}^{\text{NWA}*}/\alpha_{ew} \times \frac{\varepsilon^2}{\Gamma_W^2 M_W^2}, \\ \text{diff} &= (\text{CMS} - \text{NWA})/\alpha_{ew}, \end{aligned} \quad (\text{E.3})$$

where the virtual amplitudes in CMS and NWA have been excluded the corresponding photon exchange diagrams in Eqs.(D.4,D.5) and add the piece $B_0(M_W^2 - i\Gamma_W M_W, 0, M_W^2 - i\Gamma_W M_W) - B_0(M_W^2, 0, M_W^2 - i\Gamma_W M_W)$ in W mass renormalization constant.

Due to the reason that in the numerical calculations, it would be quite difficult to keep the very small offshellness, here we can not get the consistent result between CMS and NWA.

E.2 $e^+e^- \rightarrow Z/\gamma^* \rightarrow \mu^+\mu^-$

E.2.1 Non-resonance region

For the trivial cross checks with the symbols defined in Eq.(E.1) are presented in Fig.9.

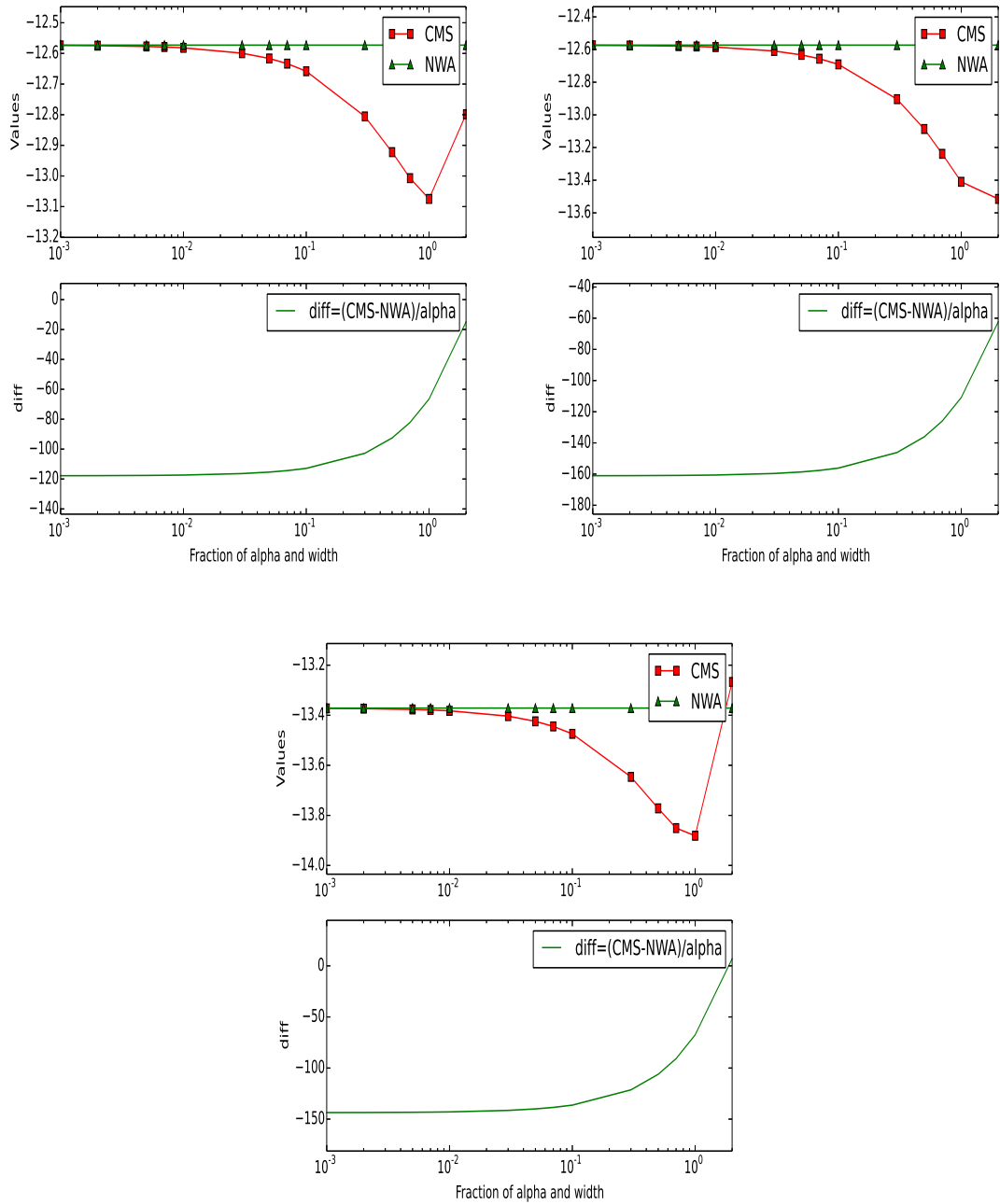


Figure 2: Trivial cross checks of the real part of the virtual for $e^+\nu_e \rightarrow W^+ \rightarrow \mu^+\nu_m$ in the non-resonance region with the correct LO width Γ_W^{LO} (upper-left panel), with the normal logarithm (upper-right panel), with the width $\Gamma_W = 1.2\Gamma_W^{\text{LO}}$ (lower panel).

The remaining cross checks we define the following notations for comparison between

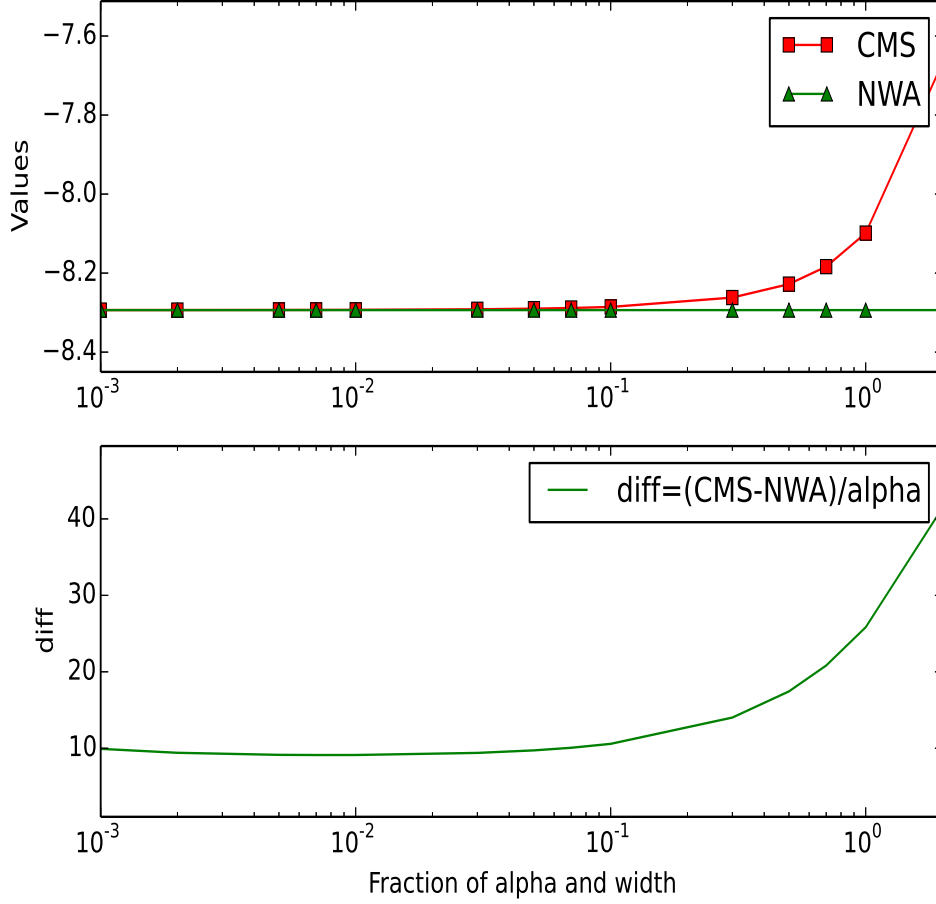


Figure 3: Cross checks for $e^+\nu_e \rightarrow W^+ \rightarrow \mu^+\nu_m$ in the non-resonance region with the correct LO width Γ_W^{LO} .

the results in CMS and NWA:

$$\begin{aligned}
\text{CMS} \times \alpha_{\text{ew}} |\mathcal{A}_{\text{Born}}^{\text{NWA}}|^2 &= 2\Im \mathcal{A}_{\text{Virtual}}^{\text{CMS}} \mathcal{A}_{\text{Born}}^{\text{CMS}*} |_{\delta Z_e=0, \delta s_w=0} \\
&\quad + 2\Im \mathcal{A}_{\text{Virtual}}^{\text{Born}} (\mathcal{A}_{\text{Born}}^{\text{CMS}*} |_{(\Gamma_Z=0 \text{ in } Z \text{ propagator only})}), \\
\text{NWA} \times \alpha_{\text{ew}} |\mathcal{A}_{\text{Born}}^{\text{NWA}}|^2 &= 2\Im \mathcal{A}_{\text{Virtual}}^{\text{NWA}} \mathcal{A}_{\text{Born}}^{\text{NWA}*}, \\
\text{diff} &= (\text{CMS} - \text{NWA})/\alpha_{\text{ew}}.
\end{aligned} \tag{E.4}$$

E.2.2 Resonance region: ε -offshellness method

Similarly, we have the following notations for comparison between the results in CMS and NWA:

$$\begin{aligned}
\text{CMS} &= 2\Re(\mathcal{A}_{\text{Virtual}}^{\text{CMS}}) \mathcal{A}_{\text{Born}}^{\text{CMS}*} / \alpha_{\text{ew}} \\
\text{NWA} &= 2\Re \mathcal{A}_{\text{Virtual}}^{\text{NWA}} \mathcal{A}_{\text{Born}}^{\text{NWA}*} / \alpha_{\text{ew}} \times \frac{\varepsilon^2}{\Gamma_Z^2 M_Z^2}, \\
\text{diff} &= (\text{CMS} - \text{NWA})/\alpha_{\text{ew}},
\end{aligned} \tag{E.5}$$

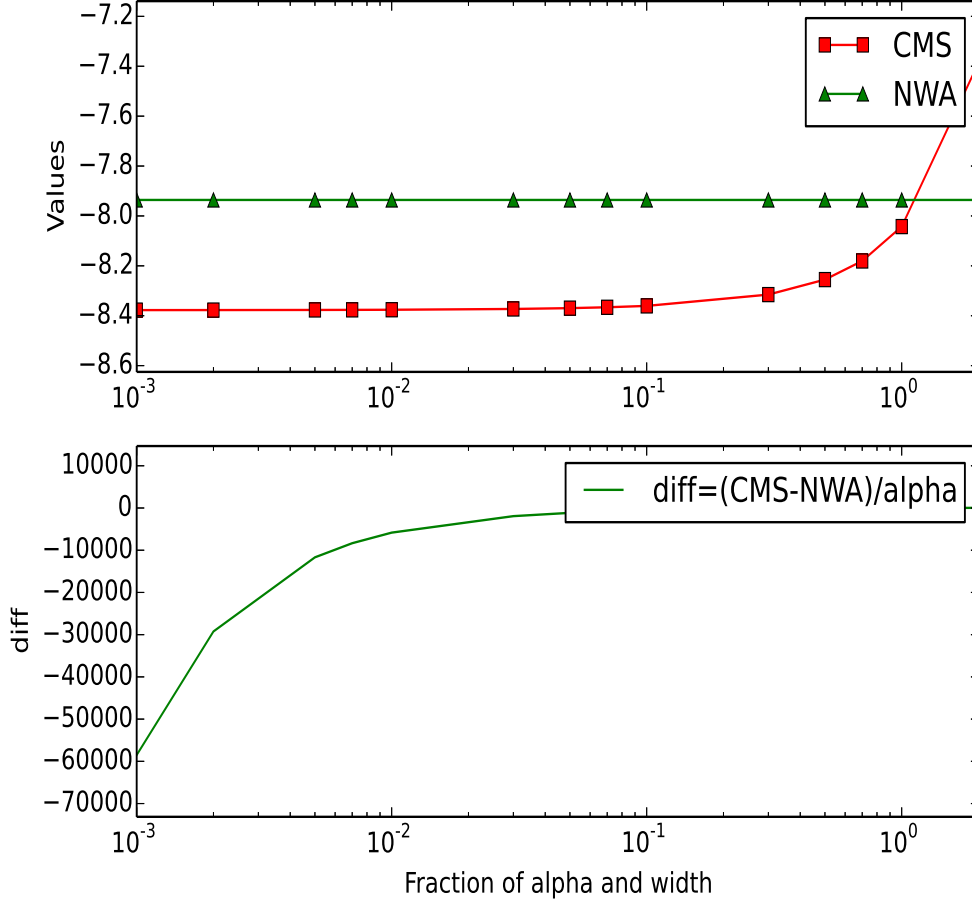
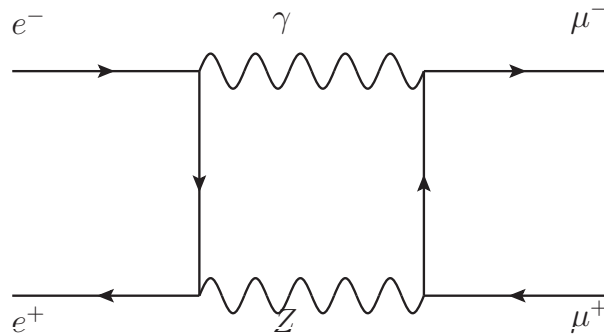


Figure 4: Cross checks for $e^+\nu_e \rightarrow W^+ \rightarrow \mu^+\nu_\mu$ in the non-resonance region with the wrong LO width, i.e. $\Gamma_W = 1.2\Gamma_W^{\text{LO}}$.

where the virtual amplitudes in CMS and NWA have been excluded the corresponding photon exchange box diagrams at least with one Z like



E.3 $e^+\nu_e \rightarrow t\bar{b} \rightarrow W^+b\bar{b}$

E.3.1 Non-resonance region

For this $2 \rightarrow 3$ process, the direct comparison between CMS and NWA of the real part

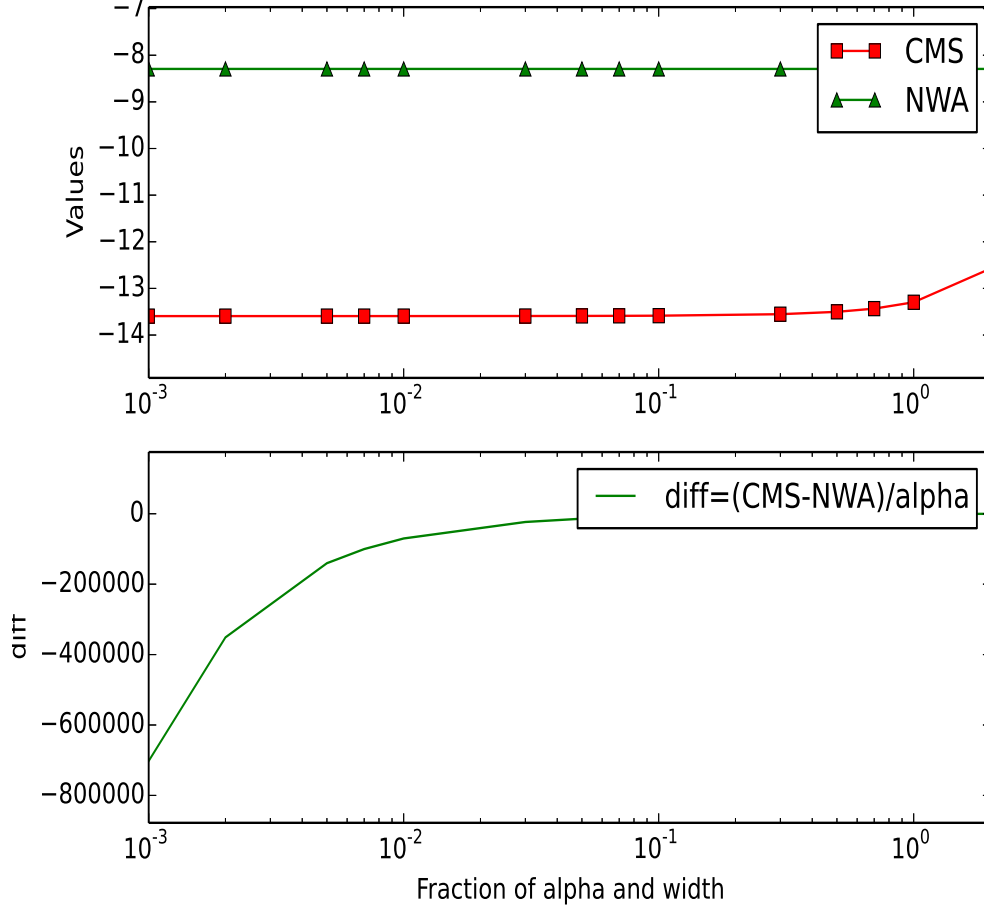


Figure 5: Cross checks for $e^+\nu_e \rightarrow W^+ \rightarrow \mu^+\nu_m$ in the non-resonance region with the correct LO width but using the normal logarithms.

in the amplitude squared would not be a trivial cross check. Hence, we can define the following variables:

$$\begin{aligned}
 \text{CMS} &= [2\Re(\mathcal{A}_{\text{Virtual}}^{\text{CMS}}\mathcal{A}_{\text{Born}}^{\text{CMS}*}) + |\mathcal{A}_{\text{Born}}^{\text{CMS}}|^2 - |\mathcal{A}_{\text{Born}}^{\text{NWA}}|^2] / (\alpha_{\text{ew}}|\mathcal{A}_{\text{Born}}^{\text{NWA}}|^2) \\
 \text{NWA} &= 2\Re(\mathcal{A}_{\text{Virtual}}^{\text{NWA}}\mathcal{A}_{\text{Born}}^{\text{NWA}*}) / (\alpha_{\text{ew}}|\mathcal{A}_{\text{Born}}^{\text{NWA}}|^2), \\
 \text{diff} &= (\text{CMS} - \text{NWA})/\alpha_{\text{ew}},
 \end{aligned}
 \tag{E.7}$$

Because the resonance in this process we want to check is the top quark resonance only¹⁷, we take all of the widths except top quark are zero. Especially, since W^+ is a final state, we should take it to be stable (i.e. $\Gamma_W = 0$) in order to maintain the unitarity of the amplitude. In Fig.15, we perform a direct comparison with the UV CTs in CMS but taking $\Gamma_{W^\pm, Z, H, G^0, G^\pm} = 0$. Apparently, CMS is not equal to NWA when $\Gamma_t, \alpha_{\text{ew}} \rightarrow 0$. The reason because one should take the NWA form (i.e. take the real part of it) of W mass and wavefunction renormalization constant and Z mass renormalization constant and Weinberg angle s_w, c_w renormalization constants instead of the CMS ones.

¹⁷There is also Z resonance, which we have $e^+\nu_e \rightarrow W^+Z \rightarrow W^+b\bar{b}$.

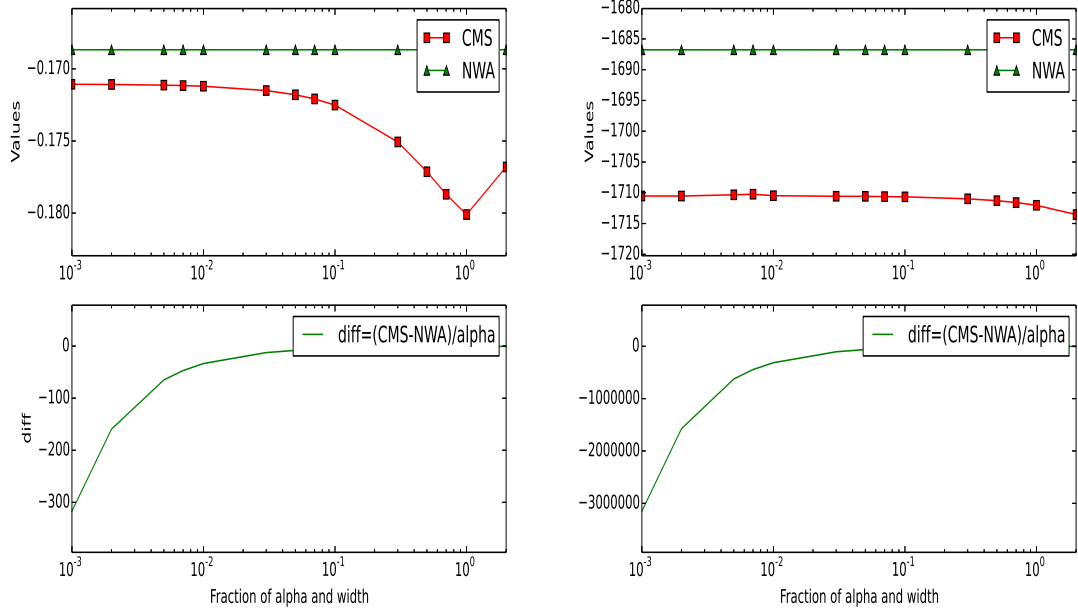


Figure 6: Cross checks for $e^+\nu_e \rightarrow W^+ \rightarrow \mu^+\nu_m$ in the resonance region with the correct LO width Γ_W^{LO} (left pannel) and $\Gamma_W = 10^{-2} \times \Gamma_W^{\text{LO}}$ (right pannel), where we take the offshellness to be $\varepsilon = p^2 - M_W^2 = 10^{-2} \times \Gamma_W^{\text{min}} M_W$.

E.4 $u\bar{d} \rightarrow W^+ + \gamma \rightarrow e^+\nu_e + \gamma$

Similar to the Eq.(E.7), we can directly compare the following variables

$$\begin{aligned}
\text{CMS} &= [2\Re(\mathcal{A}_{\text{Virtual}}^{\text{CMS}}\mathcal{A}_{\text{Born}}^{\text{CMS}*}) + |\mathcal{A}_{\text{Born}}^{\text{CMS}}|^2 - |\mathcal{A}_{\text{Born}}^{\text{NWA}}|^2] / (\alpha_{ew}|\mathcal{A}_{\text{Born}}^{\text{NWA}}|^2) \\
\text{NWA} &= 2\Re(\mathcal{A}_{\text{Virtual}}^{\text{NWA}}\mathcal{A}_{\text{Born}}^{\text{NWA}*}) / (\alpha_{ew}|\mathcal{A}_{\text{Born}}^{\text{NWA}}|^2), \\
\text{diff} &= (\text{CMS} - \text{NWA})/\alpha_{ew}.
\end{aligned} \tag{E.8}$$

Here, we don't need to take any special treatment because all of the final states are stable states.

E.4.1 Non-resonance region

E.5 $u\bar{u} \rightarrow Z/\gamma^* + \gamma \rightarrow e^+e^- + \gamma$

E.5.1 Non-resonance region

Similar to the Eq.(E.7), we can directly compare the following variables

$$\begin{aligned}
\text{CMS} &= [2\Re(\mathcal{A}_{\text{Virtual}}^{\text{CMS}}\mathcal{A}_{\text{Born}}^{\text{CMS}*}) + |\mathcal{A}_{\text{Born}}^{\text{CMS}}|^2 - |\mathcal{A}_{\text{Born}}^{\text{NWA}}|^2] / (\alpha_{ew}|\mathcal{A}_{\text{Born}}^{\text{NWA}}|^2) \\
\text{NWA} &= 2\Re(\mathcal{A}_{\text{Virtual}}^{\text{NWA}}\mathcal{A}_{\text{Born}}^{\text{NWA}*}) / (\alpha_{ew}|\mathcal{A}_{\text{Born}}^{\text{NWA}}|^2), \\
\text{diff} &= (\text{CMS} - \text{NWA})/\alpha_{ew}.
\end{aligned} \tag{E.9}$$

Here, we don't need to take any special treatment because all of the final states are stable states. Here, one can take W 's width to be zero only when its mass renormalization constant

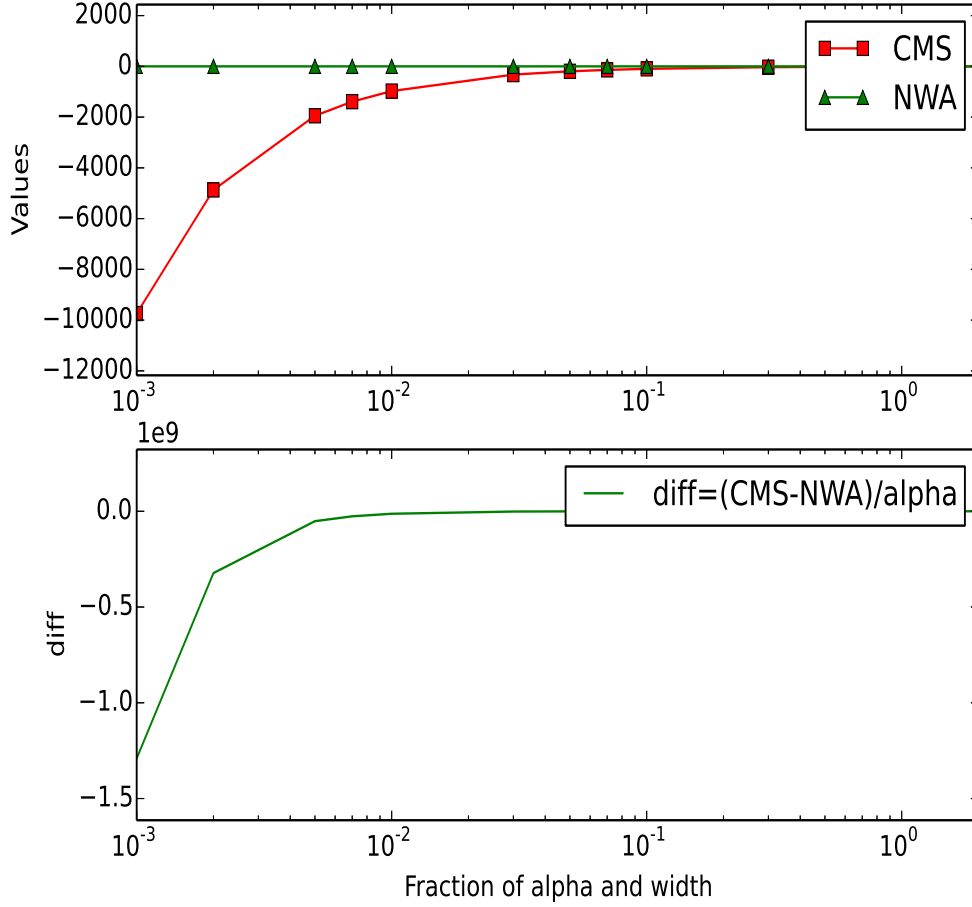


Figure 7: Cross checks for $e^+\nu_e \rightarrow W^+ \rightarrow \mu^+\nu_\mu$ in the resonance region with the correct LO width Γ_W^{LO} but using the normal logarithms, where we also take $\varepsilon = p^2 - M_W^2 = 10^{-2} \times \Gamma_W^{\text{min}} M_W$.

as well as $\delta s_w, \delta c_w$ to be in the NWA case (i.e. take the real part to the corresponding W mass renormalization in $\delta s_w, \delta c_w$). In order to avoid this problem, we keep the exact LO W width as well as the LO Z width.

E.6 $e^+\nu_e \rightarrow \mu^+\nu_\mu b\bar{b}$

E.6.1 Non-resonance region

Similar to the Eq.(E.7), we can directly compare the following variables

$$\begin{aligned}
 \text{CMS} &= [2\Re(\mathcal{A}_{\text{Virtual}}^{\text{CMS}} \mathcal{A}_{\text{Born}}^{\text{CMS}*}) + |\mathcal{A}_{\text{Born}}^{\text{CMS}}|^2 - |\mathcal{A}_{\text{Born}}^{\text{NWA}}|^2] / (\alpha_{ew} |\mathcal{A}_{\text{Born}}^{\text{NWA}}|^2) \\
 \text{NWA} &= 2\Re(\mathcal{A}_{\text{Virtual}}^{\text{NWA}} \mathcal{A}_{\text{Born}}^{\text{NWA}*}) / (\alpha_{ew} |\mathcal{A}_{\text{Born}}^{\text{NWA}}|^2), \\
 \text{diff} &= (\text{CMS} - \text{NWA}) / \alpha_{ew}.
 \end{aligned} \tag{E.10}$$

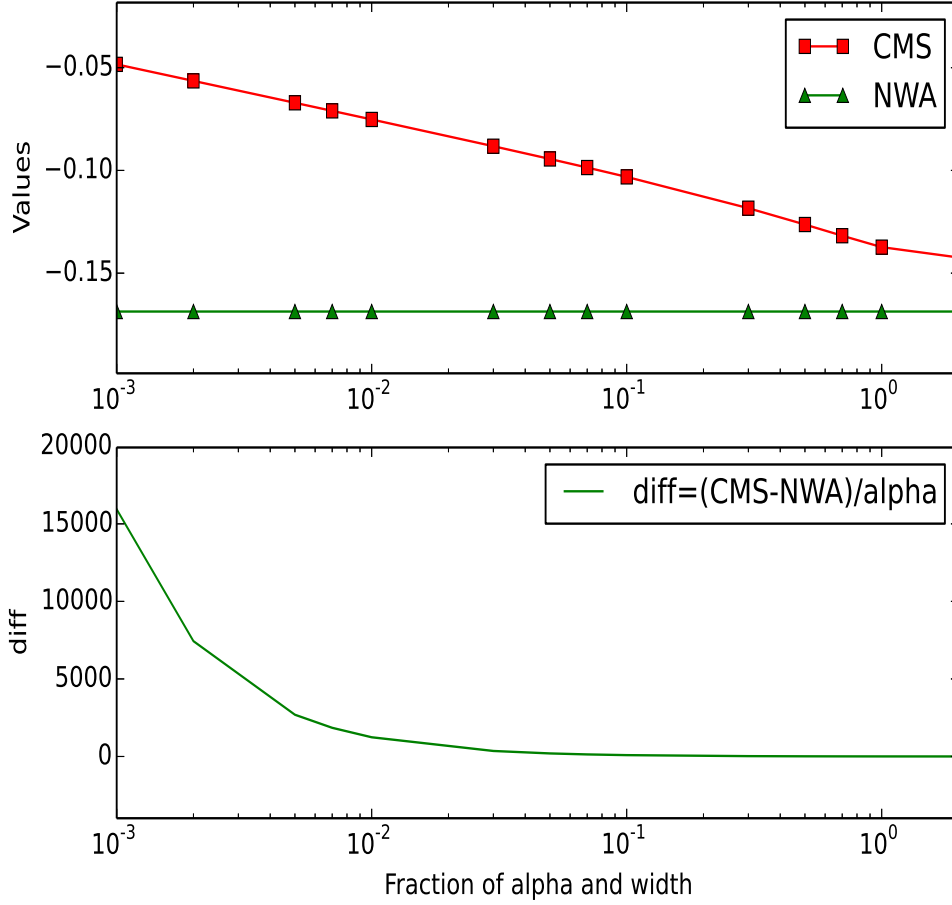


Figure 8: Cross checks for $e^+\nu_e \rightarrow W^+ \rightarrow \mu^+\nu_\mu$ in the resonance region with the correct LO width Γ_W^{LO} without adding the term $B_0(M_W^2 - i\Gamma_W M_W, 0, M_W^2 - i\Gamma_W M_W) - B_0(M_W^2, 0, M_W^2 - i\Gamma_W M_W)$ in W mass renormalization constant.

Here, we don't need to take any special treatment because all of the final states are stable states. Because there are top quark, W and Z resonances, we keep the exact LO Z, W, and top quark widths here.

E.7 $gg \rightarrow \mu^+\nu_\mu b\mu^-\bar{\nu}_\mu\bar{b}$

E.7.1 Non-resonance region

Similar to the Eq.(E.7), we can directly compare the following variables

$$\begin{aligned}
 \text{CMS} &= [2\Re(\mathcal{A}_{\text{Virtual}}^{\text{CMS}}\mathcal{A}_{\text{Born}}^{\text{CMS}*}) + |\mathcal{A}_{\text{Born}}^{\text{CMS}}|^2 - |\mathcal{A}_{\text{Born}}^{\text{NWA}}|^2] / (\alpha_{\text{ew}}|\mathcal{A}_{\text{Born}}^{\text{NWA}}|^2) \\
 \text{NWA} &= 2\Re(\mathcal{A}_{\text{Virtual}}^{\text{NWA}}\mathcal{A}_{\text{Born}}^{\text{NWA}*}) / (\alpha_{\text{ew}}|\mathcal{A}_{\text{Born}}^{\text{NWA}}|^2), \\
 \text{diff} &= (\text{CMS} - \text{NWA})/\alpha_{\text{ew}}.
 \end{aligned}
 \tag{E.11}$$

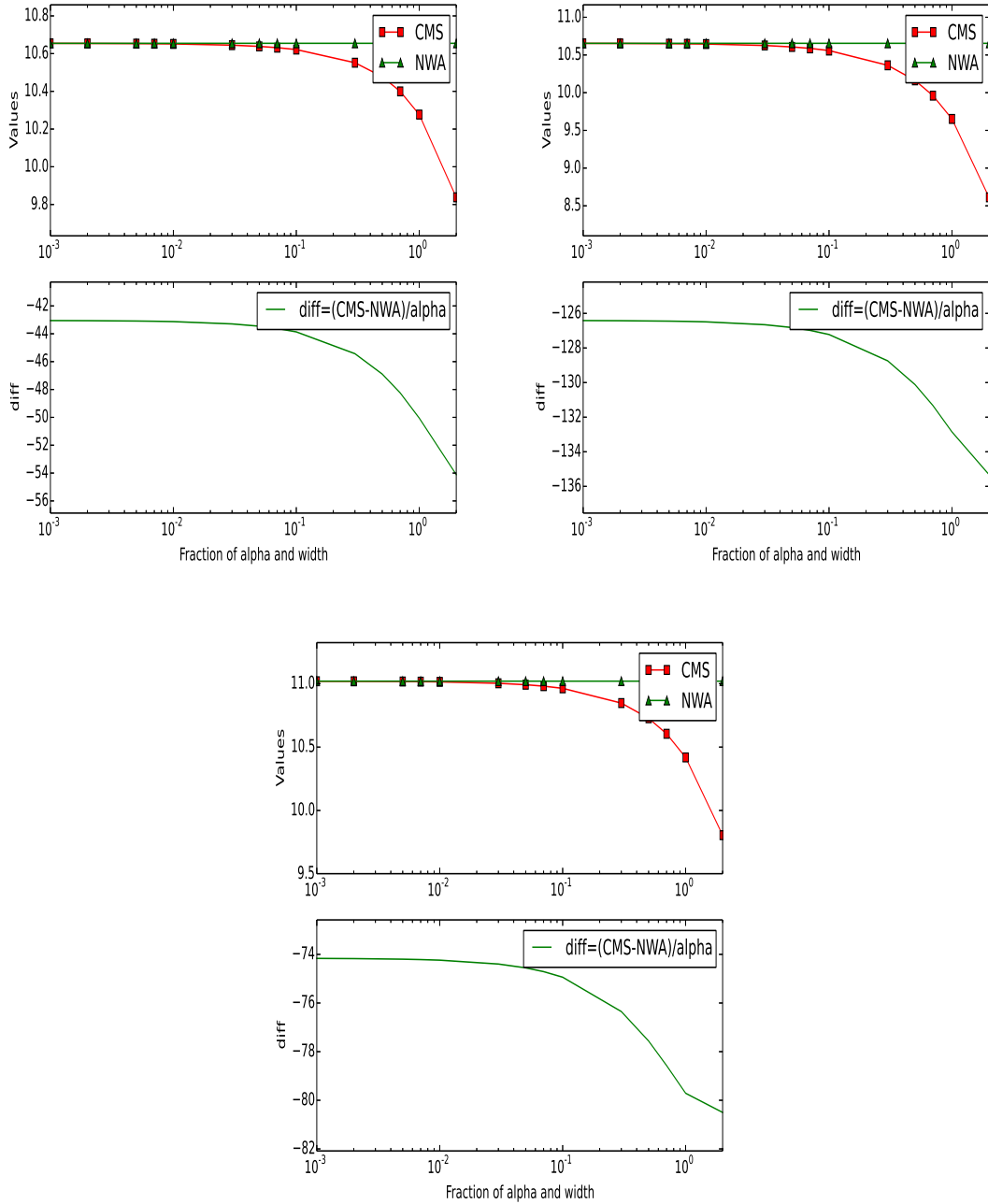


Figure 9: Trivial cross checks of the real part of the virtual for $e^+e^- \rightarrow Z/\gamma^* \rightarrow \mu^+\mu^-$ in the non-resonance region with the correct LO width Γ_Z^{LO} (upper-left panel), with the normal logarithm (upper-right panel), with the width $\Gamma_Z = 1.2\Gamma_Z^{\text{LO}}$ (lower panel).

Here, we don't need to take any special treatment because all of the final states are stable states. Because there are top quark, W and Z resonances, we keep the exact LO Z, W, and top quark widths here.

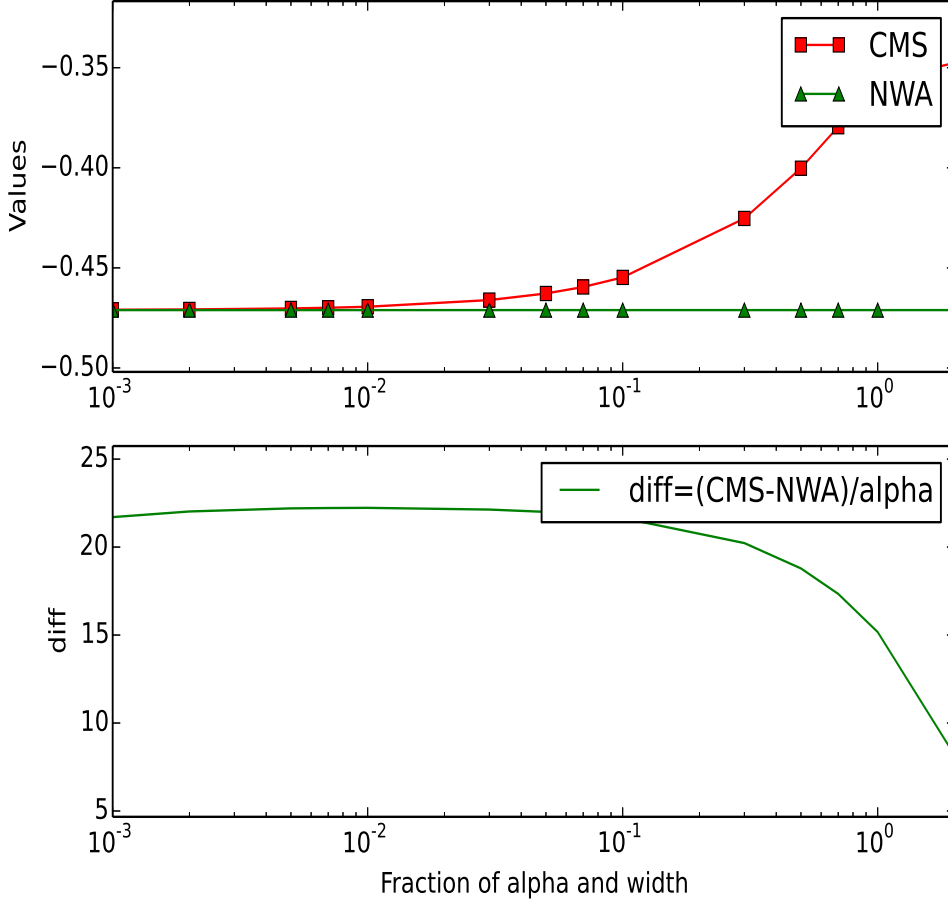


Figure 10: Cross checks for $e^+e^- \rightarrow Z/\gamma^* \rightarrow \mu^+\mu^-$ in the non-resonance region with the correct LO width Γ_Z^{LO} .

E.8 $b\gamma \rightarrow \mu^+\nu_\mu b\mu^-\bar{\nu}_\mu$

E.8.1 Non-resonance region

Similar to the Eq.(E.7), we can directly compare the following variables

$$\begin{aligned}
 \text{CMS} &= [2\Re(\mathcal{A}_{\text{Virtual}}^{\text{CMS}}\mathcal{A}_{\text{Born}}^{\text{CMS}*}) + |\mathcal{A}_{\text{Born}}^{\text{CMS}}|^2 - |\mathcal{A}_{\text{Born}}^{\text{NWA}}|^2] / (\alpha_{\text{ew}}|\mathcal{A}_{\text{Born}}^{\text{NWA}}|^2) \\
 \text{NWA} &= 2\Re(\mathcal{A}_{\text{Virtual}}^{\text{NWA}}\mathcal{A}_{\text{Born}}^{\text{NWA}*}) / (\alpha_{\text{ew}}|\mathcal{A}_{\text{Born}}^{\text{NWA}}|^2), \\
 \text{diff} &= (\text{CMS} - \text{NWA})/\alpha_{\text{ew}}.
 \end{aligned}
 \tag{E.12}$$

Here, we don't need to take any special treatment because all of the final states are stable states. Because there are top quark, W and Z resonances, we keep the exact LO Z, W, and top quark widths here.

Acknowledgments

We are grateful to Ansgar Denner for very helpful discussions. This work was performed in the ERC grant 291377 ‘‘LHCtheory: Theoretical predictions and analyses of LHC physics: advancing the precision frontier’’.

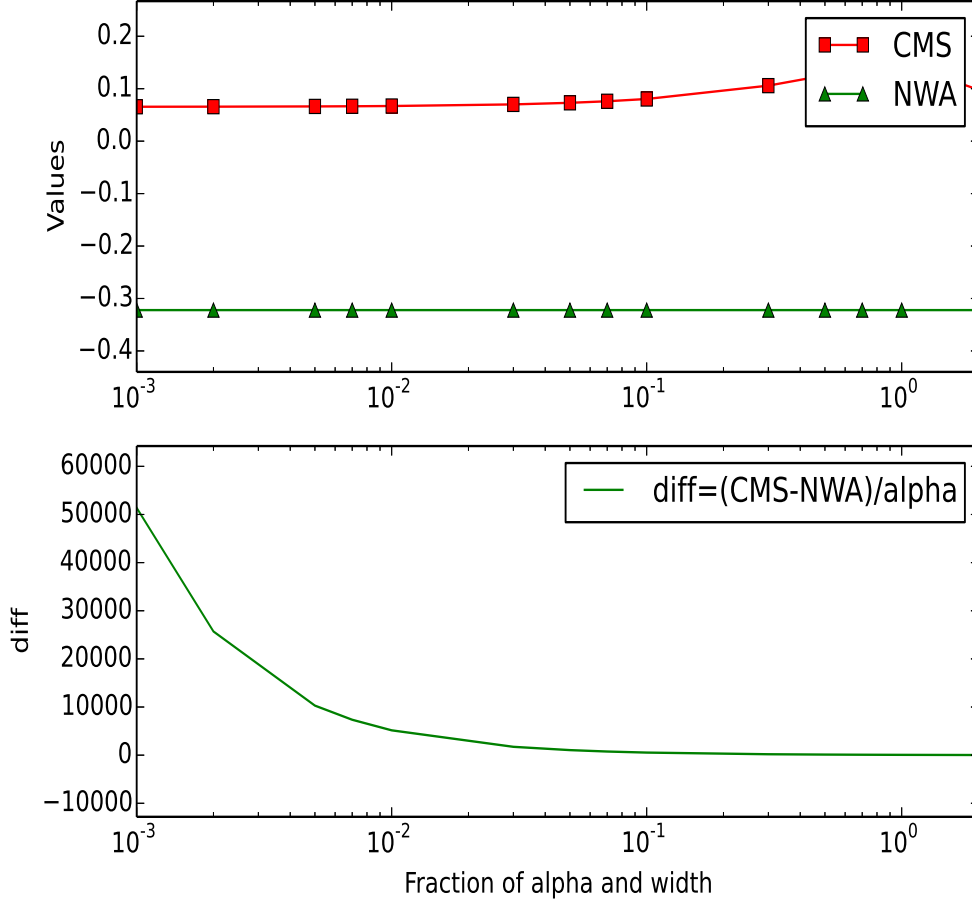


Figure 11: Cross checks for $e^+e^- \rightarrow Z/\gamma^* \rightarrow \mu^+\mu^-$ in the non-resonance region with the wrong LO width, i.e. $\Gamma_Z = 1.2\Gamma_Z^{\text{LO}}$.

References

- [1] D. Ross and J. Taylor, *RENORMALIZATION OF A UNIFIED THEORY OF WEAK AND ELECTROMAGNETIC INTERACTIONS*, *Nucl.Phys.* **B51** (1973) 125–144.
- [2] A. Denner, *Techniques for calculation of electroweak radiative corrections at the one loop level and results for W physics at LEP-200*, *Fortschr. Phys.* **41** (1993) 307–420, [[arXiv:0709.1075](https://arxiv.org/abs/0709.1075)].
- [3] H. Lehmann, K. Symanzik, and W. Zimmermann, *On the formulation of quantized field theories*, *Nuovo Cim.* **1** (1955) 205–225.
- [4] M. Veltman, *Unitarity and causality in a renormalizable field theory with unstable particles*, *Physica* **29** (1963) 186–207.
- [5] R. G. Stuart, *Gauge invariance, analyticity and physical observables at the Z0 resonance*, *Phys.Lett.* **B262** (1991) 113–119.
- [6] B. A. Kniehl and A. Sirlin, *Differences between the pole and on-shell masses and widths of the Higgs boson*, *Phys.Rev.Lett.* **81** (1998) 1373–1376, [[hep-ph/9805390](https://arxiv.org/abs/hep-ph/9805390)].

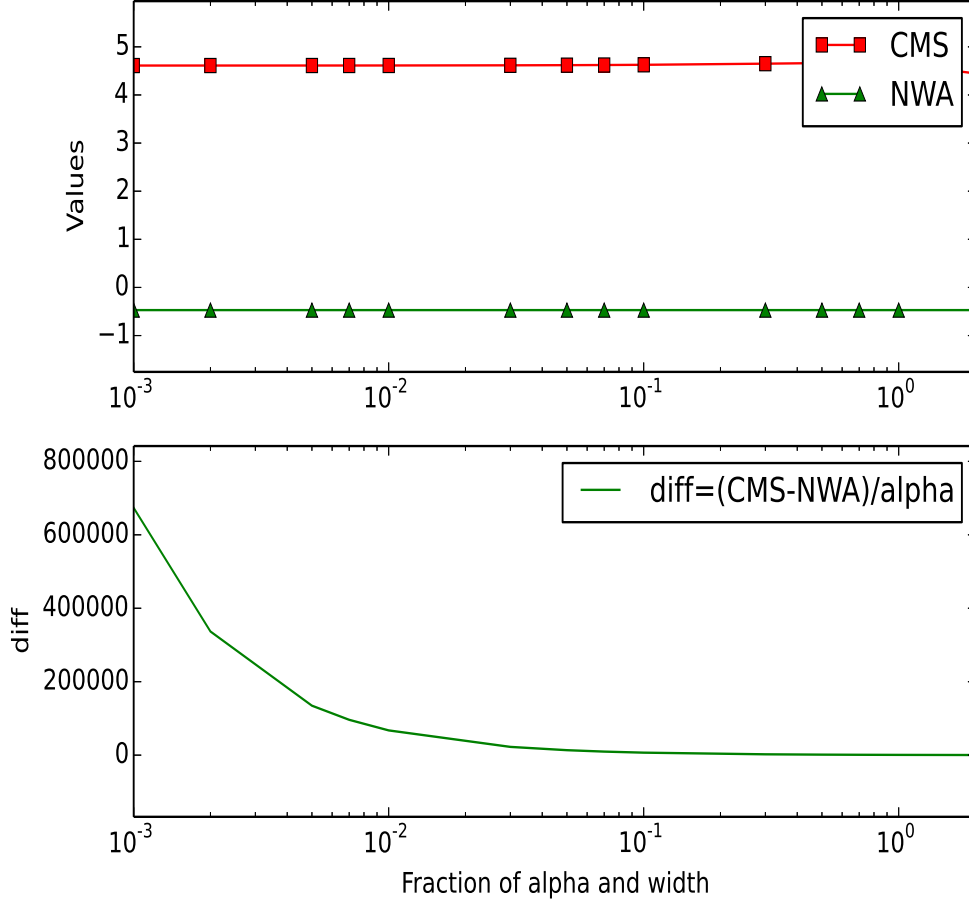


Figure 12: Cross checks for $e^+e^- \rightarrow Z/\gamma^* \rightarrow \mu^+\mu^-$ in the non-resonance region with the correct LO width but using the normal logarithms.

- [7] B. A. Kniehl, C. P. Palisoc, and A. Sirlin, *Elimination of threshold singularities in the relation between on shell and pole widths*, *Phys.Rev.* **D66** (2002) 057902, [[hep-ph/0205304](#)].
- [8] P. A. Grassi, B. A. Kniehl, and A. Sirlin, *Width and partial widths of unstable particles in the light of the Nielsen identities*, *Phys.Rev.* **D65** (2002) 085001, [[hep-ph/0109228](#)].
- [9] G. Passarino, C. Sturm, and S. Uccirati, *Higgs Pseudo-Observables, Second Riemann Sheet and All That*, *Nucl.Phys.* **B834** (2010) 77–115, [[arXiv:1001.3360](#)].
- [10] R. G. Stuart, *General renormalization of the gauge invariant perturbation expansion near the Z_0 resonance*, *Phys.Lett.* **B272** (1991) 353–358.
- [11] A. Sirlin, *Observations concerning mass renormalization in the electroweak theory*, *Phys.Lett.* **B267** (1991) 240–242.
- [12] A. Sirlin, *Theoretical considerations concerning the Z_0 mass*, *Phys.Rev.Lett.* **67** (1991) 2127–2130.
- [13] F. Dyson, *The Radiation theories of Tomonaga, Schwinger, and Feynman*, *Phys.Rev.* **75** (1949) 486–502.
- [14] G. Breit and E. Wigner, *Capture of Slow Neutrons*, *Phys.Rev.* **49** (1936) 519–531.

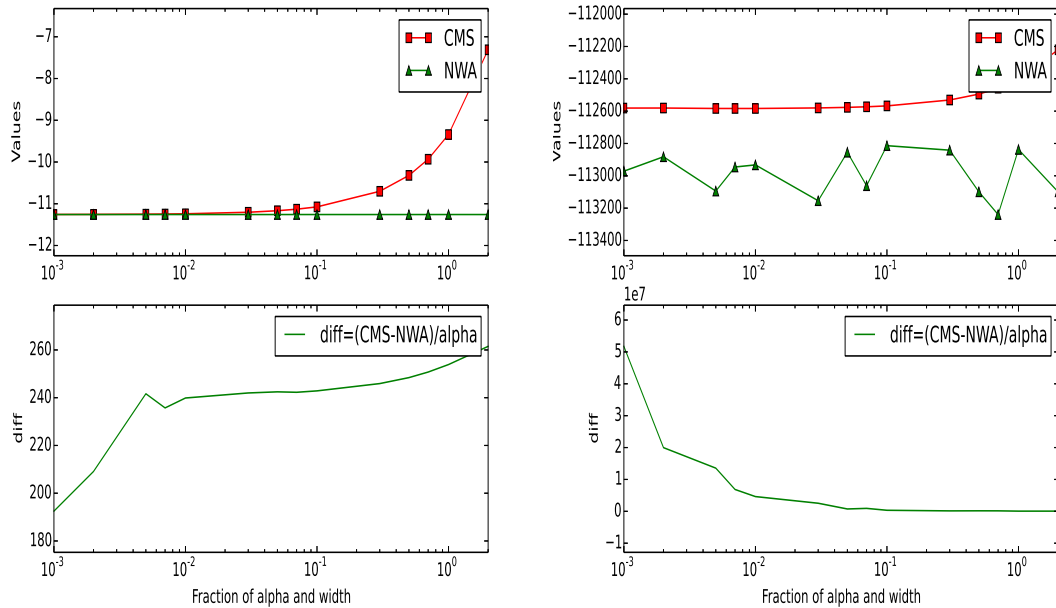


Figure 13: Cross checks for $e^+e^- \rightarrow Z/\gamma^* \rightarrow \mu^+\mu^-$ in the resonance region with the correct LO width Γ_Z^{LO} (left pannel) and $\Gamma_Z = 10^{-2} \times \Gamma_Z^{\text{LO}}$ (right pannel), where we take the offshellness to be $\varepsilon = p^2 - M_Z^2 = 10^{-2} \times \Gamma_Z^{\text{min}} M_Z$.

- [15] A. Denner, S. Dittmaier, M. Roth, and L. Wieders, *Electroweak corrections to charged-current $e^+e^- \rightarrow 4$ fermion processes: Technical details and further results*, *Nucl.Phys.* **B724** (2005) 247–294, [[hep-ph/0505042](#)].
- [16] A. Denner, S. Dittmaier, M. Roth, and D. Wackerroth, *Predictions for all processes $e^+e^- \rightarrow 4$ fermions + gamma*, *Nucl.Phys.* **B560** (1999) 33–65, [[hep-ph/9904472](#)].
- [17] A. Denner and S. Dittmaier, *The Complex-mass scheme for perturbative calculations with unstable particles*, *Nucl.Phys.Proc.Suppl.* **160** (2006) 22–26, [[hep-ph/0605312](#)].
- [18] A. Chapovsky, V. A. Khoze, A. Signer, and W. J. Stirling, *Nonfactorizable corrections and effective field theories*, *Nucl.Phys.* **B621** (2002) 257–302, [[hep-ph/0108190](#)].
- [19] M. Beneke, A. Chapovsky, A. Signer, and G. Zanderighi, *Effective theory approach to unstable particle production*, *Phys.Rev.Lett.* **93** (2004) 011602, [[hep-ph/0312331](#)].
- [20] M. Beneke, A. Chapovsky, A. Signer, and G. Zanderighi, *Effective theory calculation of resonant high-energy scattering*, *Nucl.Phys.* **B686** (2004) 205–247, [[hep-ph/0401002](#)].
- [21] T. Bauer, J. Gegelia, G. Japaridze, and S. Scherer, *Complex-mass scheme and perturbative unitarity*, *Int.J.Mod.Phys.* **A27** (2012) 1250178, [[arXiv:1211.1684](#)].
- [22] A. Denner and J.-N. Lang, *The Complex-Mass Scheme and Unitarity in perturbative Quantum Field Theory*, [arXiv:1406.6280](#).
- [23] S. Dittmaier, *Separation of soft and collinear singularities from one loop N point integrals*, *Nucl.Phys.* **B675** (2003) 447–466, [[hep-ph/0308246](#)].

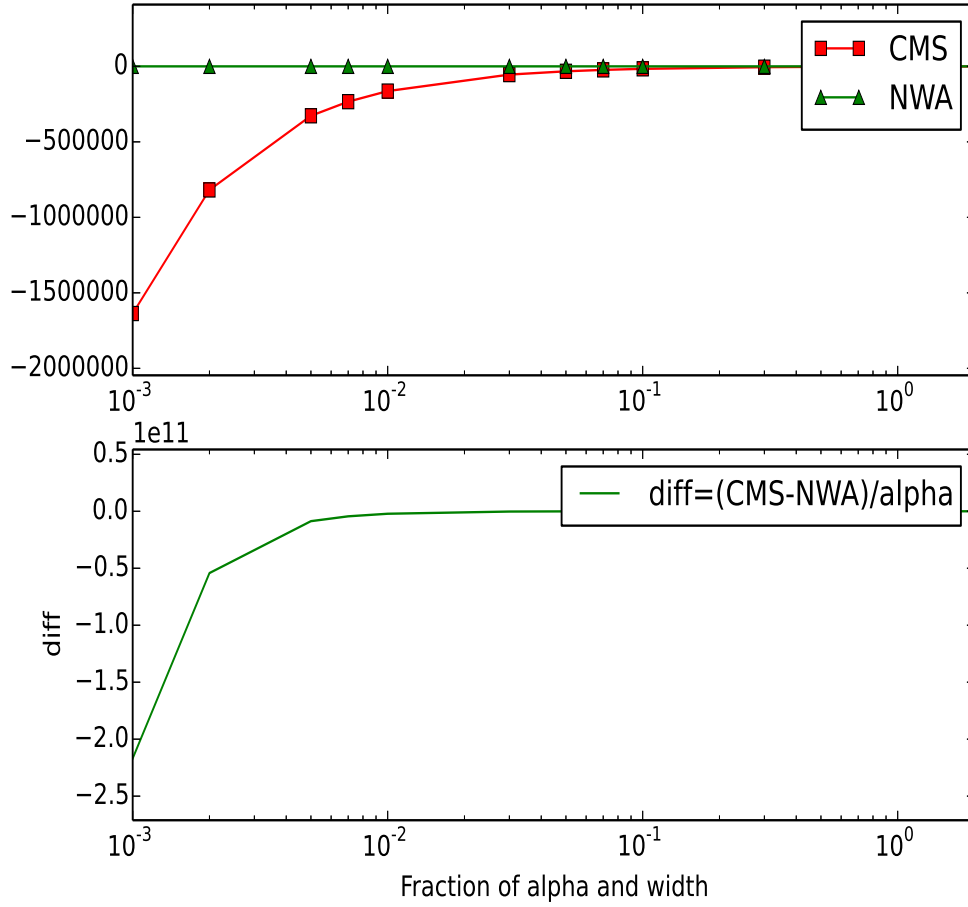


Figure 14: Cross checks for $e^+e^- \rightarrow Z/\gamma^* \rightarrow \mu^+\mu^-$ in the resonance region with the correct LO width Γ_Z^{LO} but using the normal logarithms, where we also take $\varepsilon = p^2 - M_Z^2 = 10^{-2} \times \Gamma_Z^{\text{min}} M_Z$.

- [24] S. Catani, T. Gleisberg, F. Krauss, G. Rodrigo, and J.-C. Winter, *From loops to trees by-passing Feynman's theorem*, *JHEP* **0809** (2008) 065, [[arXiv:0804.3170](#)].
- [25] M. Beneke and V. A. Smirnov, *Asymptotic expansion of Feynman integrals near threshold*, *Nucl.Phys.* **B522** (1998) 321–344, [[hep-ph/9711391](#)].

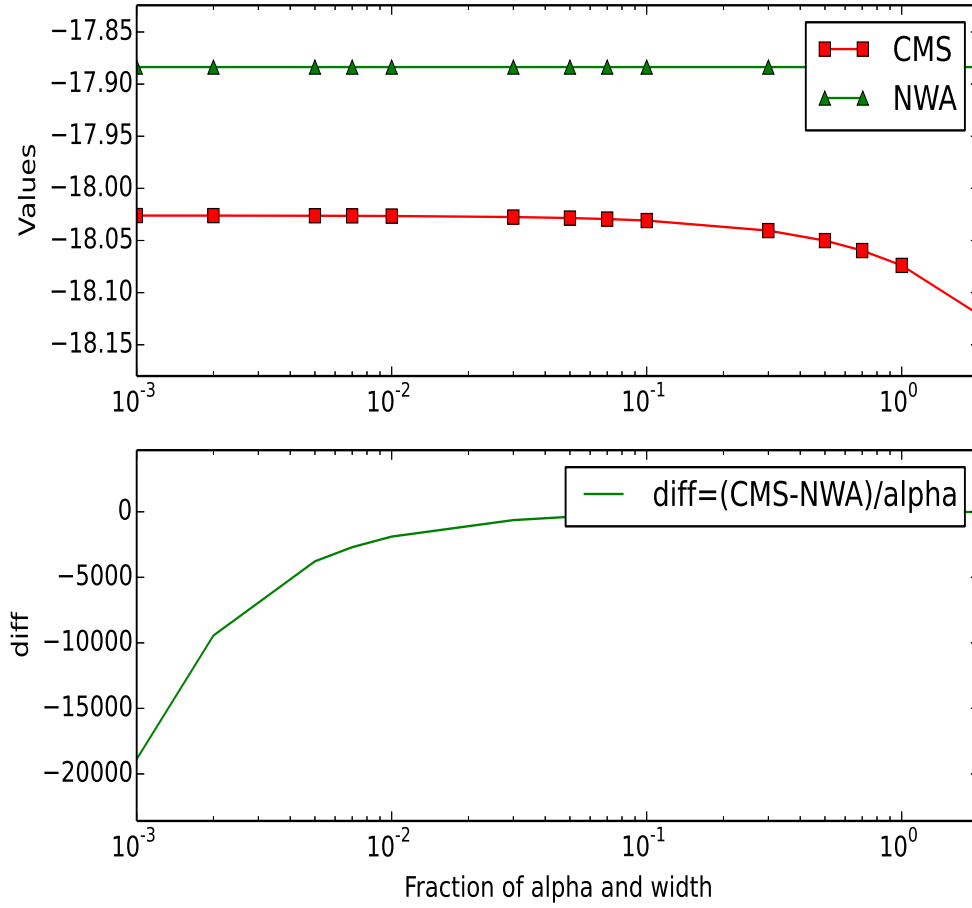


Figure 15: Cross checks for $e^+\nu_e \rightarrow t\bar{b} \rightarrow W^+b\bar{b}$ in the non-resonance region with the correct LO width Γ_t^{LO} but not taking real part to W, Z renormalization constants.

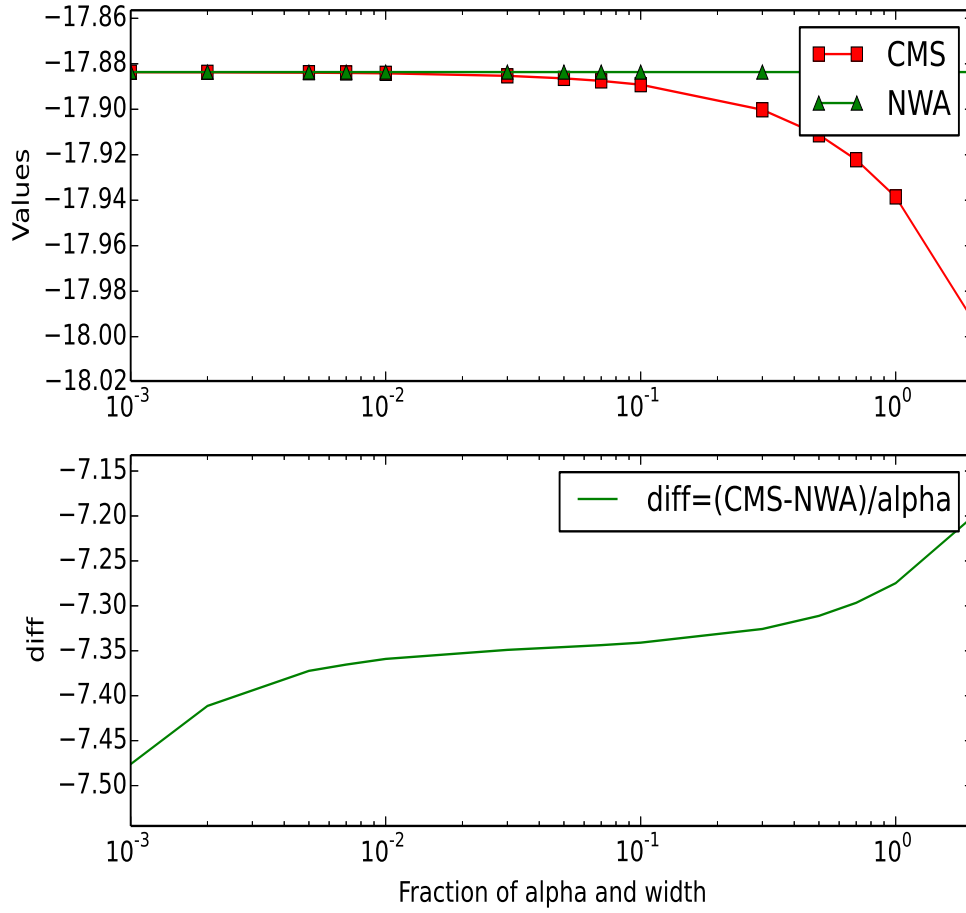


Figure 16: Cross checks for $e^+\nu_e \rightarrow t\bar{b} \rightarrow W^+b\bar{b}$ in the non-resonance region with the correct LO width Γ_t^{LO} .

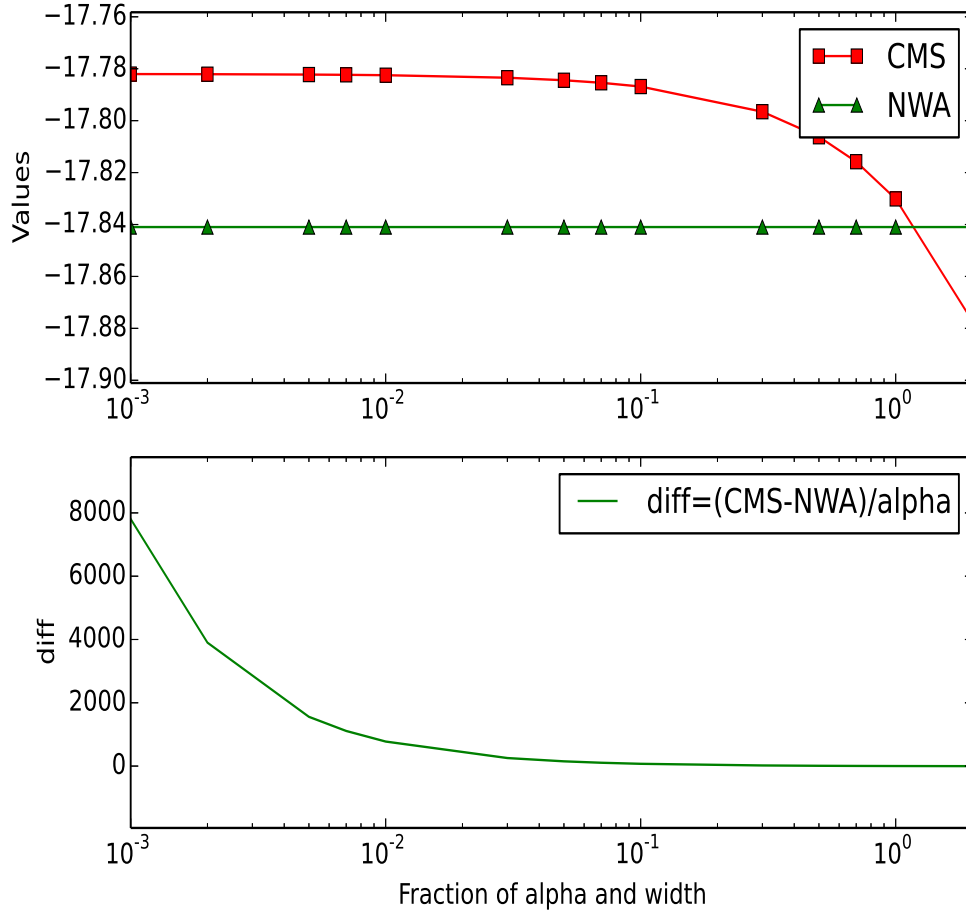


Figure 17: Cross checks for $e^+ \nu_e \rightarrow t \bar{b} \rightarrow W^+ b \bar{b}$ in the non-resonance region with the wrong LO width, i.e. $\Gamma_t = 1.2 \Gamma_t^{\text{LO}}$.

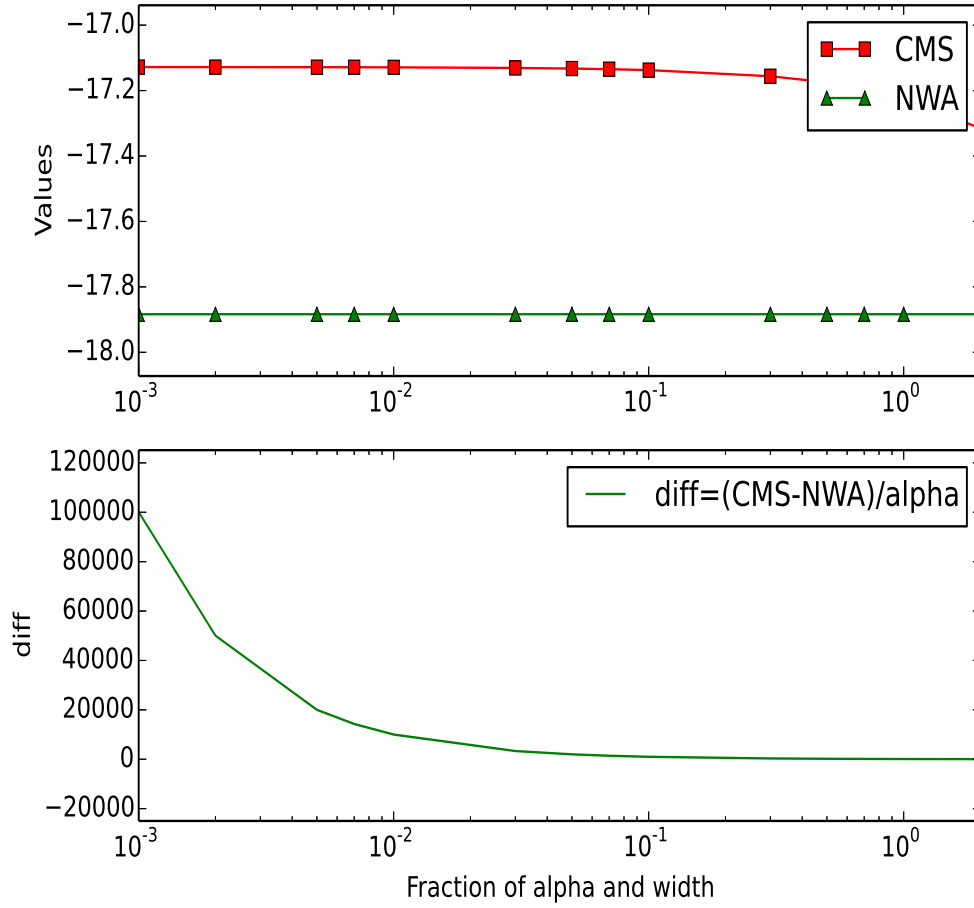


Figure 18: Cross checks for $e^+\nu_e \rightarrow t\bar{b} \rightarrow W^+b\bar{b}$ in the non-resonance region with the correct LO width but using the normal logarithms.

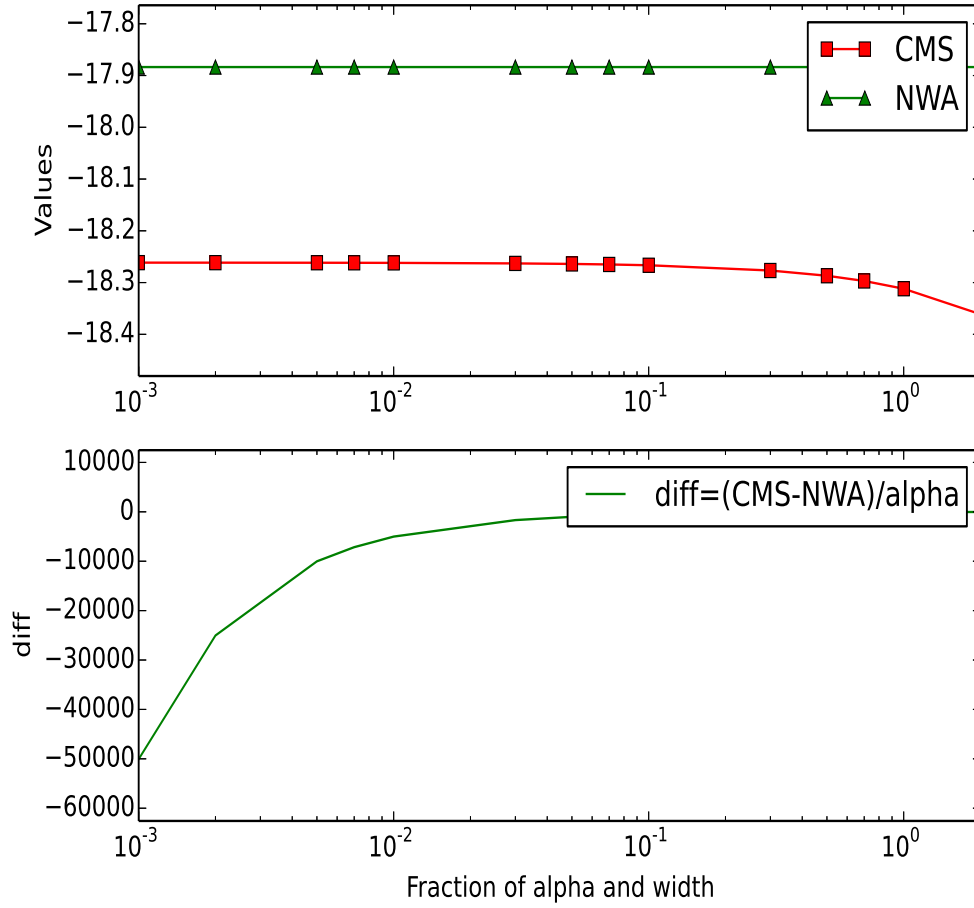


Figure 19: Cross checks for $e^+\nu_e \rightarrow t\bar{b} \rightarrow W^+b\bar{b}$ in the non-resonance region with the correct LO width without Born contributions.

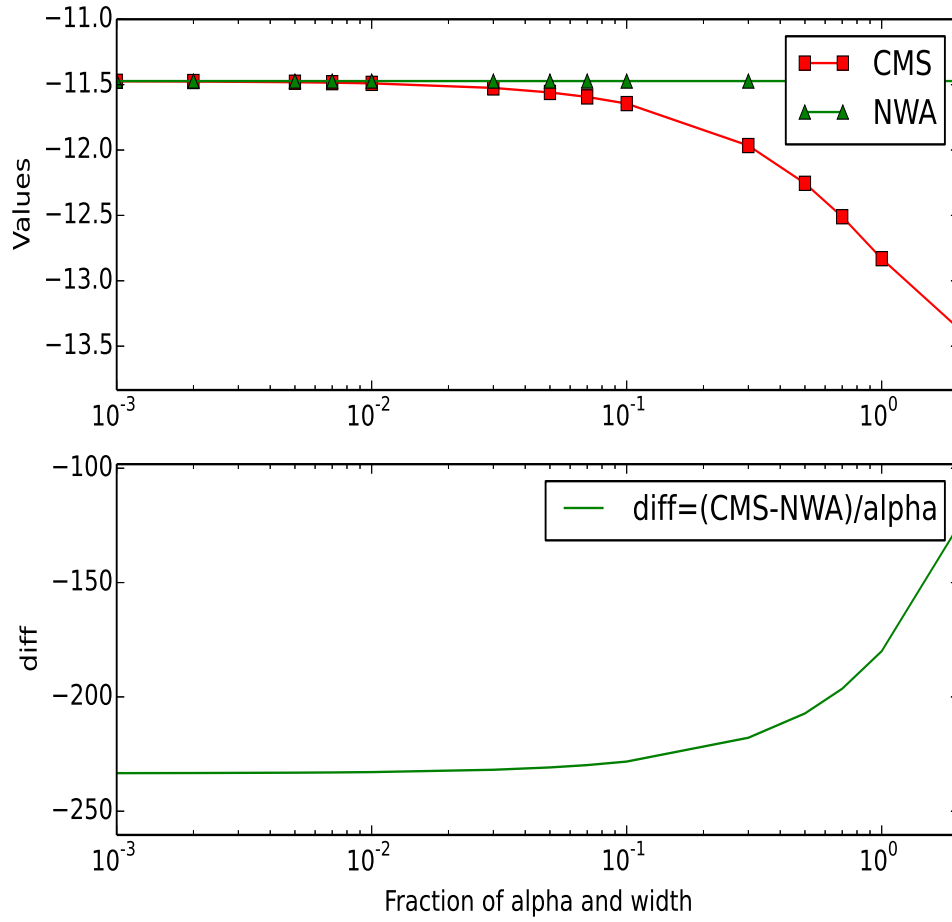


Figure 20: Cross checks for $u\bar{d} \rightarrow W^+ + \gamma \rightarrow e^+\nu_e + \gamma$ in the non-resonance region with the correct LO width Γ_W^{LO} .

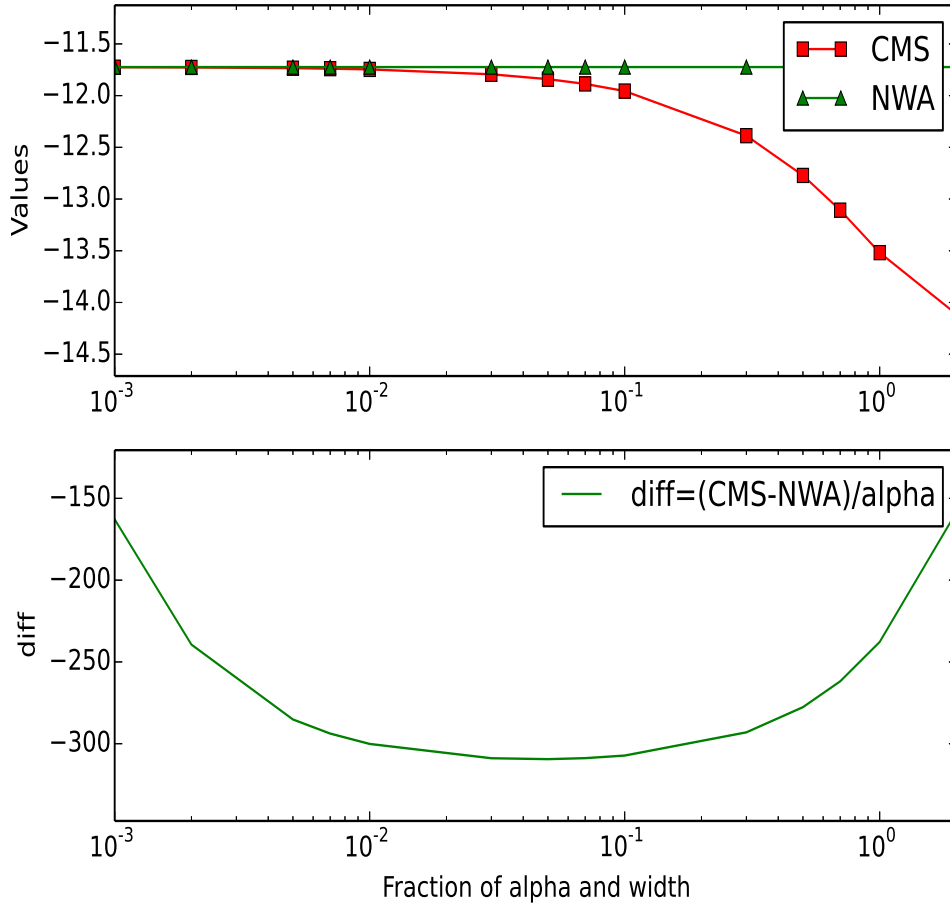


Figure 21: Cross checks for $u\bar{d} \rightarrow W^+ + \gamma \rightarrow e^+\nu_e + \gamma$ in the non-resonance region with the wrong LO width, i.e. $\Gamma_W = 1.2\Gamma_W^{\text{LO}}$.

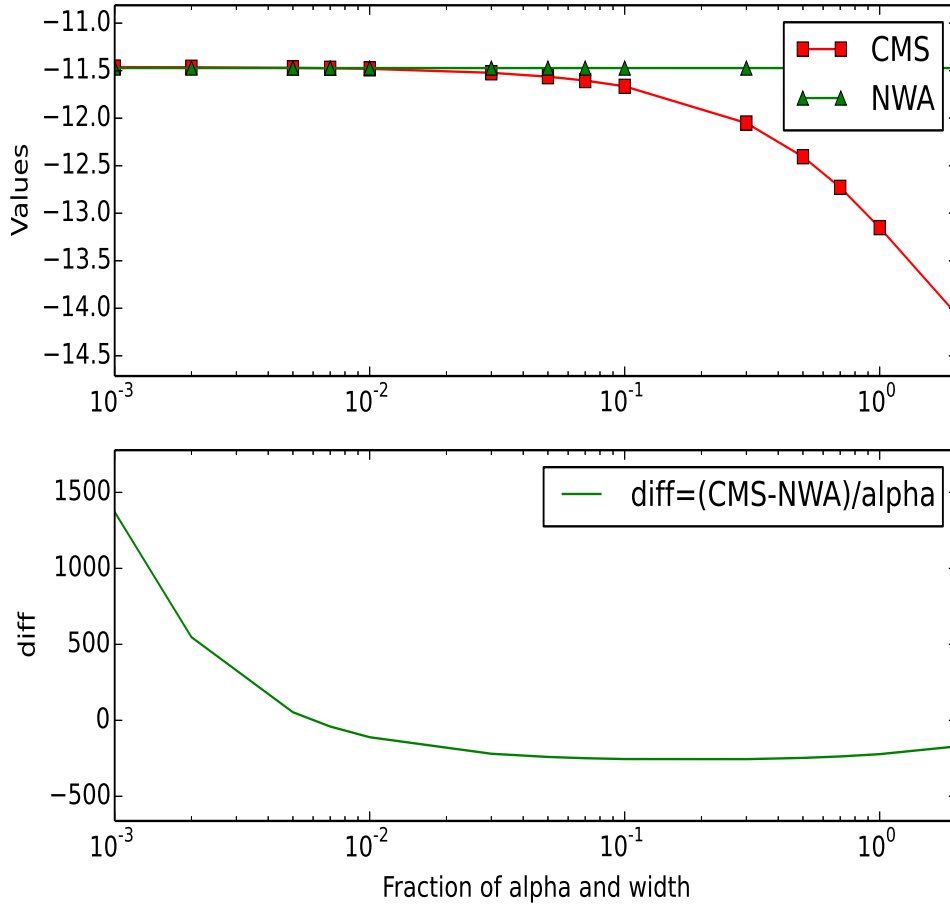


Figure 22: Cross checks for $u\bar{d} \rightarrow W^+ + \gamma \rightarrow e^+\nu_e + \gamma$ in the non-resonance region with the correct LO width but using the normal logarithms.

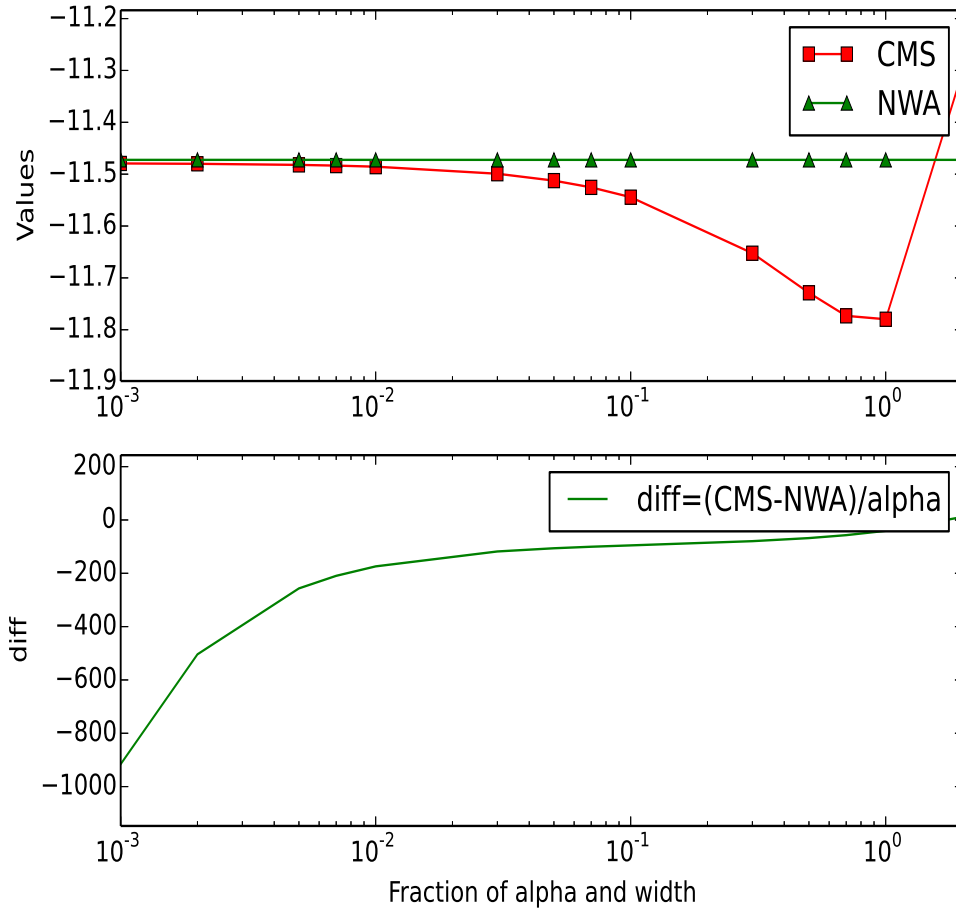


Figure 23: Cross checks for $u\bar{d} \rightarrow W^+ + \gamma \rightarrow e^+\nu_e + \gamma$ in the non-resonance region with the correct LO width without Born contributions.

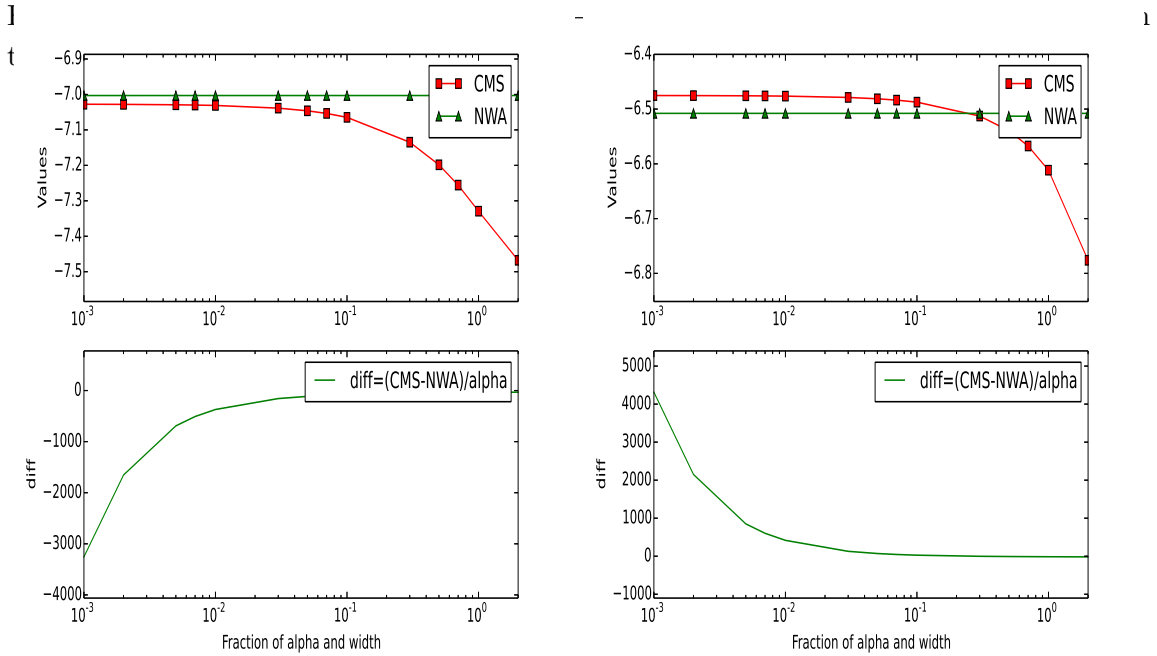
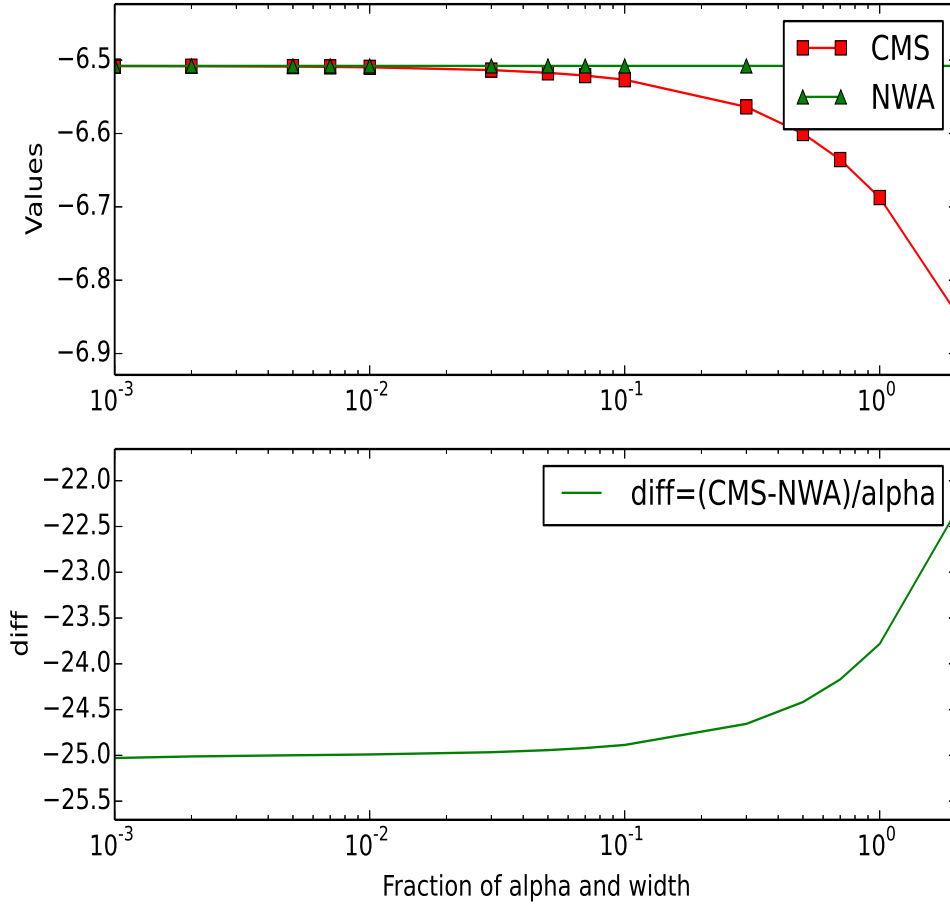


Figure 25: Cross checks for $u\bar{u} \rightarrow Z/\gamma^* + \gamma \rightarrow e^+e^- + \gamma$ in the non-resonance region with the wrong LO widths, i.e. $\Gamma_Z = 1.2\Gamma_Z^{\text{LO}}$ (left panel) and $\Gamma_W = 1.2\Gamma_W^{\text{LO}}$ (right panel).

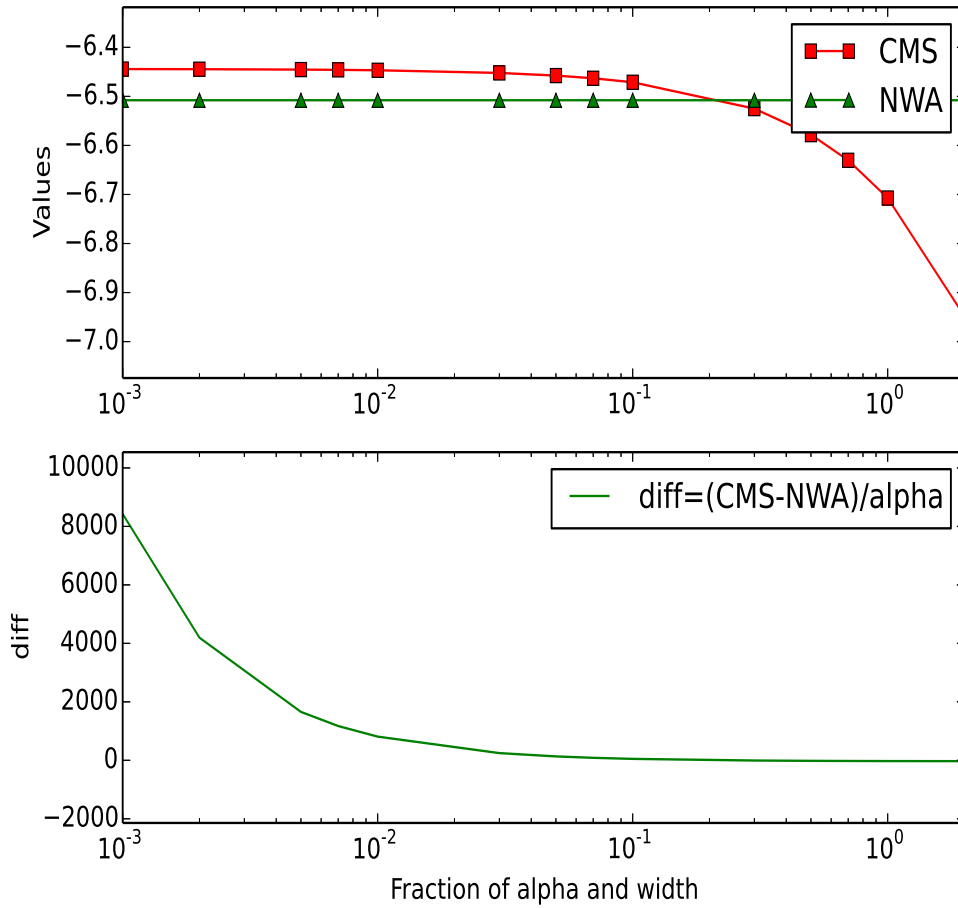


Figure 26: Cross checks for $u\bar{u} \rightarrow Z/\gamma^* + \gamma \rightarrow e^+e^- + \gamma$ in the non-resonance region with the correct LO widths but using the normal logarithms.

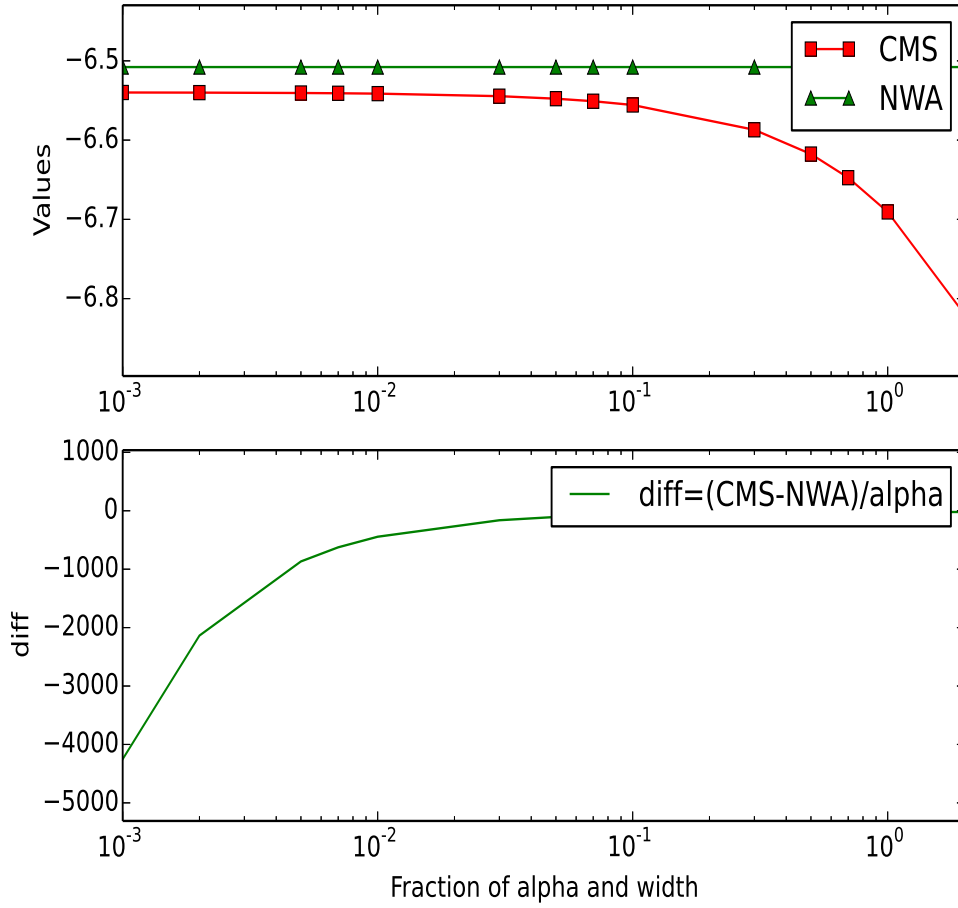


Figure 27: Cross checks for $u\bar{u} \rightarrow Z/\gamma^* + \gamma \rightarrow e^+e^- + \gamma$ in the non-resonance region with the correct LO widths without Born contributions.

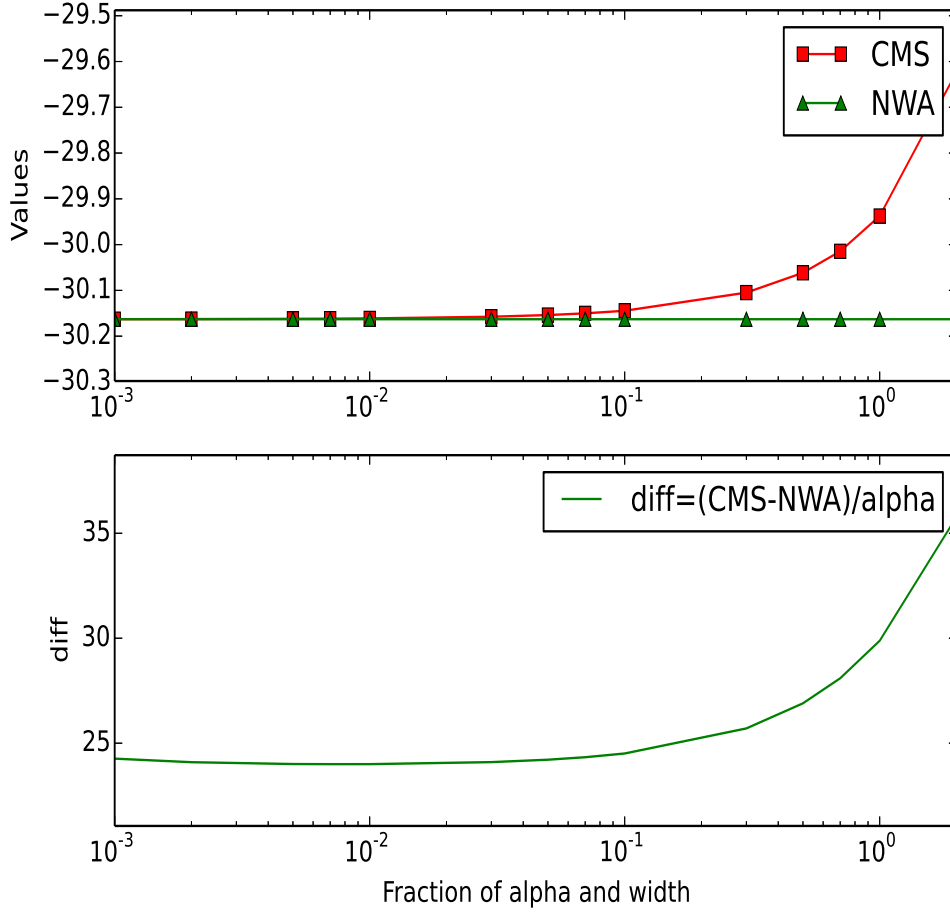


Figure 28: Cross checks for $e^+\nu_e \rightarrow \mu^+\nu_\mu b\bar{b}$ in the non-resonance region with the correct LO widths Γ_Z^{LO} , Γ_W^{LO} and Γ_t^{LO} .

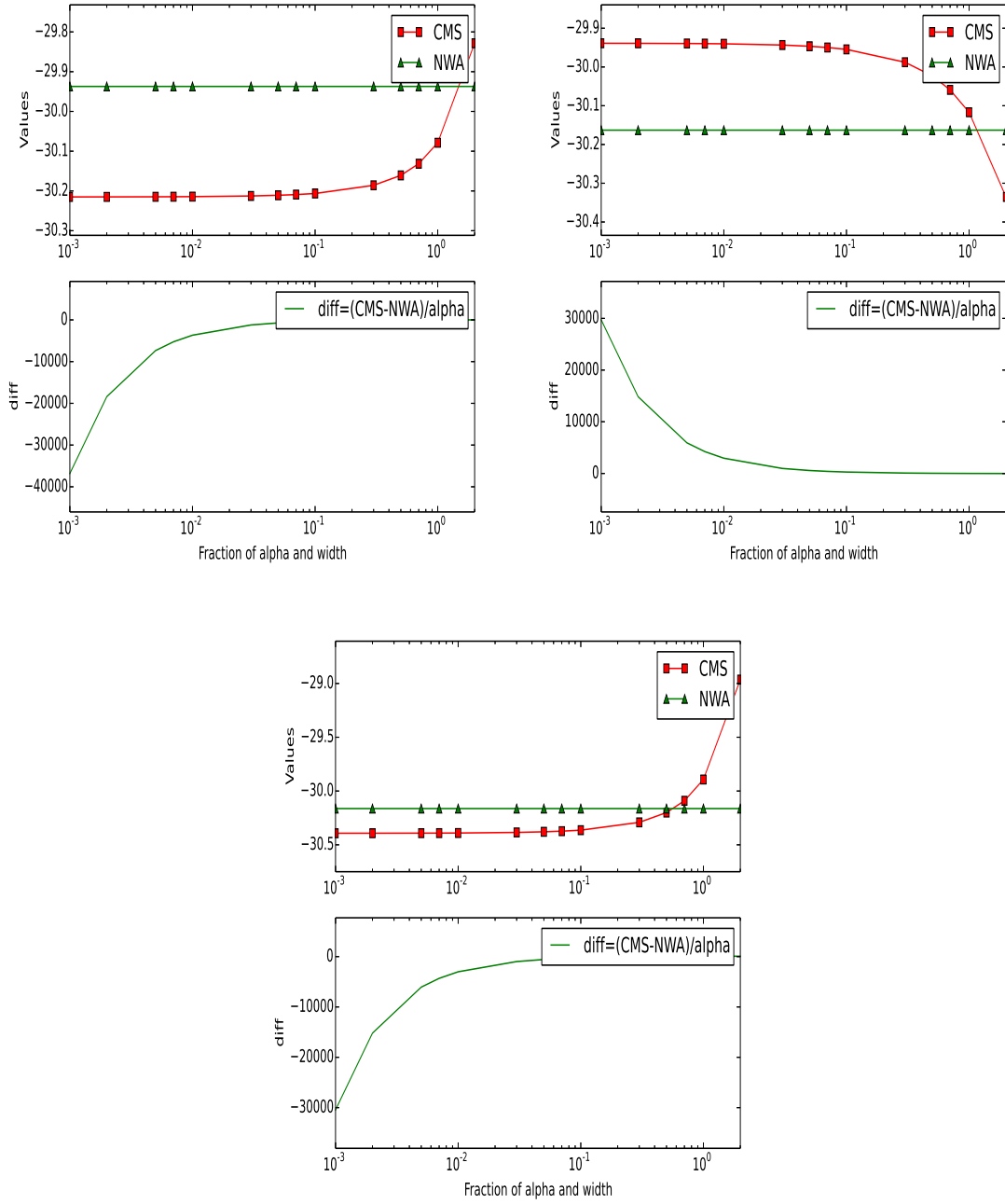


Figure 29: Cross checks for $e^+\nu_e \rightarrow \mu^+\nu_\mu b\bar{b}$ in the non-resonance region with the wrong LO widths, i.e. $\Gamma_t = 1.2\Gamma_t^{\text{LO}}$ (upper-left panel), $\Gamma_W = 1.2\Gamma_W^{\text{LO}}$ (upper-right panel) and $\Gamma_Z = 1.2\Gamma_Z^{\text{LO}}$ (lower panel).

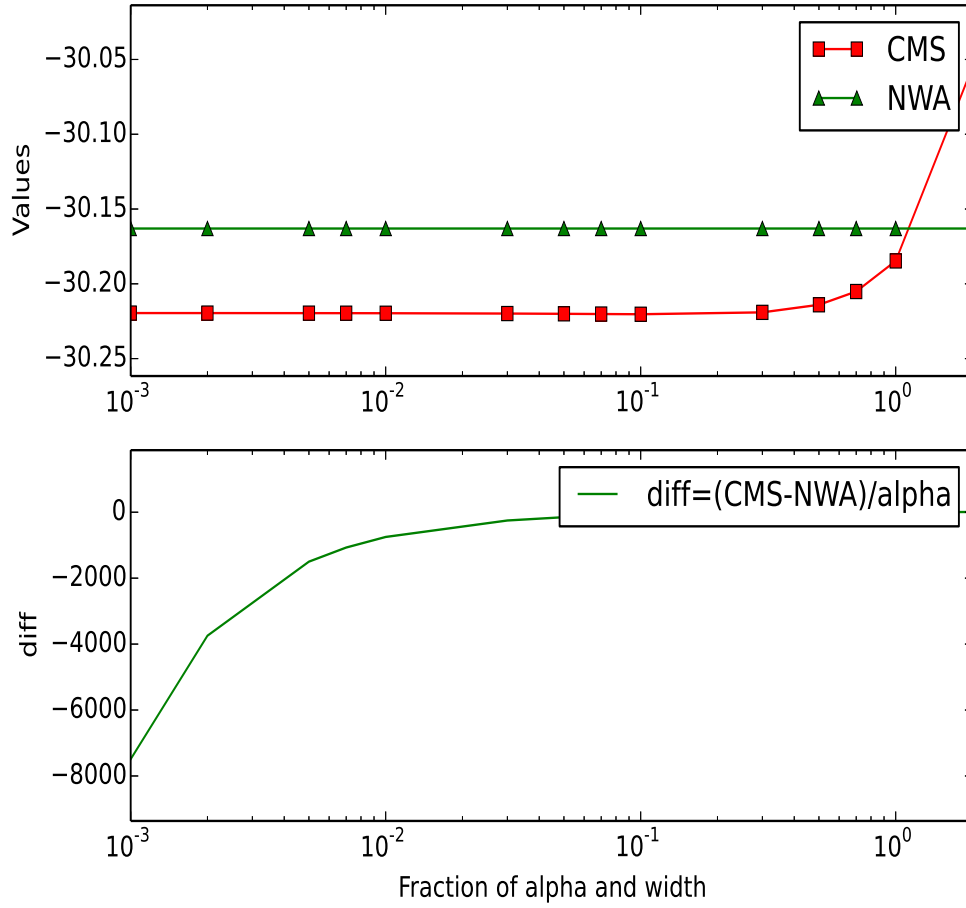


Figure 30: Cross checks for $e^+\nu_e \rightarrow \mu^+\nu_\mu b\bar{b}$ in the non-resonance region with the correct LO widths but using the normal logarithms.

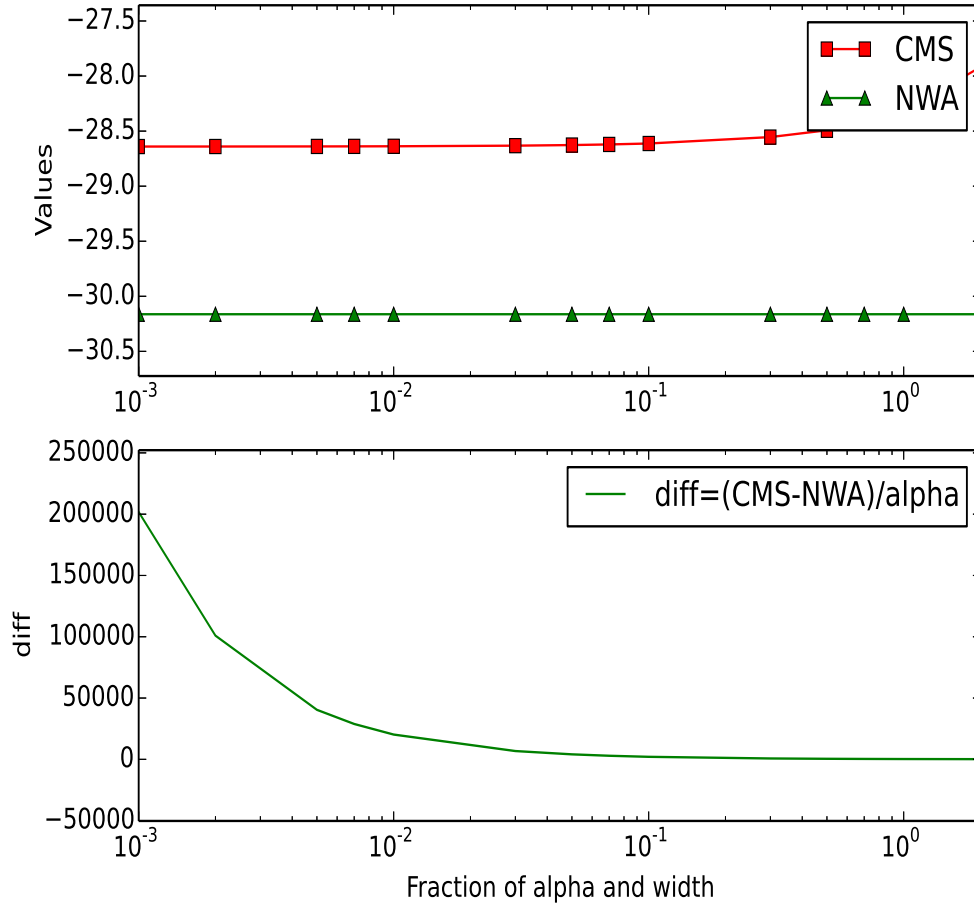


Figure 31: Cross checks for $e^+\nu_e \rightarrow \mu^+\nu_\mu b\bar{b}$ in the non-resonance region with the correct LO widths without Born contributions.

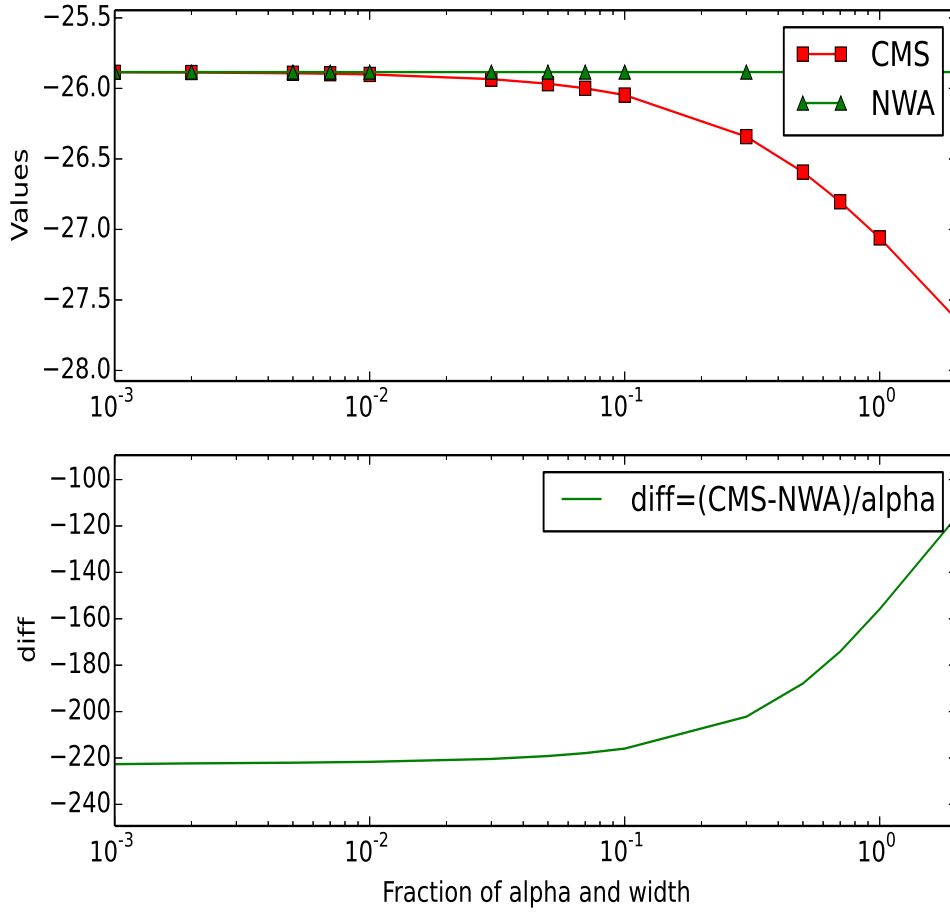


Figure 32: Cross checks for $gg \rightarrow \mu^+ \nu_\mu b \mu^- \bar{\nu}_\mu \bar{b}$ in the non-resonance region with the correct LO widths Γ_Z^{LO} , Γ_W^{LO} and Γ_t^{LO} .

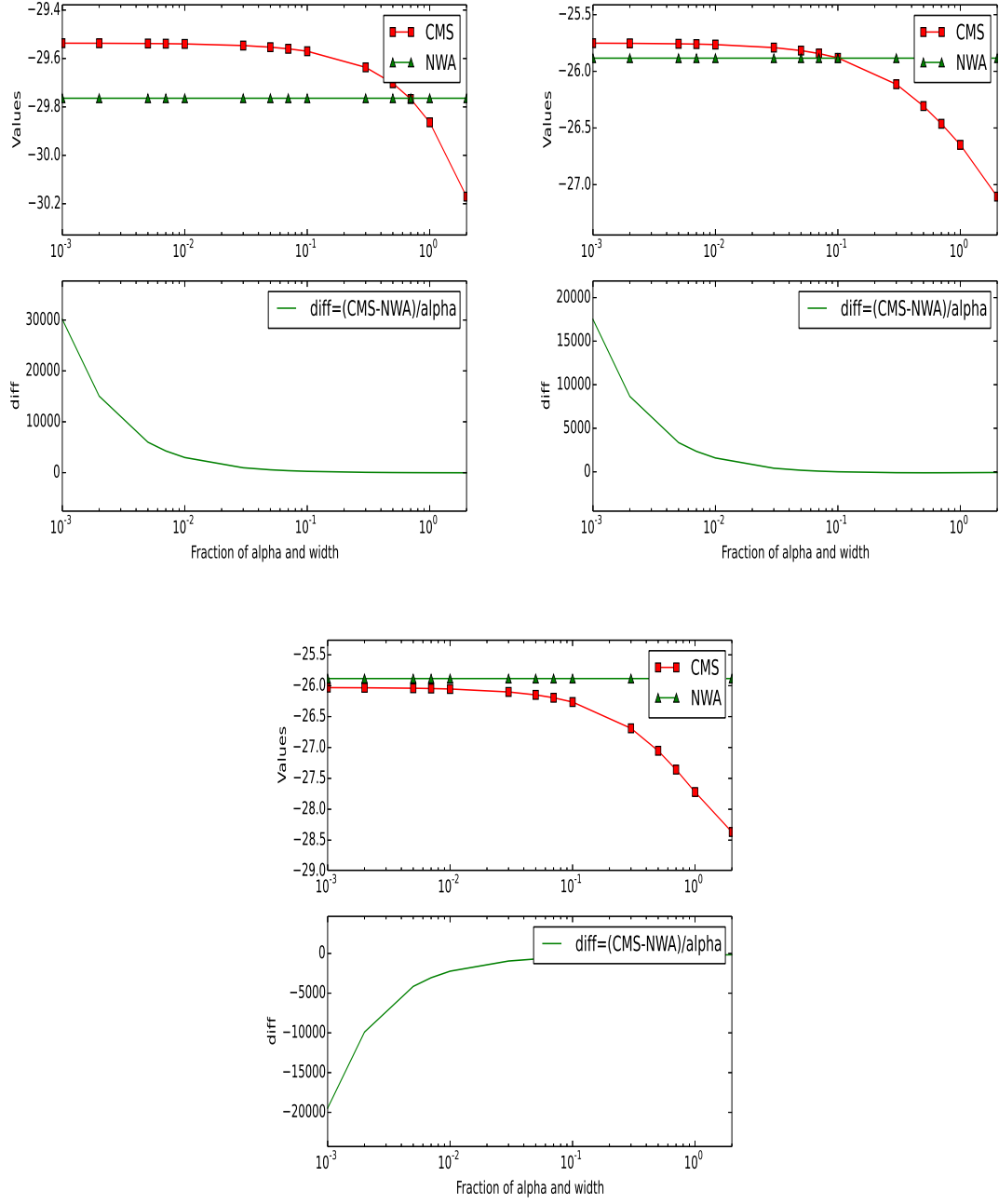


Figure 33: Cross checks for $gg \rightarrow \mu^+ \nu_\mu b \mu^- \bar{\nu}_\mu \bar{b}$ in the non-resonance region with the wrong LO widths, i.e. $\Gamma_t = 1.2\Gamma_t^{\text{LO}}$ (upper-left panel), $\Gamma_W = 1.2\Gamma_W^{\text{LO}}$ (upper-right panel) and $\Gamma_Z = 1.2\Gamma_Z^{\text{LO}}$ (lower panel).

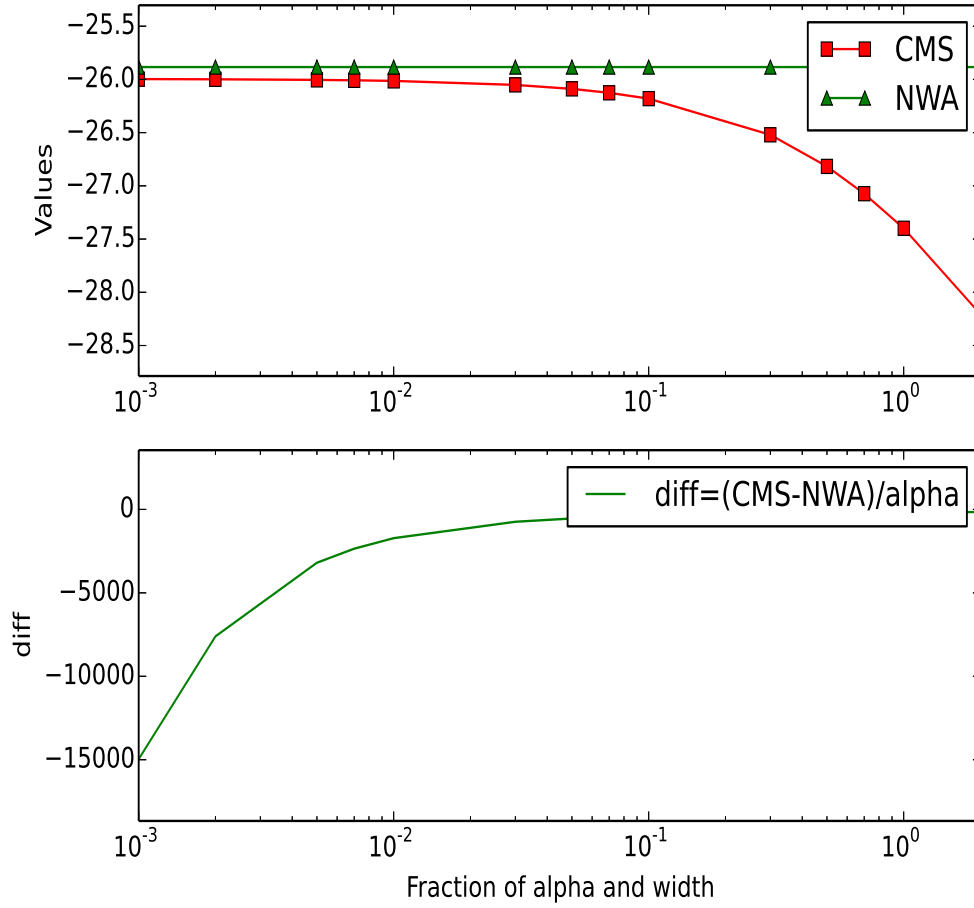


Figure 34: Cross checks for $gg \rightarrow \mu^+ \nu_\mu b \mu^- \bar{\nu}_\mu \bar{b}$ in the non-resonance region with the correct LO widths but using the normal logarithms.

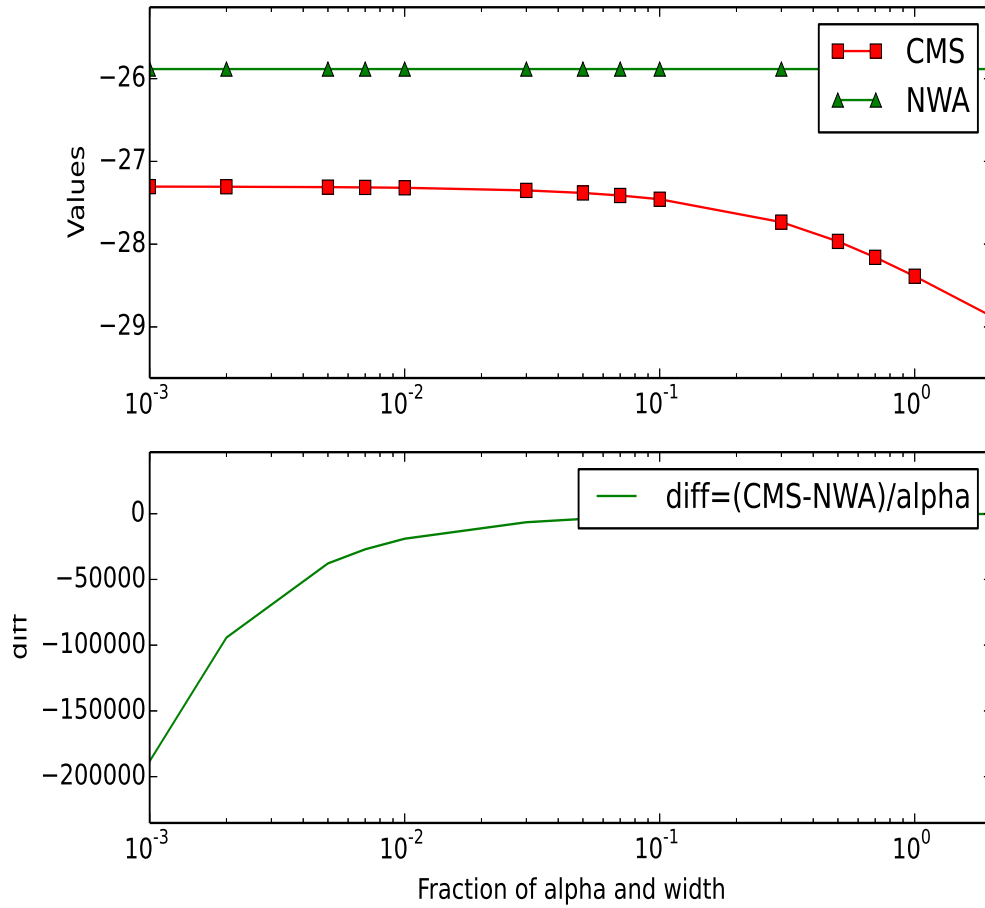


Figure 35: Cross checks for $gg \rightarrow \mu^+ \nu_\mu b \mu^- \bar{\nu}_\mu \bar{b}$ in the non-resonance region with the correct LO widths without Born contributions.

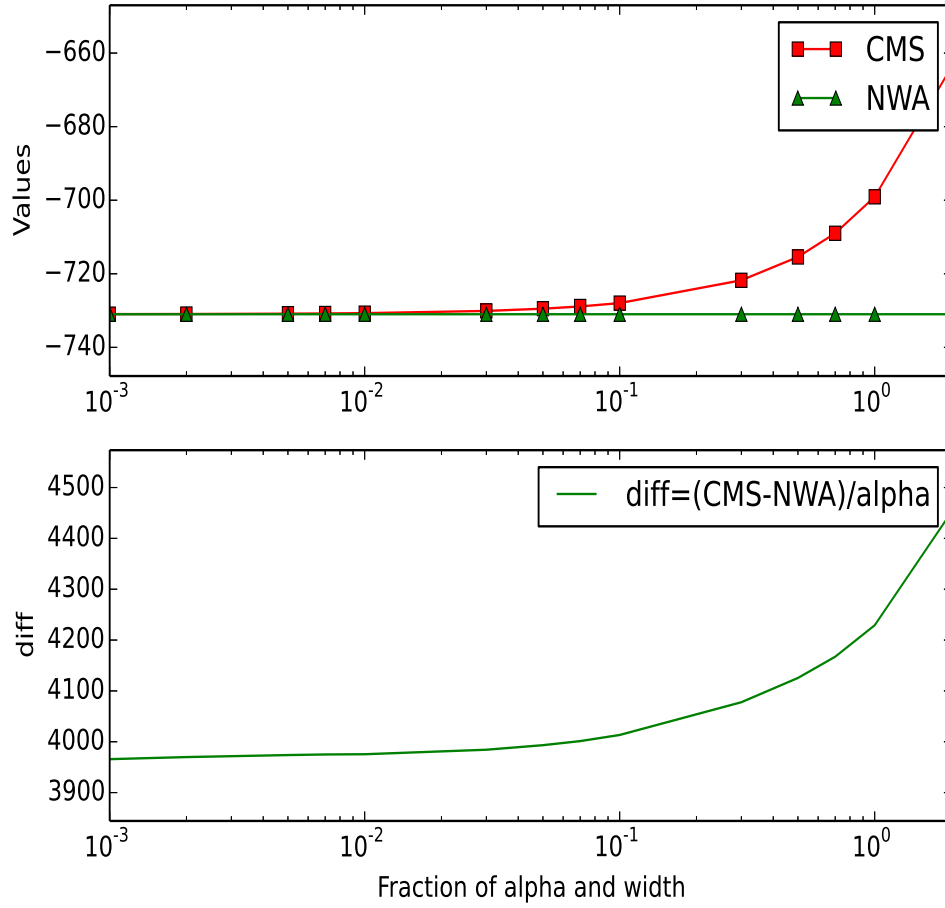


Figure 36: Cross checks for $b\gamma \rightarrow \mu^+\nu_\mu b\mu^-\bar{\nu}_\mu$ in the non-resonance region with the correct LO widths Γ_Z^{LO} , Γ_W^{LO} and Γ_t^{LO} .

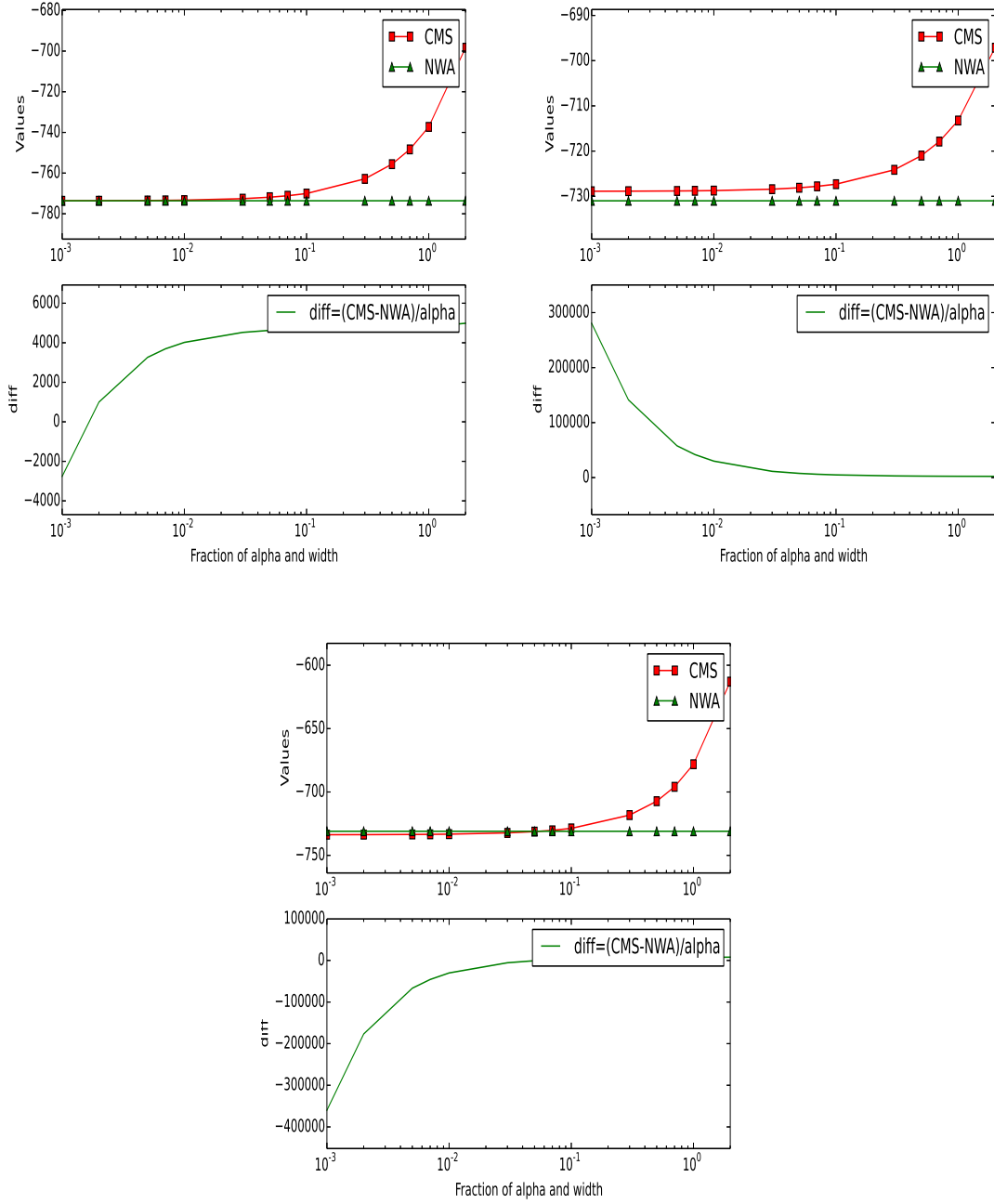


Figure 37: Cross checks for $b\gamma \rightarrow \mu^+\nu_\mu b\mu^-\bar{\nu}_\mu$ in the non-resonance region with the wrong LO widths, i.e. $\Gamma_t = 1.2\Gamma_t^{\text{LO}}$ (upper-left panel), $\Gamma_W = 1.2\Gamma_W^{\text{LO}}$ (upper-right panel) and $\Gamma_Z = 1.2\Gamma_Z^{\text{LO}}$ (lower panel).

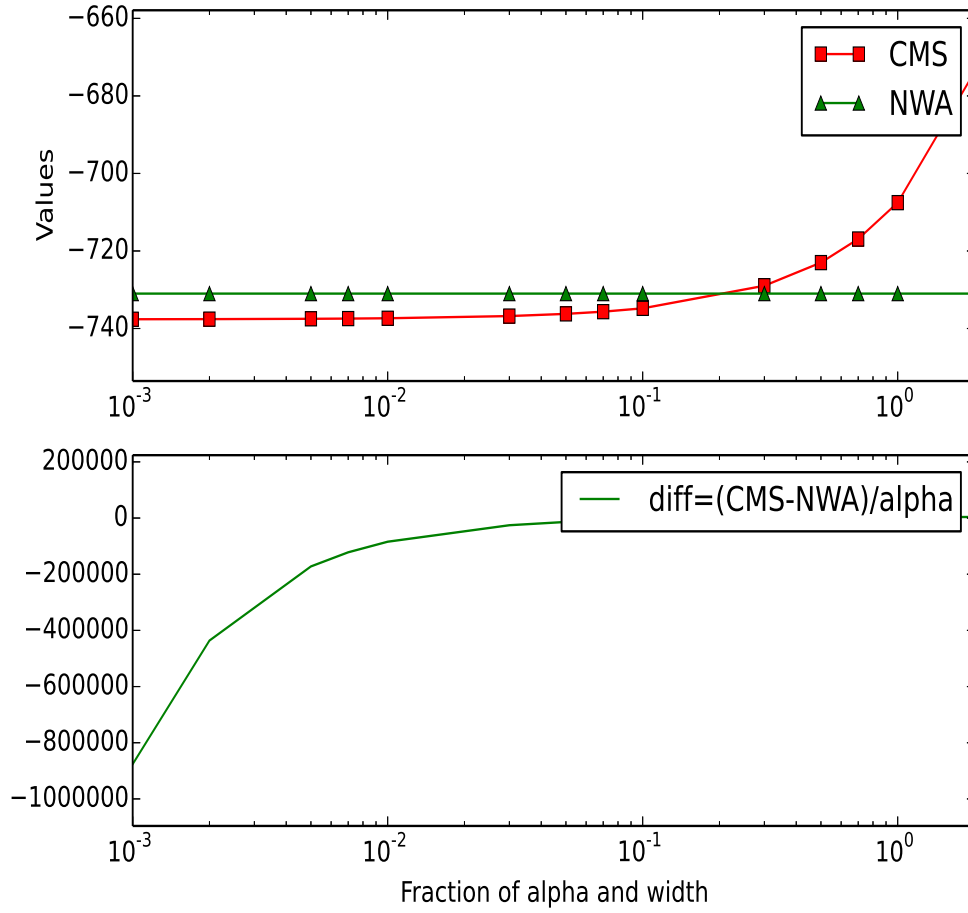


Figure 38: Cross checks for $b\gamma \rightarrow \mu^+\nu_\mu b\mu^-\bar{\nu}_\mu$ in the non-resonance region with the correct LO widths but using the normal logarithms.

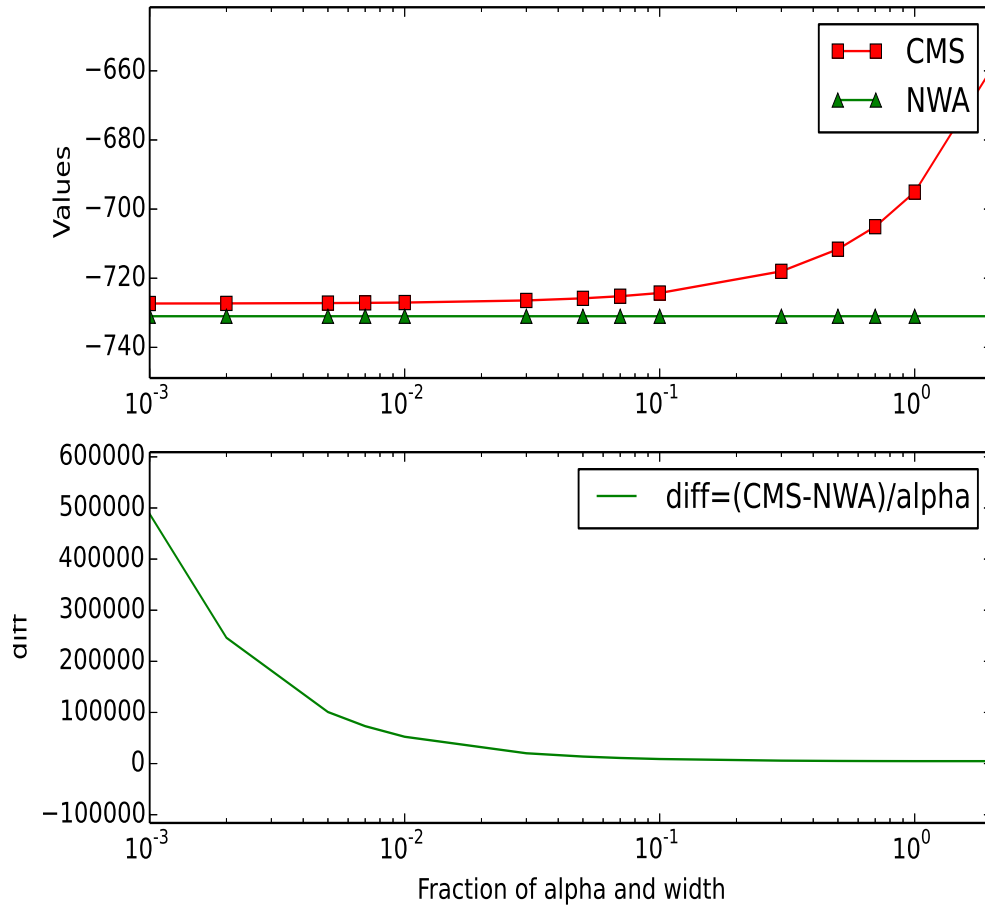


Figure 39: Cross checks for $b\gamma \rightarrow \mu^+\nu_\mu b\mu^-\bar{\nu}_\mu$ in the non-resonance region with the correct LO widths without Born contributions.